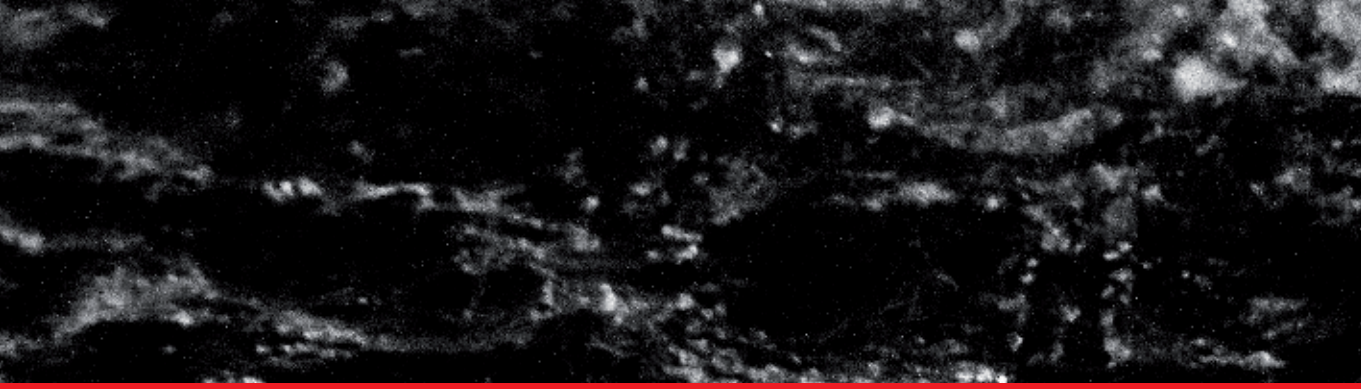

IntechOpen

Aquifers
Matrix and Fluids

Edited by Muhammad Salik Javaid and Shaukat Ali Khan

AQUIFERS - MATRIX AND FLUIDS

Edited by **Muhammad Salik Javaid**
and **Shaukat Ali Khan**

Aquifers - Matrix and Fluids
http://dx.doi.org/10.5772/intechopen.69070
Edited by Muhammad Salik Javaid and Shaukat Ali Khan

Contributors

Hsin-Fu Yeh, Fawzia Al-Ruwaih, Gunnar Jacks, Satheesachandran Thambi, Sateechandran Thambi, Amor Ben Moussa, Hatem Mejri, Sarra Bel Haj Salem, Mohamed Metwaly, Adebayo Olayinka Salako, Adepelumi Abraham A., Abdullah Faruque, Muhammad Salik Javaid, Shaukat Ali Khan

Notice

First published in London, United Kingdom, 2018 by IntechOpen
eBook (PDF) Published by IntechOpen, 2019
IntechOpen is the global imprint of INTECHOPEN LIMITED, registered in England and Wales, registration number: 11086078, The Shard, 25th floor, 32 London Bridge Street
London, SE19SG – United Kingdom
Printed in Croatia

British Library Cataloguing-in-Publication Data
A catalogue record for this book is available from the British Library

Additional hard and PDF copies can be obtained from orders@intechopen.com

Aquifers - Matrix and Fluids
Edited by Muhammad Salik Javaid and Shaukat Ali Khan

p. cm.

Print ISBN 978-1-78923-490-9

Online ISBN 978-1-78923-491-6

eBook (PDF) ISBN 978-1-83881-370-3

Meet the editors

For the past four decades, Dr. Muhammad Salik Javaid has been working in the fields of academics, research, development, execution, management, and policy formulation assignments with the Corps of Engineers and engineering universities within Pakistan and abroad. He also worked as the chief consulting engineer for the Engineer-in-Chief and Director General Planning for the Reconstruction and Rehabilitation Authority after the 2005 earthquake in Pakistan. He is a graduate of Georgia Tech, Atlanta, USA, where he undertook his Master's and Doctoral studies in the fields of dam overtopping and ocean bed hydrodynamics.

Presently, he is the chairman of the Department of Civil Engineering at Abasyn University at Islamabad Campus, Pakistan. He has also conducted courses on applied hydrology, hydraulics engineering, and river engineering for civil engineering students at various campuses.

Dr. Shaukat Ali Khan is a graduate of NUST, Pakistan; University of Calgary, Canada; and University of Sheffield, UK, where he received his BSc, MS, and PhD degrees, respectively.

Dr. Shaukat has a multidisciplinary teaching, research, and practical experience of over 25 years in civil engineering. His experience includes design and implementation of buildings, bridges, and heavy irrigation/hydraulic structures in Pakistan, Canada, and the UK. His research interests include risk and vulnerability assessment, strengthening and design of irrigation and hydraulic structures, as exhibited by numerous publications. Currently, Dr. Shaukat is serving as the associate dean, Faculty of Engineering, at Abasyn University, Peshawar.

Contents

Preface

If you search for the word "aquifer" using any search engine on the Internet, you would come across a lot of published material including numerous articles and books on this specific topic. In the plethora of these books and articles, one wonders at the need for yet another book on this subject. Anyone even remotely linked with the field of rocks and water would vouch that there are so many facets to this little word "aquifer" that despite the availability of so much literature in the water world, this immense literary aquifer is not enough to quench the thirst of many. People have been concerned with aquifers since time immemorial. Stakeholders of aquifers include water users such as domestic house owners, agriculturists, industrialists in arid regions, water conservationists and environmentalists in desert zones, politicians in transboundary regions, even military tacticians and economic strategists in water scarce countries and regions.

Our interest with the field of aquifers was initiated by a series of courses on "flow through porous media" taken during postgraduate studies. These developed the prime concepts of the nature, composition, formation, structure, fracture, and dynamics of rocks carrying various types of fluids, be it water, hydrocarbons, or any chemicals spilled and percolated in the ground. Because aquifers are hidden under the ground, it requires multidisciplinary, unconventional, as well as state-of-the-art conventional techniques to fully comprehend the aura of aquifers. Fascinated as we were by what moves under the ground, that fascination still continues.

"Health of aquifers" is one major research area for present-day scientists and engineers. Aquifers became prone to manmade contamination even before the beginning of the industrial age. Due to increased intensity of pollution because of modern-day lifestyles, concerns for the well-being of aquifer rocks and aquifer fluids are on the rise. All stakeholders are concerned for passing on this resource of life, intact and in usable condition, to the next generations.

In addition to the introductory section, the main text of this book comprises two additional sections, one each on "porous rocks" and the "fluids" they carry. The first section contains research chapters on the physical aspects, structure, and dynamics of the geologic strata called aquifers. The second section contains research chapters dealing with the quality, quantity, pollutions, purification, treatment, and characteristics of water contained in these geologic strata. This book is intended to catch the attention of practicing professionals, the research community, and students and teachers working in areas pertinent to the subject. Readers, for their consumption, will find diversified material in this presentation.

This book provides a collection of diversified papers on understanding and highlighting some critical aspects that address various issues related to aquifers. It provides a deep understanding of the issues and problems related to aquifers that may be used by academi-

cians, researchers, and professionals working in this field. The book project *Aquifers* could not have been possible without the hard work of many eminent professionals, hydrologists, geologists, water resources engineers, scholars, and scientists the world over who undertook analysis of problems and issues, conducted research, found out remedies and solutions, and authored these chapters.

The steadfast attitude, focus on results, and concern for timelines displayed by Ms. Renata Sliva and Ms. Ivana Glavic, Author Service Managers of Intech Open Access Publisher, are recognized for constantly reminding us of the deadlines to be met. The forbearance of our spouses, Sultana Salik and Maher Nigar Shaukat, during the period we were working on this book is heartily appreciated. The management of Abasyn University is also thanked for providing us with the academic platform and institutional resources to undertake this assignment.

Finally, the entire concept of IntechOpen Access Publishing is lauded for its global outreach and universal benefit to the human race.

Dr. Muhammad Salik Javaid,
Abasyn University, Islamabad Campus
Pakistan

Dr. Shaukat Ali Khan
Abasyn University, Peshawar Campus
Pakistan

Section 1

Aquifers: The Resource

Chapter 1

Introductory Chapter: Aquifers Today and Tomorrow

Muhammad Salik Javaid and Shaukat Ali Khan

Additional information is available at the end of the chapter

http://dx.doi.org/10.5772/intechopen.75800

1. Introduction

As defined in many scientific texts "An aquifer is an underground layer of water bearing permeable rock, rock fractures or unconsolidated material from which groundwater can be extracted using water well" [1]. Related terms used are aquitard, which is a bed of low permeability along an aquifer, and aquiclude, which is a solid, impermeable area underlying or overlying an aquifer, making an aquifer confined or unconfined. Aquifer system is a series of two or more aquifers hydraulically connected with each other. If an aquifer or an aquifer system spans more than one state, it is called transboundary aquifer [2]. An aquifer is therefore the combination of both; an underground rock structure, and water mass existing in the pores and voids. Aquifers contain by far the largest volume of unfrozen fresh water on earth thus making it an enormously important natural resource, entrusted to us by the Mother Nature for equitable use and safe custody for the next generations to come. Because of the fact that aquifer is hidden to the eye, therefore till today they are poorly known and understood by the common masses and decision makers alike.

2. Aquifers today

Aquifer, the solid rock structure and fluid occupying the interstices, being a transitional resource has been prone to exploitations, silent revolutions and progressive pollutant attacks inherent to modern lifestyles. A considerable amount of risk and uncertainty is therefore attached to the aquifers because of stresses on groundwater systems produced inherent to modern domestic and industrial life patterns. At present, the key issues related to the aquifers may be summed up as:

Falling groundwater levels and storage depletion.

Groundwater quality and resource pollution.

Effect of climate change and sea level rise.

Effect of natural hazards and emergencies on aquifers.

Management of transboundary aquifers.

In the absence of well installation and pump operation laws in many countries of the world and lack of enforcement of these laws wherever these do exist, excessive pumping leading to mining of the aquifers is a constant source of depletion of aquifers. It is feared that in many arid, semi-arid, and increasingly water-scarce areas around the world, dependency on aquifer water will increase because of storage buffers rendering the groundwater a better option than dwindling surface waters. There is, thus, a dire need that laws be made and regulations be implemented to effectively monitor the excessive pumping from aquifers. According to a recent news in the city of Cape Town, the water taps will cease to supply water to the entire city in April 2018 because water supplies are likely to deplete to unmanageable lower limits.

Aquifer quality degradation is another major issue that has been and is bothering the stakeholders the world over. At conventional drilling depths, the water found is usually of potable quality, fit for municipal, agriculture and industrial consumption. However, exhaustive use of micropollutants in particular pharmaceuticals and personal care products and endocrine disruptive compounds is drastically affecting the quality of aquifer waters for all purposes. It remains a major global, regional and local concern to protect the groundwater against quality degradation in all respects.

Inherently aquifers are very resilient to the effects of atmospheric variations above ground, surface hazards and climate change effects and therefore are preferred over the surface waters, making them as more dominant sources of water. However, climate change adversely alters the aquifer's groundwater recharge thus introducing uncertainties in the recharge estimates and spatial pattern definitions. Climate change alters the mean annual groundwater recharge and mean annual surface water flows and their distribution in time. The water demand and water use have also been found to have been affected by the climate change phenomena.

Artificial recharge is the planned human activity of augmenting the amount of groundwater available through works designed to increase the natural replenishment or percolation of surface waters into the groundwater aquifers. Artificial recharge is also used for the purpose of disposal of floodwaters, control of salt water intrusion, water storage to reduce pumping and piping costs, temporary regulation of groundwater abstraction, and water quality improvement by removal of suspended solids. Managed aquifer recharge is increasingly being used to facilitate water recycling in areas where it is possible to improve scarcity by harvesting urban storm water and wastewater. Pretreating injection water should be made obligatory.

Natural treatment can be achieved in the aquifer during managed aquifer recharge, resulting removal of pathogens, nutrients and micropollutants.

Aquifer storage transfer and recovery (ASTR) in contrast to aquifer storage and recovery (ASR) uses separate wells for injection and for recovery, allowing an attenuation zone to exist around the recharge zone [3].

Aquifer management and groundwater governance are very complex phenomena and need to be tailored to local conditions and socio-politico-economic environments. For transboundary aquifer systems, due to international dimension coming into play, this complexity is even greatly enhanced. International cooperation and wide range international initiatives could add significant value to aquifer management. International cooperation could be in the form of enhancing and disseminating technical data about aquifers and groundwater, developing and promoting approaches and tools for aquifer management, and raising global commitment for priority action when required.

Administrative and political borders dividing transboundary aquifer systems provide great barriers and obstacles to the coordinated development and management of aquifers, making this even more complex in nature. Lack of information or information gaps, conflicting interests of states and a lack of coordination across the boundaries, easily lead to the problems that may otherwise be preventable. A study on international law revealed that very few institutional arrangements and legal instruments exist to resolve such conflicts of interests [4]. In its 66th session, the United Nations General Assembly passed a resolution on "Law of Transboundary Aquifers" [5]. Salient of the resolution being:

States concerned to make appropriate bilateral or regional arrangements for proper management of their transboundary aquifers, taking into account the provisions of the resolution.

Encourages International Hydrological Program (IHP) of United Nations Economic Scientific and Cultural Organization (UNESCO) to offer further scientific and technical assistance to the states concerned.

To formally legislate on "the law of transboundary aquifers."

3. Aquifers tomorrow

Due to excessive demand of water by the ever increasing population, the necessity of artificial recharge of aquifers is increasing day by day. Extensive research is being conducted to explore new and novel techniques for artificially recharging the aquifers to enhance their capacity, water quantity, and improve the water quality. Kavuri et al. have reviewed the existing methods of artificial recharge such as infiltration basins and canals, water traps, cut waters, surface run off, drainage wells, etc. [6]. Modern techniques like direct surface and subsurface recharge including seepage from surface reservoirs like Khanpur reservoir, and indirect recharge have been thoroughly explored and improved for achieving better efficiency in meeting the artificial recharge goals like storage of fresh waters within saline aquifers, secondary oil recovery, and wastewater disposal, etc. [7]. Indirect methods include installation of groundwater pumping facilities, hydraulically inducing infiltration in the drainage basins, modification of aquifers or construction of new aquifers.

The latest trend in aquifers is the modification of existing aquifers or creation of new artificial aquifers or underground reservoirs for water. Aquifers can be modified by structures that impede outflow of groundwater. Groundwater barriers or dams have been built underground to obstruct or detain flow in/out of the aquifers. Recent example is the creation of artificial aquifer

under Liwa desert in south of Abu Dhabi, United Arab Emirates which can provide water at the rate of 600 l per day per person. Reportedly Liwa Strategic Water Reserve (Liwa ASR) can store 26 billion liters of water, and it will take approximately 26 months to fill it up [8].

4. Conclusion

Since groundwater as a natural resource is very vital for survival of human race on this planet earth, the present generation is answerable to the future generations for its safe custody, upkeep and maintenance of quality and quantity. Therefore, all endeavors must be made in understanding the nature and behavior of aquifers, their protection, their maintenance and sustainable development for use by all stakeholders concerned.

Author details

Muhammad Salik Javaid[1]* and Shaukat Ali Khan[2]

*Address all correspondence to: msalikj@abasynisb.edu.pk

1 Abasyn University, Islamabad, Pakistan

2 Abasyn University, Peshawar, Pakistan

References

[1] Dunn MG, editor. Exploring Your World: The Adventures of Geography. Washington, DC: National Geographic Society; 1993

[2] UNGA. Resolution 63/124 on "Law of Transboundary Aquifers". New York: United Nations General Assembly; 2008

[3] Dillon P, Pavelic P, Page D, Beringen H, Ward J. Managed Aquifer Recharge: An Introduction. Canberra: National Water Commission, Australian Government; 2009. Waterlines Report Series No. 13

[4] Burchi S, Mechlem K. Groundwater in International Law: Compilation of Treaties and Other Legal Instruments. Rome: FAO; 2005. FAO Legislative Study 86

[5] Official Records. General Assembly, 63rd and 66th Session, 6th Committee Meetings. New York: United Nations; 2011

[6] Kavuri M, Boddu M, Annamdas VGM. New methods of artificial recharge of aquifers: A review. In: Proceedings of 4th International Perspective on Water Resources and Environment, IPWE 2011. Singapore: University of Singapore; 2011

[7] Jamil SM, Nawab A, Salik JM, Sarfraz A. Geo-Technical Evaluation of Seepage Remedial Measures of Khanpur Dam. International Conference on GeoTechnical Engineering. Lahore; 2010

[8] Haider H. Emergency water storage project begins in Liwa desert. Khaleej Times. Abu Dhabi, UAE; Sep 24, 2010

Section 2

Aquifers: The Structure

Chapter 2

Aquifer, Classification and Characterization

Salako Adebayo O and Adepelumi Abraham A

Additional information is available at the end of the chapter

http://dx.doi.org/10.5772/intechopen.72692

Abstract

Aquifers in geological terms are referred to as bodies of saturated rocks or geological formations through which volumes of water find their way (permeability) into wells and springs. Classification of these is a function of water table location within the subsurface, its structure and hydraulic conductivities into two namely; Confined Aquifers and Unconfined Aquifers and then characterized these aquifers. The characterization of aquifers could be done using certain geophysical techniques like Electrical Resistivity, Electromagnetic Induction, Ground Penetrating Radar (GPR) and Seismic Techniques. Aquifer Characterization is dependent on the petro-physical properties (porosity, permeability, seismic velocities etc.) of the subsurface. Results of this Aquifer Characterization could be observed and analyzed using varying geophysical software (WinRESIST, RADpro etc.) to better image the subsurface.

Keywords: aquifers, unconfined aquifer, confined aquifer, aquifer characterization, electrical resistivity, electromagnetic induction, ground penetrating radar, seismic techniques

1. Introduction

To explore the term "Aquifer", it is paramount to understand a bit about the natural occurring resource groundwater depended on by vast majority of people and how it relates to Aquifers.

Groundwater is defined as fresh water (from rain, melting of ice and snow) that soaks into the soil and is stored between pore-spaces, fractures and joints found in within rocks and other geological formations. Groundwater occurs in various geological formations, the ability of geological formations to store water is a function of its textural arrangement. The source of groundwater most times could be linked to surface run-off and infiltration of rainwater into the subsurface and streams from which it leads to the establishment of the water table and serve as a primary supplier of streams, springs lakes, bays and oceans. The textural arrangement (uniformly or tightly arranged texture, loosely arranged texture) found within

most geological formations and rocks have a strong role to play in *water retention* and *storative* capacity of any rock or geological formation. Rocks/Geological formation with uniformly or tightly arranged texture have high water retaining ability (porosity) but less transmitting or mobility ability (permeability) while those with higher porosity and higher permeability have sufficiently enough to yield significant quantities of groundwater to wells and springs as such any geological formation with such characteristic is been referred to as an Aquifer. Let us now consider other definitions for aquifers and look at the different types that exist based on its classification and what influences these classifications.

An **aquifer** according to word web dictionary refers to any underground layer of water-bearing rock or geological formation that yields sufficiently groundwater for wells and springs. According to geological terms an Aquifer could be referred to as a body of saturated rock or geological formation through which water can easily move (permeability) into wells and streams (**Figure 1**). The top of the water level in an aquifer is called the water table. An aquifer fills with water from rain or melted snow that drains into the ground. In certain areas, water could pass through the soil of the aquifer while in other areas it enters through joints and cracks in rocks where it moves downwards until it encounters rocks that are less permeable. Aquifers generally are known to serve as reservoirs and could dry up when people drain them faster than they are been refilled by nature.

Aquifers must not only be permeable but must also be porous and are found to include rock types such as sandstones, conglomerates, fractured limestone and unconsolidated sand, gravels and fractured volcanic rocks (columnar basalts). While some aquifers have high porosity and low permeability others have high porosity and high productivity. Those with high porosity and low permeability are referred to as poor aquifers and include rocks or geological formation such as granites and schist while those with high porosity and high permeability are regarded as excellent aquifers and include rocks like fractured volcanic rocks.

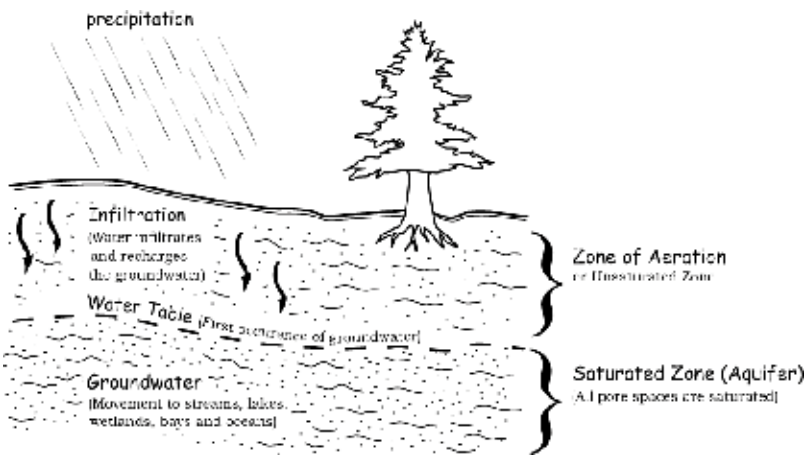

Figure 1. Aquifer formation (as adapted from http://water.usgs.gov/ogw).

http://dx.doi.org/10.5772/intechopen.72692

2. Classification of aquifers

Aquifers are generally been classed into two main categories namely confined aquifer and unconfined aquifers.

2.1. Confined aquifers

Confined Aquifers are those bodies of water found accumulating in a permeable rock and are been enclosed by two impermeable rock layers or rock bodies. Confined Aquifers are aquifers that are found to be overlain by a confining rock layer or rock bodies, often made up of clay which might offer some form of protection from surface contamination. The geological barriers which are non-permeable and found exist between the aquifer causes the water within it to be under pressure which is comparatively more than the atmospheric pressure. The presence of fractures, or cracks in bedrocks is also capable of bearing water in large openings within bedrocks dissolving some of the rock and accounts for high yields of well in karst terrain counties like Augusta, Bath within Virginia. Groundwater flow through aquifers is either vertically or horizontally at rates often influenced by gravity and geological formations in these areas.

Confined aquifers could also be referred to as "Artesian aquifers" which could be found most above the base of confined rock layers. Punctured wells deriving their sources from artesian aquifers have fluctuation in their water levels due more to pressure change than quantity of stored water. The punctured well serve more as conduits for water transmission from replenishing areas to natural or artificial final points. In terms of storativity, confined aquifers (**Figure 2**) have very low storativity values of 0.01 to 0.0001.

2.2. Unconfined aquifer

Unconfined Aquifer unlike confined aquifers are generally found located near the land surface and have no layers of clay (or other impermeable geologic material) above the water table although they are found lying relatively above impermeable clay rock layers. The uppermost

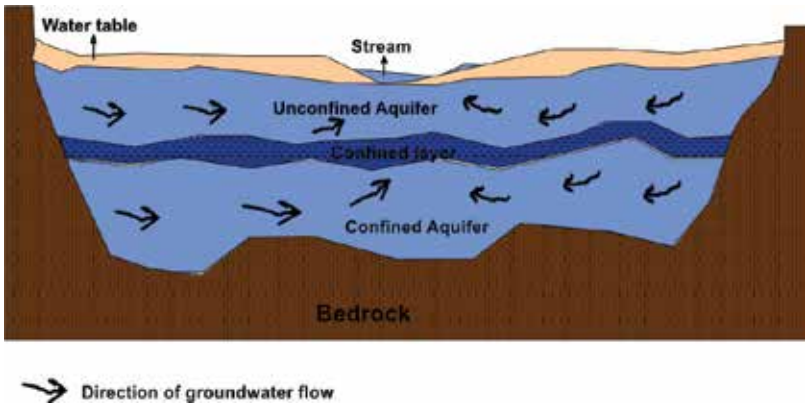

Figure 2. Schematic cross-section of aquifer types (source: http://en.m.wikipedia.org>wiki>Aquifer).

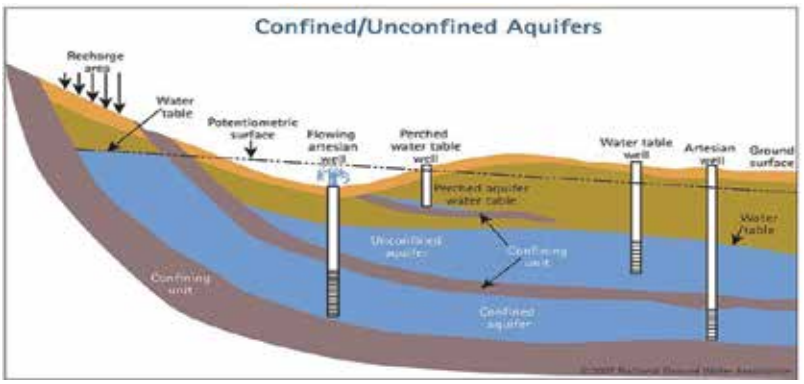

Figure 3. Schematic cross-section of aquifer types (source: coloradogeologicalsurvey.org>wateratlas).

boundary of groundwater within the unconfined aquifer is the water table, the groundwater in an unconfined aquifer is more vulnerable to contamination from surface pollution as compared to that in confined aquifers this been so due to easy groundwater infiltration by land pollutants. Fluctuation in the level of groundwater varies and depends on the stored up groundwater in the space of the aquifer which in turn affects the rise or fall of water levels in wells that derive their source from aquifers. Unconfined aquifers have a storative value greater than 0.01. "Perched aquifers" (**Figure 3**) are special cases of unconfined aquifers occurring in situation where groundwater bodies are separated from their main groundwater source by relatively impermeable rock layers of small areal extents and zones of aeration above the main body of groundwater The quantity of water found available in this type of aquifer is usually minute and available for short periods of time.

3. Petro-physical properties of aquifers

Petro-physical properties of aquifers are properties that help in the defining and characterizing aquifers. Some of the properties considered are:

3.1. Hydraulic conductivity

Hydraulic Conductivity could be described as the relative ease with which a fluids (groundwater) flows through a medium (in this case a geological formation or rock) which is quite different from intrinsic permeability in that though it describes the water-transmitting property of the medium it is however not influenced by the temperature, pressure or the fluid passing through the geological formation. Hydraulic conductivity of a soil or rock or geological formation depends on a variety of physical factors amongst which includes porosity, particle size and distribution, arrangement of particles and other factors.

Mathematically hydraulic conductivity could be defined by the formula below:

http://dx.doi.org/10.5772/intechopen.72692

$$K = k\frac{\rho g}{\mu} \tag{1}$$

where K is the hydraulic conductivity (cm/s or m/s), k is the intrinsic permeability, ρ is the density of fluid, μ is the dynamic viscosity of fluid.

Note: seconds (s) could be converted to days by time conversions.

Generally, for unconsolidated porous media, hydraulic conductivity varies with particle size as such clayey materials exhibits low values of hydraulic conductivity as compared to sands and gravels that exhibits high values of hydraulic conductivity (150 m/day for coarse gravels, 45 m/day for coarse sand and 0.08 m/day for clay). This is so because the small particle size arrangements (fine grained) in geological formations contained mainly of clayey materials though porous is not permeable enough to allow groundwater flow within it however in sands and gravels (medium to coarse grained) we have medium to coarse arrangement of particle sizes which results to a porous and permeable geological formations or rocks that allows a higher ease of groundwater flow. It is however essential to point out that we could have geological formations or rock that exhibit medium values of hydraulic conductivity, this is in the case where you have a geological formation made up of moderate amounts of clayey material and sandy materials. It should also be noted that variations in hydraulic conductivity values of geological formations or rocks is dependent on factors such as weathering, fracturing, solution channels and depth of burial.

3.2. Porosity

Porosity of a geological formation or rock or soil could be described as the measure of the contained voids or interstices expressed as a ratio of the volume of voids to the total volume. It could also be defined as the volume of pores within a rock or soil sample divided by the total volume of the rock matrix (pores and solid materials contained with the rock). When a rock is emplaced by either cooling from an igneous melt or induration from loose sediment or soil formation from weathering of rock materials, it possess an inherent porosity known as primary porosity which reduces with time by actions of cementation or compaction. However, when joints, fissures, fractures or solution cavities formed within rocks after the must have been emplaced it is referred to as secondary porosity. Therefore, total porosity is the sum of primary and secondary porosities.

If all the pores found contained in a rock are not connected, then only a certain fraction of the pores would allow for water movement. The fraction that allows for water movement is known as the effective porosity example of which includes pumice, glassy volcanic rock (solidified froth) probably would float in water because its total porosity is high and it contains much entrained gas.

Porosity of a rock is determined to a large extent by the packing arrangement of particle sizes and the uniformity of its grain-size distribution. As such a cubic packing (**Figure 4A**) would give a porosity of 47.65%, the greatest and most ideal a rock with uniform spherical grains can achieve as the centers of eight such grains from vertices of a cube. However, if the packing

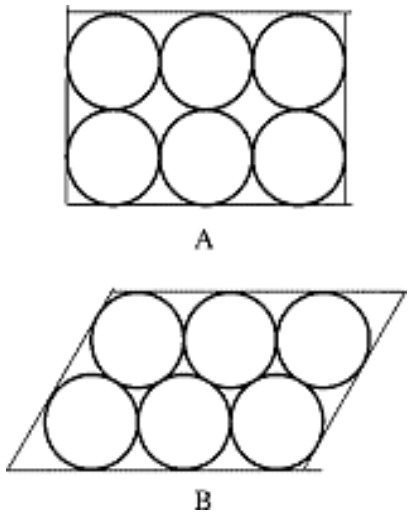

Figure 4. (A) Cubic packing (B) Rhombohedral packing.

arrangement of the rock where to change to be that of a rhombohedral (**Figure 4B**) then, its porosity would reduce to 25.85% as the centers of the eight adjacent spheres form the vertices of rhombus.

Mathematically porosity (n) is given by the formula below:

$$Porosity\ (n) = \frac{Vp}{Vt} \tag{2}$$

where Vp is the pores of rock or soil sample, Vt is the total volume of pores and solid material.

3.3. Transmissivity

Transmissivity (T) more simply could be defined as the property of aquifer to transmit water. It could also be defined as the amount of water that can be transmitted horizontally through an aquifer unit by full saturated thickness of the aquifer under a hydraulic gradient of 1 or as the rate at which water of prevailing kinematic viscosity is transmitted through a unit width of aquifer under a unit gradient.

It could be mathematically defined as:

$$T = Kb\ \left(m^2/day\right) \tag{3}$$

where T is the transmissivity, K is the hydraulic conductivity, b is the saturated thickness of the aquifer.

Aquifers are characterized by petro-physical properties such as *hydraulic conductivity* (alternatively called *permeability*), *transmissivity* (product of hydraulic conductivity and aquifer thickness) and *diffusivity* (ratio of transmissivity and storage coefficient). These properties could be examined using geophysical techniques such as Electrical Resistivity, Seismic techniques.

4. Aquifer characterization – electrical techniques

In geophysical investigations using electrical techniques, two primary properties of interest been considered are electrical conductivity or dielectric constant.

Electrical techniques make involves *profiling* and *sounding* mode of data collection which both involves the use of direct currents or low frequency altering currents passing through the subsurface. While profiling use of the terms profiling involves the inferring of subsurface measurements based on lateral changes in electrical properties over constant subsurface, Sounding infers subsurface measurements of single location as a function of changes in petrophysical properties as function of depth (**Figure 5**). The use of either of the two modes for data collection is function of the purpose of the investigation.

4.1. Electrical resistivity

Electrical resistivity (ER) is more frequently been used as compared to other electrical techniques in groundwater investigations of which includes the characterization of aquifers. Electrical Resistivity (ER) involves the introduction of time – varying direct current (DC) or very low frequency (<1 Hz) current into the ground between two current electrodes to generate potential differences as measured at the surface with units of Ohm-meters (Ω-m). A deviation from the norm in the pattern of potential differences expected from homogeneous proffer the necessary information on the form and electrical properties of subsurface inhomogeneities.

A typical Electrical Resistivity (ER) investigation made up of a 2 – electrode system would include 2 – current electrodes and 2 – potential electrodes. As current is been injected into the ground, corresponding potential differences (ΔV) is measured. This measurement coupled with known current (I) and a geometric factor (K) that is a function of the particular electrode configuration, can be used to calculate resistivity (ρ) following Ohm's law:

$$\rho = \frac{\Delta V}{I} K \tag{4}$$

The expression in Eq. (4) for a homogeneous ground is also the same applied for heterogeneous ground; however the general term "apparent resistivity (ρa)" is substituted for resistivity (ρ) in

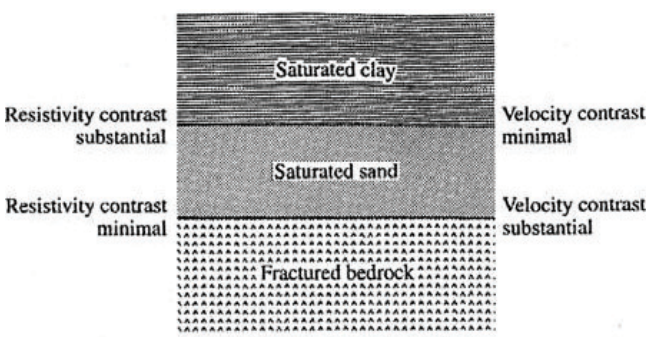

Figure 5. Schematic geological section and associated resistivity and velocity contrasts at interfaces (from Burger [2]. With permission.

Eq. (4). Apparent resistivity (ρa) is used here rather than the actual resistivity of the subsurface due to the non-homogeneity nature of the subsurface.

A four – electrode configurations is been used most commonly when it comes to measuring apparent resistivity of the subsurface. The simplest of these configurations is the Wenner configuration (**Figure 6a**) where the outer two current electrodes C_1 and C_2, apply a constant current, and the inner two potential electrodes, labeled P_1 and P_2, measures voltage difference created by this current. The electrode spacing has a fixed value a, and the apparent resistivity of the subsurface sampled by this array could be computed using the equation:

$$\rho a = \frac{\Delta V}{I} 2\pi a \tag{5}$$

Asides the Wenner array mode of electrode configuration, another commonly used electrode configuration is the Schlumberger array (**Figure 6b**), where the spacing (MN) between the potential electrodes (P_1, P_2) is much smaller as compared to the spacing (2 L) between the current electrodes (C_1, C_2).

The electrode configuration in (**Figure 6**) represents that of a dipole – dipole array where the potential electrode pair and current electrode is closely spaced, however there exist significant distances between the two sets of electrodes (**Figure 6c**) Unlike the cases of the Wenner and Schlumberger arrays, where data collected through either profiling or sounding mode depends a lot on the electrode array geometry.

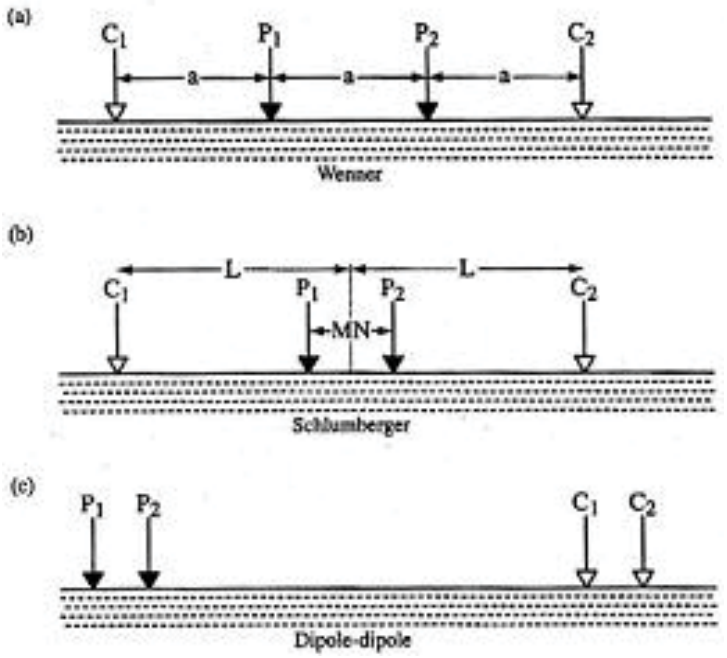

Figure 6. Common electrode configuration used to measure apparent resistivity of the subsurface C_1 and C_2 are the current electrodes and P_1 and P_2 are the potential electrodes. (a) Wenner Array (b) Schlumberger array (c) dipole – Dipole array. (from Burger [2]. With permission).

http://dx.doi.org/10.5772/intechopen.72692

To illustrate, we consider the Wenner array. Profiling involves the lateral movement of the entire array along the surface at fixed distances to obtain apparent resistivity measurements as a function of distance. The values of the measurements are assigned to the geometric center of the electrode array. Interpretation of measurements is usually with its data aimed at location of geological structures buried stream channels, aquifers or water bearing formations etc.

Sounding unlike profiling involves gradual and progressively expansion of expansion of the array about a fixed central point with current and potential electrodes being maintained at a relative spacing with depth been a function of electrode spacing and subsurface resistivity contrasts(**Figure 7a–c**). The dashed lines representing current flow lines in an homogeneous environment while bold lines represents actual current flow in single interface that separates units with different resistivities. Next we look how electrode spacing, current and its' influence on depth of penetration. In **Figure 7a**, when the electrode spacing is close, it is observed that the current only upper interface (i.e. the interface of lower resistivity). The scenario in **Figure 7b** is different; as electrode spacing has increased resulting in greater penetration depth and higher apparent resistivity values due to the influence of the lower (higher resistivity) layer. Lastly when the electrodes are farther apart, only substantial current amounts are found to flow through the resistivity layer (**Figure 7c**).

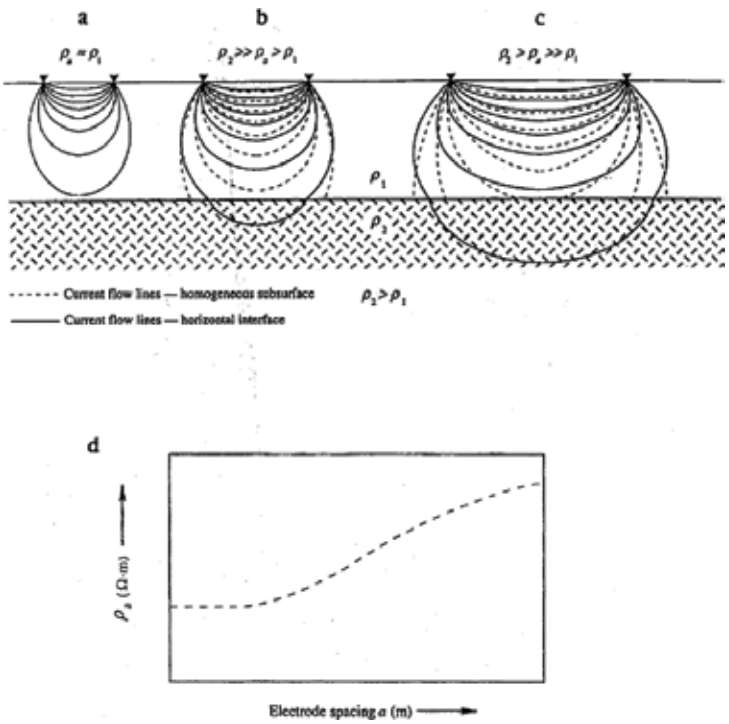

Figure 7. Effects of electrode spacing and presence of an interface on apparent resistivity measurements. The dashed lines represent current flow lines in the absence of the interface and the solid lines represent actual current flow lines (a–c) as the current electrode spacing is increased, the current lines penetrate deeper and the apparent resistivity measurements are influenced by the lower (more resistive) layer. (d) the qualitative variations in apparent resistivity as a function of electrode spacing are illustrated by the two-layer sounding curve (from Burger [2]. With permission).

The curve (**Figure 7d**) reveals qualitative variations in apparent resistivities which increases with electrode spacing, a, this curve is known as a sounding curve revealing geology of the subsurface with resistivity increasing with depth provided geology is homogeneous. However in the case where the geology is inhomogeneous it results in a complex sounding curve whose interpretation is non-unique. To interpret electrical resistivity sounding data, various curve-fitting or computer inversion schemes are used or measured and compared with model computations [1]. A classic example where both modes of data acquisition (profiling and sounding) is been used is in the location of a buried stream channel (**Figures 8a** and **6a**) using Wenner array. The contour map (**Figure 8a**) produced from resistivity measurements of several profiles collected near San Jose, CA, using an a-spacing (**Figure 6a**) of 6.1 [1, 2] reveals contours of equal apparent resistivity delineating an approximately east–west trending high apparent

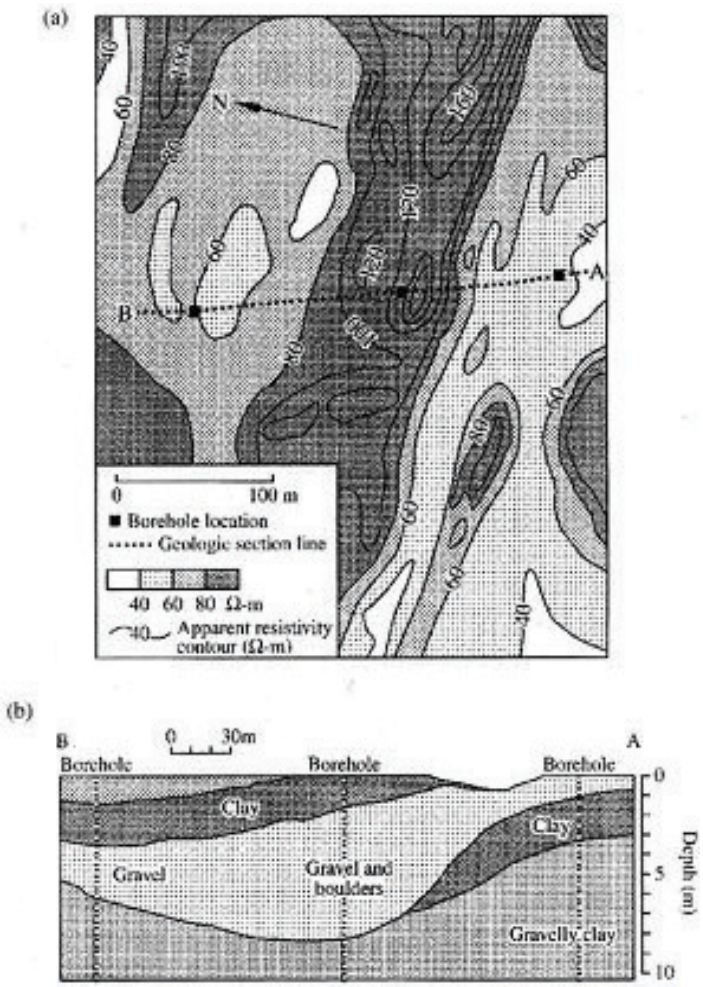

Figure 8. Resistivity survey used to delineate lateral and vertical variations in subsurface stratigraphy. (a) Contour map produced from resistivity measurements, (b) a geologic cross-section (BA) revealing high-resistivity trend in a zone of gravel and boulders that define the location of a buried stream channel (from Ref. [1] application of surface geophysics to groundwater investigations).

resistivity values. To understand the cause of high apparent resistivity values here, a geological cross-section (BA) was drawn across the map. The geological cross-section (BA) drawn is based on four expanding – spread traverses (soundings), apparent resistivity profile information and information from three boreholes whose locations are indicated on the cross-section. The critical observation of the cross-section shows that the area with high-resistivity as on the apparent resistivity map (**Figure 8b**) is a zone of gravels and boulders that defines the location of a buried stream channel (subsurface structure).

Aside the mapping of subsurface structure and stratigraphy, electrical resistivity measurements could be channeled towards the inferring lithological information and hydrogeological parameters needed for the mapping groundwater. For groundwater mapping, electrical conduction (inverse of electrical resistivity) is considered. Here the interest is the delineation of connected pore spaces, void spaces, interstices, fractures within rocks that are water filled which leads to a reduced resistivity values and high conductivity. However more information is still needed as high conductivity within rock formation or units could be due to a number of things asides water some of which includes presence of clay minerals, contamination plumes etc.

Common earth materials have wide range of electrical resistivity values revealed in **Table 1**, however some of these values are known to overlap for different earth materials. Values commonly vary over 12 orders of magnitude and have a maximum range of 24 orders of magnitude [3]. The following statements as regarding electrical resistivity holds;

- Resistivity is sensitive to moisture content; thus unsaturated sediments usually have higher resistivity values than saturated sediments.
- Sandy materials generally have higher resistivity values than clayey materials
- Granitic bedrock generally has a higher resistivity value than saturated sediments and frequently offers a large apparent resistivity contrast when overlain by these sediments.

Asides the use of sounding curves, empirical formulae have also been adapted in relating measurement of apparent resistivity with hydrological parameters of interest as this relates to aquifers. The empirical formula developed in the laboratory by Archie [4] relates these parameters:

$$\rho_r = a\varnothing^{-m} S^{-n} \rho_w \tag{6}$$

where ρ_r is the electrical resistivity of the rock, ρ_w is the pore water resistivity, $\varnothing$ is the fractional porosity, S is the fractional water saturation.

And n, a, and m are constants {$n \approx 2$, $0.6 \leq a \leq 1.0$, and $1.4 \leq m \leq 2.2$; Ward [5]}. Though Archie's law was formulated using lithified materials, Jackson et al. [6] posited its' accurate usability for unconsolidated materials also. The equation presented by Eq. (6) is used generally for well log interpretation however if ρ_r, ρ_w, and $\varnothing$ can be measured separately such that a and m are estimated reasonably then the fractional water saturation could also be inferred using electrical surveys [5]. This concept was utilized by Pfeifer and Anderson [7] to observe and monitor the migration of tracer-spiked water through the subsurface using resistivity array.

In conclusion, it could be said that the complexities that exist in the interpretation of sounding curves and the non-unique solution it gives, suggests the suitability of surface resistivity in

Material	Resistivity (ohm-m)	Dielectric Constant
Sand (dry)	10^3–10^7	3–6
Sand (saturated)	10^2–10^4	20–30
Silts	10^2–10^3	5–30
Shales	10–10^3	5–15
Clays	1–10^3	5–40
Humid soil	50–100	30
Cultivated soil	200	15
Rocky soil	1000	7
Sandy soil (dry)	7100	3
Sandy soil (saturated)	150	25
Loamy soil (dry)	9100	3
Loamy soil (saturated)	500	19
Clayey soil (dry)	3700	2
Clayey soil (saturated)	20	15
Sandstone (saturated)	25	6
Limestone (dry)	10^9	7
Limestone (saturated)	40	4–8
Basalt (saturated)	100	8
Granite	10^3–10^5	4–6
Coal	10^4	4–5
Fresh water	30–10^4	81
Permafrost	10^2–10^5	4–8
Dry snow	10^5–10^6	1
Ice	10^3–10^5	4–12

Table 1. Resistivity and dielectric constants for typical near-surface materials (data from Ref. [13]).

determined subsurface geology. Also due to its sensitivity to parameters like moisture content it's been termed a useful tool in hydrological investigations as reviewed by Ward [5], Van Nostrand and Cook [8].

4.2. Electromagnetic induction

Electromagnetic (EM) techniques as tool for geophysical exploration has dramatically increased in recent years served as a useful tool for groundwater and environmental site assessment. It involves the propagation of continuous-wave or transient electromagnetic fields in and over the earth through resulting in the generation of time-varying magnetic field. For any of such surveys to be carried out three components are essential; a transmitters, receivers, buried conductors or conductive subsurface. These three form a trio of electric-circuit coupled by an EM induction with currents been introduced into the ground directly or through inductive means by the transmitters.

The Primary field travels from the transmitter coil to the receiver coil via paths above and below the surface. Where a homogenous subsurface is detected no difference is observed between the fields propagated above, below and within the surface other than a slight reduction in amplitude. However, the interaction of the *time-varying field* with a *conductive subsurface* induces eddy currents, which gives rise to a secondary magnetic field (**Figure 9**). The attributes

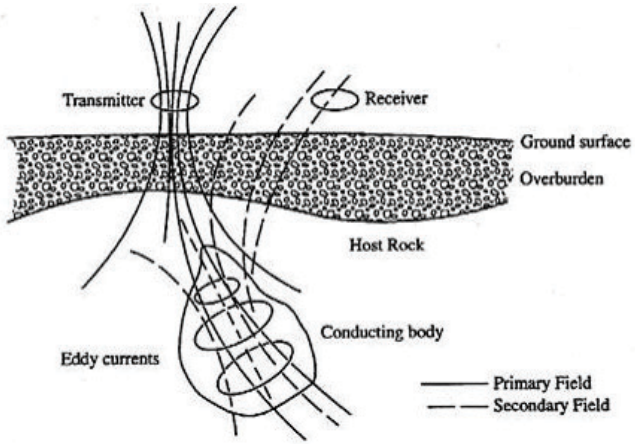

Figure 9. Electromagnetic induction technique (from Ref. [9]).

of the fields generated, such as amplitude, orientation and phase shift can be measured by the receiver coil and compared with those of the primary field as such information about the presence of subsurface conductors, or subsurface electrical conductivity distribution can be inferred.

It's paramount to recall that electrical conductivity is an inverse of electrical resistivity; as such electrical conductivity measurements made using electromagnetic methods is also dependent on subsurface texture, porosity, presence of clay minerals, moisture content and the electrical resistivity of the pore fluid presence. The acquisition of EM data requires less time, achieving greater depth of investigation than resistivity techniques. However, the equipment used are expensive and the methods used to qualitatively interpret data from EM surveys is complicated than those used in resistivity methods. This is because a conductive subsurface environment is essential to set up a secondary field measured with inductive EM methods (**Figure 9**). Electromagnetic methods as a tool for geophysical investigation and exploration is most suited for the detection of water—bearing formation (aquifers) and high – conductive subsurface target such as salt water saturated sediments.

Instrumentation could take in varying forms; but mainly consist of a source and receiver or receiver units. The source (transmitter) transmits time-varying magnetic fields with the receiver measuring components of the total (primary and secondary) field, magnetic field, sometimes the electric field and the necessary electronic circuitry to process, store and display signals [9, 10]. Data obtained from electromagnetic surveys, like their resistivity counterpart can be collected in profile and sounding mode with their information been presented as maps or pseudo-section to give a better picture of the subsurface. Acquisition, resolution and depth of investigation from this survey are been governed by mostly by conditions of the subsurface and domain of measurement.

EM surveys are divided into two domain system of measurement namely; frequency and time domain system. For frequency domain EM systems, we have the transmitter classed as either high or low frequency transmitters; high transmitter frequencies permits high- resolution investigation of subsurface conductors at near-surface or shallow depths while lower transmitter frequencies allows for deeper depth of investigation at the expense of resolution. This implies

that high frequency EM surveys yield better result for near-surface due to high resolution, however if interested in deeper subsurface investigation (low frequency EM surveys) then we have need a way around the low resolution. In the case of time domain system, secondary magnetic field is measured as a function of time, with early – time measurement being suited best for near-surface information while late- time measurement yields results of the deeper subsurface. It is paramount to note that depth of penetration or investigation and resolution is also been governed by coil configuration; while measurements from coil separations are influenced by electrical properties thus the larger coil separation investigates greater depths while smaller coil separation investigates near-surface.

Because Electrical Conductivity is related inversely to Electrical Resistivity, as such discussions relating electrical resistivity to lithology or hydrological properties can be applied in an inverse manner to measurements involving electrical conductivity. Electrical conductivity for example is higher for *saturated sediments*, clayey materials than for *unsaturated sediments* and sandy materials respectively. Some examples of investigations involving EM surveys include Sheets and Hendricks [11], who used EM induction methods to estimate soil water content and McNeill [12] that discussed the relation between electrical conductivity and hydrogeological parameters of porosity and saturation.

5. Aquifer characterization – ground waves techniques

5.1. Ground penetrating radar

Ground Penetrating Radar (GPR) as a geophysical technique is relative new and becoming increasingly popular critically understanding the events of the near-surface or shallow subsurface. Davis and Annan [13] viewed the Ground Penetrating Radar (GPR) as a technique of imaging the subsurface at high resolution using electromagnetic waves transmitted at frequencies between 10 to 1000 MHz. GPR could also be viewed as a non-destructive geophysical technique due to its successful geological applications in urban and sensitive environments. Some of these applications include the subsurface mapping of water table soils and rocks structures (e.g. groundwater channels) at high resolutions. It is similar in principle to seismic reflection profiling in however, propagation of radar waves through the subsurface is controlled by electrical properties at high frequencies.

The GPR survey system is made up of three vital components; a *transmitter, a receiver* directly connected to the *antenna* and the control unit (**Figure 10**). The transmitter radiates EM waves into the subsurface that could be refracted, diffracted or primarily reflected depending on the dielectric permittivity and electrical conductivity nature of the subsurface interfaces encountered. Recorded *radar data* received after the survey is first been observed, analyzed and interpreted by the aid of inbuilt radar processing software like RADPro, Ekko depending on the system type and make. These data are presented in form of *radargrams* which could either be presented as 2D or 3D subsurface images depending on the combination of the different axes (x, y and z) involved. Interpreting of radargrams is performed by interface mapping which is quite similar to the technique used in interpreting of seismograms. Here each band within on a radargram is presumably classed and identified as a distinct geological horizon;

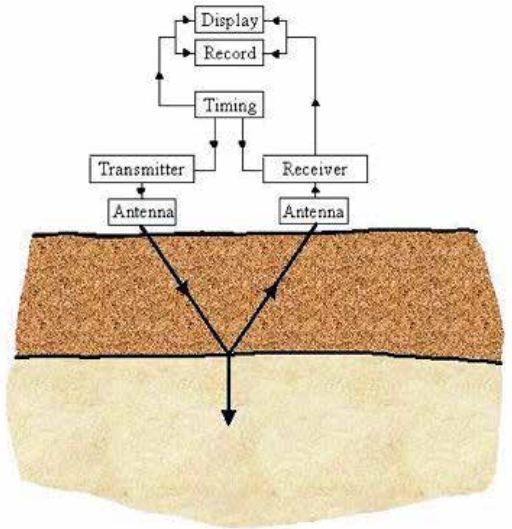

Figure 10. Flow chart for a typical GPR system (after [13]).

this would have been correct except for the effects of multiples, interference with previous reflections, noise etc. All this effects on the radargram need to be removed to correctly identify the different geological horizons and geological structures as present within the radargram as such radargram are subjected to varying radar processing operations depending on the aims, objective of the survey been undertaking through the help of inbuilt system radar processing software like RADpro, Pulse Ekko system software etc.

Processing of the radargram could be simplified by processing operations such as dewowing (removal of low frequency components), Gain Control (strengthen weaker events), deconvolution (restores shape of downgoing wave train such that primary events could be recognized more easily), Migration (useful in removing diffraction hyperbolae and restoring dips). The resultant radargram when correlated with the subsurface geology shows varying interfaces, geological structures that might be present (**Figure 11a** and **b**). Though GPR has successfully been utilized in unsaturated (non-electrically conductive or highly resistive) and saturated (electrically conductive) environment [14], however performance is higher in unsaturated (non-conductive) than in saturated (conductive) such as non-expanding clay environment such as at Savannah River Site in South Carolina [15].

The depth of penetration or investigation of GPR survey is function of the frequency of the EM waves or radar waves and nature of the subsurface material been investigated as shown in **Figure 12** for varying subsurface materials at frequencies ranging between 1 and 500 MHz. If the nature of subsurface material is highly resistive and has low conductivity then we expect a higher depth of penetration however for subsurface materials that are less resistivity and very conductive we expect low depth of penetration. Depth of penetration asides from been dependent on nature of the subsurface material (i.e. resistivity or conductivity nature) is also a function of frequencies which in turn affects resolution of subsurface imagery or radargram. Thus at low frequencies, we expect a greater depth of penetration at the expense of resolution while at high frequencies, we achieve a lower depth of penetration at higher resolution.

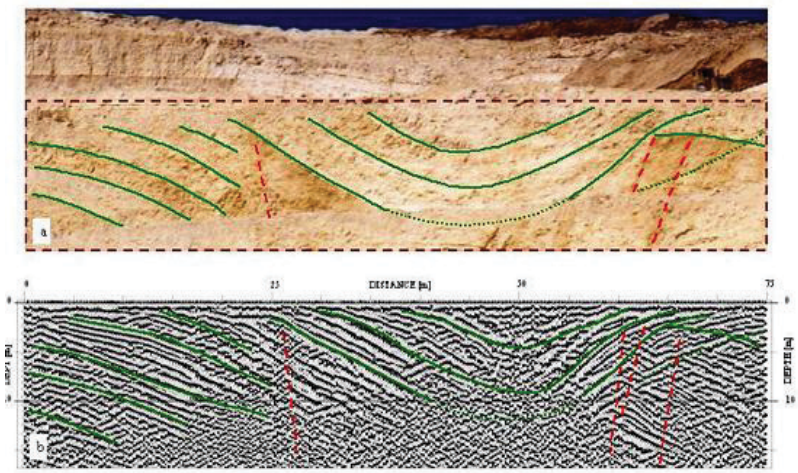

Figure 11. (A) Interpretation of a GPR profile image (B) interpretation of the prominent stratigraphic units, structures and faults.

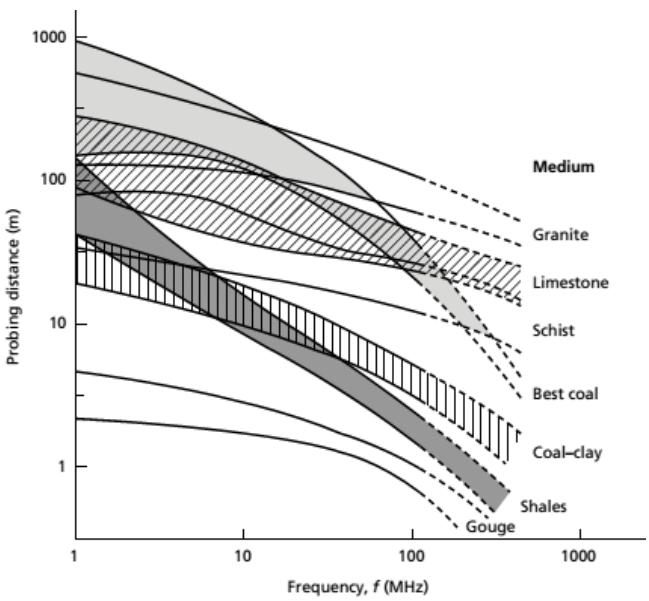

Figure 12. The relationship between probing distance and frequency for different materials (after Cook 1975).

Ground Penetrating Radar (GPR) data have been successful utilized in the hydrogeological investigations to locate the water table and to delineate shallow, unconsolidated aquifers [16].

5.2. Seismic techniques

The use of Seismic techniques in subsurface characterization is based on the propagation of elastic waves generated from a seismic controlled source, propagated through the subsurface,

boreholes, received by receivers (geophones or hydrophones) and displayed on seismographs (as a combination of waves velocities and attenuation). From these, properties of the subsurface like porosity, hydraulic conductivity, elastic moduli and water saturation which could help us better understand the subsurface could be derived.

Subsurface investigation involving Seismic techniques are categorized into three; Seismic Refraction, Cross-hole transmission (tomography) and Seismic Reflection.

With Seismic Refraction, the incident ray is refracted along the target boundary before returning to the surface (**Figure 13**). The arrival times gotten from the refracted energy are displayed as function of distance from the source with their interpretation been made manually using simple software or forward modeling techniques. The relationship between arrival times and distances could be used to obtain velocity information directly. Seismic Refraction techniques are the most

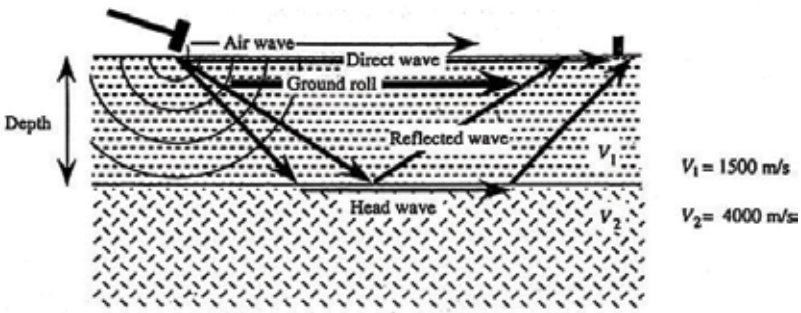

Figure 13. Major ray paths of P-wave energy (from Burger [2]).

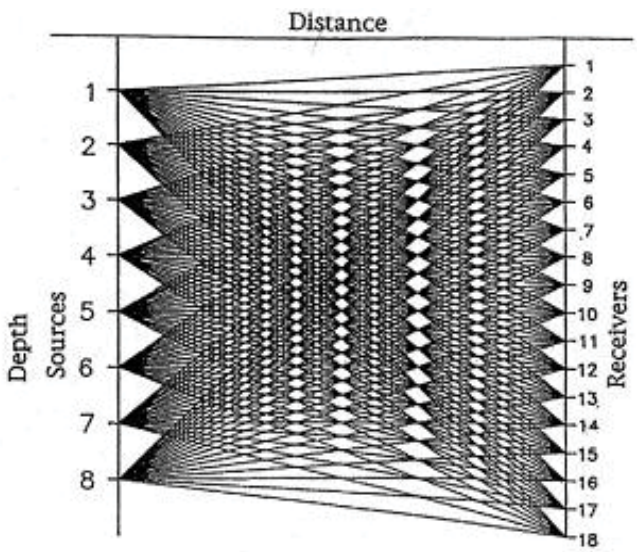

Figure 14. Cross-hole tomography geometry for seismic and radar methods. Sources and receivers are located in separated boreholes, and energy from each source is received by all geophones. Cross-holes acquisition geometries have also been used with electrical resistivity and EM methods.

appropriate for a few shallow (50 m) targets of interest, or where one is interested in identifying gross lateral velocity variations or changes in interface dip [17]. Though Seismic Refraction yields lower resolution than Seismic Reflection and Seismic Cross-hole tomographic, it is however chosen over Reflection as they are inexpensive and help to determining the depth to the water table (buried refractor) and to the top of bedrock, the gross velocity structure, or for locating significant faults. The buried refractor is usually saturated and has a greater velocity than the unsaturated equivalent soil unit and the bedrock surface [18].

Cross-hole transmission (tomography) data acquisition is possible using several techniques amongst which includes seismic techniques, electrical resistivity, electromagnetic, radar with seismic being the most common. Majority of cross – hole tomographic seismic data have been collected for research however the those collected over extremely high resolution of up to 0.5 m are better suited for site characterization. **Figure 14** shows a typical example of seismic cross-hole survey. The multiple sampling of the intra-wellbore area permits very detailed estimation of the velocity structure [19]. As seismic P-wave velocities can be related to lithological and hydrogeological parameters as discussed above, this extremely high resolution method is ideal for detailed stratigraphic and hydraulic characterization of interwell areas [20].

6. Conclusion

In conclusion, Aquifers could be classified into confined or unconfined aquifers on the basis of the presence or absence of the positioning of water table. Its characterization is a function of variations in subsurface petro-physical properties (porosity, hydraulic conductivities, and permeability) measured using geophysical techniques like electrical resistivity, electromagnetic induction, ground penetrating radar and Seismic techniques.

7. Recommendations

Having considered, what aquifers are and their characterization based on petro-physical properties of the aquifers. It is also essential to note that these properties help in selecting suitable techniques for aquifer exploration, characterization and its exploitation. However the most widely used and suitable of these techniques is the electrical methods particularly use of the electrical resistivity technique because of its speed, reliability and the fact that it is more economical in terms of use for exploration and exploitation.

Glossary

Aquifer: A permeable geological formation or body that will yield water in economical amounts.

Confined Aquifer: An aquifer overlain by an impermeable layer such that the piezometric head rises above the top of the aquifer.

Cross-hole tomographic: involves the measurement of the travel times of seismic ray paths between two or more boreholes in order to derive an image of seismic velocity in the intervening ground.

Dielectric Constant: A measure of the separation (polarization) of opposite electrical charges within a material that has been subjected to an external electrical field.

Effective Conductivity: The coefficient multiplying the expected value of the head gradient to yield the expected value of the flux.

Electrical Profiling: An electrical survey made at several surface locations using a constant electrode separation distance. Electrical profiles, also called constant spread profiles or resistivity profiles, provide information about lateral changes in apparent resistivity.

Electrical Resistivity: A measure of the ability of electrical current to flow through materials, measured in Ohm-m. Electrical resistivity is an intrinsic property of a material and is the inverse of electrical conductivity.

Electrical Sounding: An electrical survey made at a single surface location by moving electrodes progressively farther apart. Electrical soundings, also called expanding spread profiles, provide information about apparent electrical resistivity as a function of depth.

Normal Moveout Correction (NMO): Adjusting seismic or radar velocity estimates to flatten the parabolic appearance of reflectors due to offset between sources and receivers.

Radargram: A picture of the subsurface profile (graph like) representing a profile length along x-axis and y-axis or A radar image of mineral deposits or a planetary surface.

Reflection: Energy that bounces back from a surface due to a change in physical properties, such as seismic impedance in the case of sound waves resolution.

Transmitter: A transmitter is an electronic device used to produce radio waves in order to transmit or send data with the aid of an antenna during a geophysical investigation.

Receiver: A receiver is a device used to receive signals and decode signals and transform them into information the computer understands during a geophysical investigation.

Seismograms: Is an instrument used for measuring earthquake (seismic) signals which could also be adapted to be used for other geophysical investigations. These are held in a very solid position either on the bedrock or on a concrete base.

Seismic Refraction: Is a geophysical principle governed by Snell's law. Used in the fields of engineering geology, geotechnical engineering and exploration geophysics, seismic refraction traverses are performed using a seismograph(s) or geophone(s) in an array and an energy source.

Seismic Reflection: Is a method of exploration geophysics that uses the principles of seismology to estimate the properties of the earth's surface from reflected seismic waves. It's the most common geophysical methodology used for oil and gas exploration which exhibits the highest degree of technical sophistication in terms of both data acquisition and signal processing capabilities.

Unconfined Aquifer: An aquifer that has no overlying confining impermeable layer.

Author details

Salako Adebayo O[1,2]* and Adepelumi Abraham A[1,2]

*Address all correspondence to: salakoademi@gmail.com

1 Department of Geological Services, Ministry of Industry and Solid Mineral Development, Kwara State, Nigeria

2 Department of Geology, Obafemi Awolowo University, Ile-Ife, Nigeria

References

[1] Zodhy AA, Eaton GP, Mayhey DR. Applications of Surface Geophysics to Groundwater Investigations. Techniques of Water Resources Investigations of the U.S. Geological Survey, Book 2, Chapter D1; 1974

[2] Burger HR. Exploration Geophysics of the Shallow Subsurface. Englewood Cliffs, NJ: Prentice Hall; 1992

[3] Telford WM, Geldart LP, Sheriff RE. Applied Geophysics. 2nd ed. Cambridge University Press; 1990

[4] Archie GE. The electric resistivity log as an aid in determining some reservoir characteristics. Transactions of AIME. 1942;**146**:54-62

[5] Ward S. Geotechnical and Environmental Geophysics, in Geotechnical and Environmental Geophysics: Environmental and Groundwater. S.E.G. Investigations in Geophysics 5. Boca Raton, FL, U.S.A.; 1990

[6] Jackson PD, Taylor-Smith D, Stanford PN. Resistivity-porosity-particle shape relationships for marine sands. Geophysics. 1978;**43**:1250-1268

[7] Pfeifer MC and Anderson HT. CD-resistivity array to monitor fluid flow at the INEL-infiltration test. Proceedings of the Symposium on the Application of Geophysics to Engineering and Environmental Problems; Orlando, FL, April 23-26; 1995. pp. 709-718

[8] Van Nostrand RG, Cook KL. Interpretation of Resistivity Data, U.S. Geological Survey Professional Paper, PO499; 1966. 310pp

[9] Best ME. Geological Association of Canada Short Course Notes. Vol. 10. Wolfville, Nova Scotia: CRC Press LLC; Springer Ver-lag GmbH and Co. KG, May 28-29; 1992

[10] Kumar CP. Aquifer Parameter Estimation. Roorkee, India: National Institute of Hydrology; 2009

[11] Sheets KR, Hendricks JMH. Noninvasive soil water content measurement using electromagnetic induction. Water Resources Research. 1995;**31**(10):2401-2409

[12] McNeill JD. Use of electromagnetic methods for groundwater studies. In: Ward S, editor. Geotechnical and Environmental Geophysics Vol. 1: Review and Tutorial. SEG Investigations in Geophysics No. 5. Boca Raton, FL, U.S.A.; 1990. pp. 191-218

[13] Davis JL, Annan AP. Ground-penetrating radar for high-resolution mapping of soil and rock stratigraphy. Geophysical Prospecting. 1989;**37**:531-551

[14] Fisher E, McMechan G, Annan AP. Acquisition and processing of wide-aperture ground-penetrating radar data. Geophysics. 1992;**57**(3):495-504

[15] Wyatt DE, Waddell MG, Sexton GB. Geophysics and shallow faults in unconsolidated sediment. Ground Water. 1996;**34**(2):326-334

[16] Beres M Jr, Haeni FP. Application of ground penetrating radar methods in hydrogeologic studies. Ground Water. 1991;**29**(3):375-386

[17] Lankston RW. 1990. High-resolution refraction seismic data acquisition and interpretation, In: Ward S, editor. Geotechnical and Environmental Geophysics Vol. 1: Environmental and Groundwater, S.E.G. Investigations in Geophysics 5. Boca Raton, FL, U.S.A.; 45-73

[18] Sverdrup KA. Shallow seismic refraction survey near-surface groundwater flow. Ground Water Monitoring Review. 1986;**6**(1):80-83

[19] Hyndman DW, Harris JM, Gorelick SM. Capled seismic and tracer test inversion for aquifer property characterization. Water Resources Research. 1994;**30**(7):1965-1977

[20] Hyndman DW, Gorelick SM. Estimating lithologic and transport properties in three dimensions using seismic and tracer data, the Kesterson aquifer. Water Resources Research. 1996;**32**(9):2659-2670

Chapter 3

Effect of Hydrofracking on Aquifers

Abdullah Faruque and Joshua Goldowitz

Additional information is available at the end of the chapter

http://dx.doi.org/10.5772/intechopen.72327

Abstract

Geologists have understood the presence of shale gas and shale oil since the early twentieth century but always considered it unattainable due to shale's low permeability. The shale gas revolution in the USA, brought about by the combination of horizontal drilling and hydraulic fracturing, has proven the feasibility of economically accessing this resource and significantly increasing the world's proven reserve. As we enter the era of application of this technology worldwide, countries will have to weigh the promise of increased energy independence and hydrocarbon revenue against the potential damage to water supplies. Hydrofracking's voracious thirst for water and potential to pollute will impact surface water bodies and aquifers. We review the basic technique, and potentially contaminating fracking fluid additives. We examine the potential damage to water quality and the potential effect on water availability in China, Mexico, South Africa, and Algeria.

Keywords: aquifer, hydrofracking, shale gas, water resources, water

1. Introduction

Hydrofracking is a simple technique that has revolutionized oil and gas production and transformed the USA into the world's largest oil producer, and yet the technique remains controversial. Along with the promise of increased production comes the real threats of surface water and groundwater pollution. An additional threat is posed by the release of methane, a potent greenhouse gas. Modern hydrofracking combines horizontal drilling through thousands of feet of hydrocarbon-bearing rock with a formation fracturing injection of high-pressure fracking fluid. The fracking fluid is both the elixir that unlocks the tightly held hydrocarbons and the source of potential pollution. It is a mixture of millions of liters of water under extreme pressure to fracture the rock, sand grains to prop the new fractures open, lubricants to decrease friction and better deliver the pressurized water to the rock, and toxic chemicals to

prevent microbial growth. There is a worldwide debate related to the environmental impact of hydrofracking causing some countries to ban the practice, and some countries to declare a moratorium on hydrofracking. Even in the USA, where hydrofracking was invented, there are states and even counties within states that have banned hydrofracking.

One of the many risks and concerns of hydrofracking is methane releases and its impact on climate change, but the biggest concern expressed in both the popular press and scientific journals is the contamination of groundwater. One aspect of the debate related to the contamination of groundwater to be explored in this chapter in more detail is the argument that the hydrofracking is happening kilometers below the ground level, and therefore the hydrofracking layer is separated from usable aquifer layers by more than a 1000 meter of impermeable bedrock. In this chapter the authors will lay out the history of hydrofracking and the technological improvements that have optimized the process. The authors will describe the real and perceived threats to the environment and communities within the path of the hydrofracking boom.

2. History of hydrofracking technique

What is called hydrofracking in the popular vernacular is actually two technologies. It is a combination of horizontal drilling and high-volume hydraulic fracturing. The first is horizontal drilling, in which the well drills horizontally through the oil- or gas-bearing rock layer. The second is high-volume hydraulic fracturing in which highly pressurized water is used to fracture the oil- or gas-bearing rock formation and sand transported with the high-pressure water props the fractures open.

Neither is an entirely new technology. Directional drilling was used to drill for offshore oil in southern California in the 1920s. Drillers would drill vertically from an onshore location and then cause the drill bit to angle west to tap formations below the ocean [1]. From that time the technology has steadily advanced until the present day where drillers have excellent control of the depth and angle of the turn from vertical, the ultimate depth of the horizontal portion, and the 3D orientation of the drilling.

3. Purpose of hydrofracking and typical geologic targets

Horizontal drilling followed by high-volume hydraulic fracturing is an expensive, heavy technology, potentially polluting activity, so why has it become popular? Comparing the process to conventional drilling explains the overwhelming benefits of the technique in the appropriate geologic setting.

In a conventional oil or gas production setting, a well would be advanced from the ground surface vertically down through overlying sediment and rock layers and ultimately through the oil- or gas-bearing formation. Typically, the target would be an oil- and/or gas-bearing sandstone or limestone layer of rock possibly tens to hundreds of feet thick. The portion of the well casing within the hydrocarbon-rich zone would be perforated or screened. The relatively large pores in the sandstone or limestone would allow the fluid to flow toward the well.

The limits to fossil fuel production in such a well are the thickness of the formation that is screened, tens to hundreds of feet, and the ability of the hydrocarbons to flow through the solid rock. To glean natural gas or oil from a shale formation offers a unique challenge due to the size of the rock's pores. Normally, reservoir rocks have pore throat openings in the range of 2 μm or more. Hydrocarbon-rich shales have pore throat openings in the range of 0.1–0.005 μm [2].

These inherent limits on production of hydrocarbons from shale are overcome with the combination of horizontal drilling and high-volume hydraulic fracturing. In this technique, a well is drilled vertically down to a few hundred feet above the top of the reservoir rock then bored in an arc towards horizontal, then continuing as a horizontal borehole. The horizontal borehole is positioned to be somewhere in the middle of the depth of the reservoir rock and extended thousands of feet horizontally through the formation. The entire length of the horizontal borehole through the reservoir rock will eventually be screened and open for hydrocarbon flow. To overcome the low pore size and porosity of the shale, portions of horizontal well casing will be perforated, and then the rock surrounding the well bore will be fractured using high-pressure water. The fracturing creates interconnected secondary porosity that allows hydrocarbons to flow toward the thousands of feet of horizontal well. This combination of horizontal drilling and high volume hydraulic fracturing is what has converted shale gas into a recoverable resource.

4. Effect of hydrofracking in the USA and worldwide oil and gas proven reserve

The rapid rise of combined horizontal drilling and high-volume hydraulic fracturing has opened up large, previously unavailable natural gas and oil resources within the lower 48 states of the USA. The opening-up of unconventional "tight gas" formations to exploration and production has greatly increased estimates of technically recoverable US shale gas reserves. Geologists at the US Geological Survey, US Energy Information Administration, as well as in academic settings and energy producers have known the vast natural gas resource locked within the tight shale formations. It is only with the development of horizontal drilling and the perfection of hydrofracking that portions of this resource have been converted to proven reserves, that is, portions of the resource that are able to be economically extracted. **Figure 1** shows the increase in shale gas as a percentage of all natural gas produced in the USA between 2000 and 2015 and indicates the dramatic rise from less than 3% of US natural gas production in 2003 to over 65% of US natural gas production in 2015.

The technological revolution that has increased US natural gas production in the USA has spilled over into and dramatically increased US oil production as well. Oil exploration and extraction are a mature industry in the USA, having begun in the 1860s. US oil production, as well as US proven reserves, had been in a long-term steady decline since 1970. That decline was reversed in 2008, and since 2014 more than half of the oil production in the USA comes from hydrofracked wells. In fact US oil production increased from under 5 million barrels per day in 2008 to over 9 million barrels per day in 2015, and the US Energy Information Administration projects that US oil production will reach 10 million barrels per day by 2018 [3].

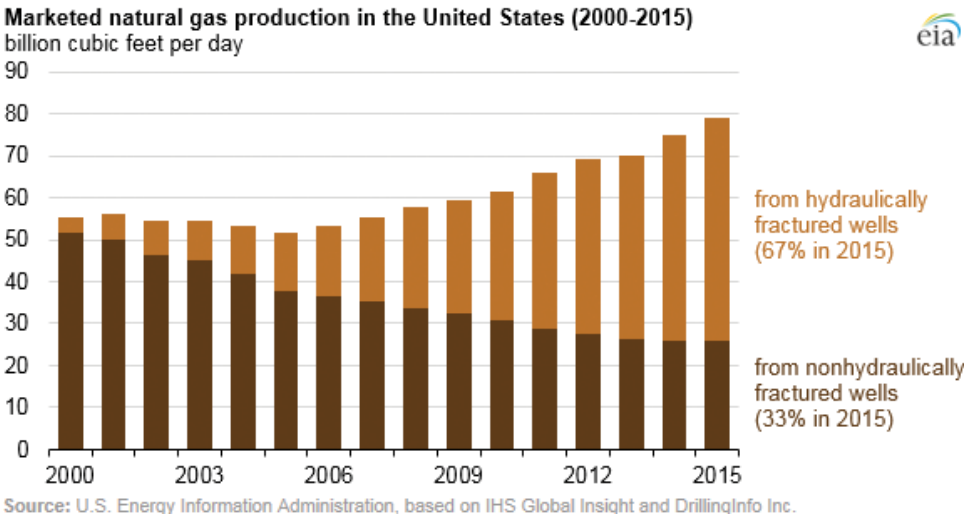

Figure 1. Natural gas production in the USA in billion cubic feet per day (2000–2015) [5]. Conventional gas shown in dark shading and shale gas shown in light shading.

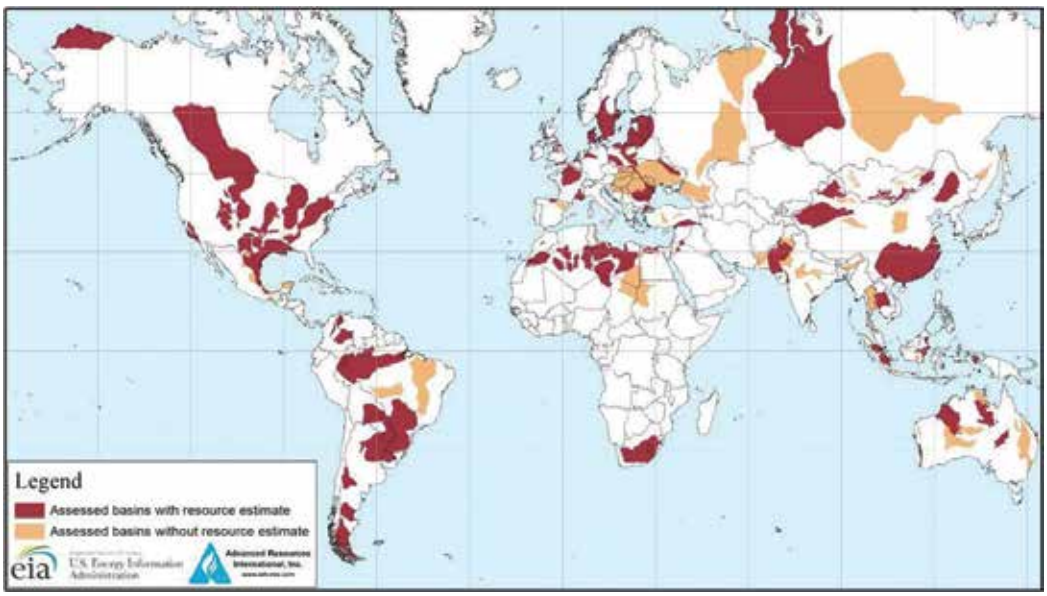

Figure 2. Basins with assessed shale oil and shale gas formations [6].

The technological revolution that has transformed the oil and gas proven reserve and production story in the USA is beginning to affect production worldwide. The US Energy Information Administration has found that tight shale gas and tight shale oil resources are distributed around the world (**Figure 2**).

Rank	Country	Shale oil (billion barrels)		Rank	Country	Shale gas (trillion cubic feet)	
1	Russia	75		1	China	1,115	
2	U.S.[1]	58	(48)	2	Argentina	802	
3	China	32		3	Algeria	707	
4	Argentina	27		4	U.S.[1]	665	(1,161)
5	Libya	26		5	Canada	573	
6	Australia	18		6	Mexico	545	
7	Venezuela	13		7	Australia	437	
8	Mexico	13		8	South Africa	390	
9	Pakistan	9		9	Russia	285	
10	Canada	9		10	Brazil	245	
	World Total	345	(335)		World Total	7,299	(7,795)

[1]EIA (Energy Information Administration) estimates used for ranking order. ARI (Advanced Resources International) estimates in parentheses.

Table 1. Top 10 countries with technically recoverable shale oil and shale gas resources [6].

Countries with the highest technically recoverable tight shale oil and shale gas, as shown in **Table 1**, are found on every inhabited continent. The US Geological Survey has estimated that the technically recoverable shale gas represents a 47% increase in the world's total technically recoverable natural gas and that the technically recoverable shale oil represents an 11% increase [4]. The capital and know-how intensive hydrofracking revolution has only begun in a handful of countries, most notably China, Argentina, Mexico, and Algeria.

5. Aquifers and water resources: hydrofracking's threat to water quantity and water resources

In terms of aquifers, hydrofracking presents two threats: it uses too much water, and the water it uses becomes polluted and unfit for any other use. This section will address the threat hydrofracking poses to water resources due to imposing a new demand on already stretched water resources. Hydraulic fracturing as a technology is well known as a water hog. The volume of water used per well depends on the length of the horizontal borehole and the formation, but it is not unheard of for a single well to use 20 million liters. This is a consumptive use of water, in that once the hydrofracking chemicals are added and the water is injected into the subsurface, it cannot be reused. For perspective, consider that 20 million liters of sufficient water to meet the basic needs and few health concerns arise for approximately 200,000–400,000 people, according to the World Health Organization [7]. And, that is just the water used for a single well!

As with the most water resource problems, the geographic distribution of available water resource and water need may not align. A look at the hydrofracking experience in the USA is illustrative. Some shale gas formations underlie areas of abundant water, such as the Marcellus shale and Utica shale in the Northeastern USA. This area is well supplied with rivers, lakes, and abundant groundwater. The area is humid and receives on the order of 100 cm of precipitation annually. In contrast the Uinta-Piceance Province in Colorado, located in the Western USA,

is located mainly in an area of high desert. The waters of the Colorado River are already over allocated, yet energy companies have secured over a million acre-feet (1.25 billion cubic meters) of water rights. Many of the shale gas formations poised to make a significant contribution to the world's natural gas production are also found in areas already experiencing water stress.

The World Resources Institute reports that China, India, Pakistan, Mexico, and South Africa are among the top 20 countries in the world in terms of shale gas potential, but each may have insufficient unallocated water to develop this resource [8]. Currently, farmers in China, India, and Pakistan use tube wells and electric pumps to pull 400 billion cubic meters of groundwater out of aquifers annually. This volume exceeds recharge by an estimated 170 billion cubic meters per year [9]. The three countries combined are responsible for more than half of the world's agricultural use of groundwater. Water is in such short supply near major cities in parts of Asia that untreated sewage is used to irrigate crops. It is estimated that a quarter of all of Pakistan's vegetables are irrigated with sewage. These are not countries with excess water waiting to be used for hydrofracking! **Table 2** lists 20 countries with the largest technically recoverable shale gas resources by average exposure to baseline water stress over shale play area.

If a significant shale gas resource exists in a water short area, the problem is likely not that there will be insufficient water to develop the lucrative natural gas resource. The problem is more likely that the water for hydrofracking will be diverted from some of the use. There will be winners and losers.

One country to consider is China. It is estimated that China has twice the shale gas resource of the USA, over 1100 trillion cubic feet. This is enough to be a significant factor in China's transition toward a cleaner energy future. China currently uses coal to provide 62% of its total energy output [10]. It has been said that shale gas on its worst day is better than coal on its best day; so to any extent possibility, a transition from coal to shale gas could be a positive development. Shale gas, photovoltaics, and wind power will likely all be part of the mix used to wean China away from coal as it strives to meet its obligations under the Paris agreement.

China is the world's most populous country. In his book *When the Rivers Run Dry*, Fred Pearce states that "If northern China were a separate country it would be one of the most water-stressed in the world." The World Bank estimates that China has already lost 14 billion dollars in industrial production due to water shortages. More than a quarter of China's landmass is already a desert. The Gobi, the fastest-expanding desert on earth, grows toward Beijing at a rate of 2 miles per year. It has been estimated that the country lost more than 6% of its farmland to desertification between 1997 and 2008 [11].

Extremely high	High	Medium to high	Medium to low	Low
Pakistan (105)	China (1115)	USA (567)	Argentina (802)	Australia (437)
	Mexico (545)	Paraguay (75)	Canada (573)	Russia (287)
	S. Africa (390)		Poland (148)	Brazil (245)
	India (96)		France (137)	Venezuela (167)
			Ukraine (128)	Columbia (55)

Estimated shale gas in trillion cubic feet in brackets. Data source: [8].

Table 2. Baseline water stress over shale play area.

http://dx.doi.org/10.5772/intechopen.72327

Some of China's potential shale gas fields underlie areas already experiencing water stress. The statement of [12] indicates that fracking in the Sichuan Basin will compete with domestic water needs in an area that is already water stressed, but the specter of additional desertification and diversion of water for hydrofracking has not deterred multinational oil and gas companies. Chinese energy companies Sinochem, Sinopec, and CNOOC have invested in US shale gas operations such as Chesapeake Energy partly to gain access to hydrofracking experience. Major western energy companies including ExxonMobil and Chevron have initiated joint ventures in Chinese shale gas. The US shale gas boom in formations such as the Bakken in Texas and the Marcellus in Pennsylvania has taken place in nearly horizontal, relatively shallow formations. Many of China's most promising formations are deeper and in more complex geology, indicating that it will take even more water per well to successfully frack the formations [13].

Figures 3 and **4** show current water scarcity in China and shale gas plays in China, respectively. Development of shale gas basins in the northern area in particular will compete with other uses for scarce water. Both the Bohai Bay Basin and the Ordos Basin are found in areas already classified as under extreme water scarcity. Population will grow, industry will expand, and agriculture will struggle to keep up with growing food demand; each of these areas will continue to be at least as water short as they are presently.

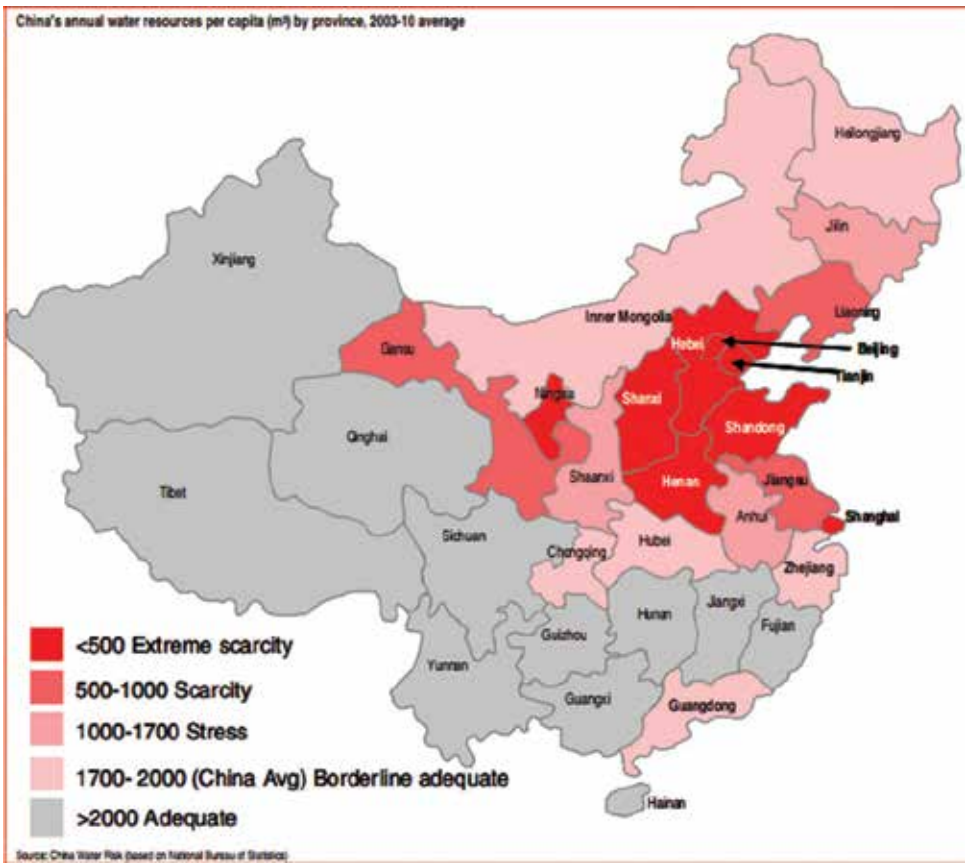

Figure 3. China's annual water resources per capita (m^3) by province (2003–2010 average) [15].

Figure 4. China's shale gas distribution [16].

A rather extreme case of competition between current water demand and the coming demand from hydrofracking is illustrated by Algeria. Algeria is estimated to have the third largest reserve of technically recoverable shale gas in the world, after China and Argentina. Its two significant shale gas formations are the Frasnian Shale and the Tannezuft Shale. These are found in multiple basins throughout the southern portion of the country [14]. Algeria is dependent on domestic gas production for energy. More than 60% of Algeria's energy needs are currently met with domestic production of conventional gas, but the output has been declining. Algeria will not be able to leave the shale gas in the ground.

Few countries on earth are as dry as Algeria. Over 80% of the country is located within the Sahara desert. Only the northern coastal portion of the country is temperate, but it becomes hotter and dryer away from the coast and the coastal mountains. The majority of the country located above the shale gas formations receives little to no rainfall. Annual precipitation is less than 10 cm per year for the majority of the country. Except for the coastal area, all surface water is ephemeral, with wadis draining to sebhkas—closed internal basins with high evaporation [17].

Figure 5 shows annual precipitation in Algeria. **Figure 6**, showing the location of shale gas basins in Algeria, indicates that all of the resource exists in areas of the country that receive less than 10 cm of precipitation annually. The population away from the coastal areas is entirely dependent on water pumped from deep aquifers. In that there is no recharge, they are essentially mining their non-renewable groundwater from aquifers below the Sahara. The aquifers used for water supply include moderate to high permeability unconsolidated material, sedimentary rock layers, and karst rock layers.

http://dx.doi.org/10.5772/intechopen.72327

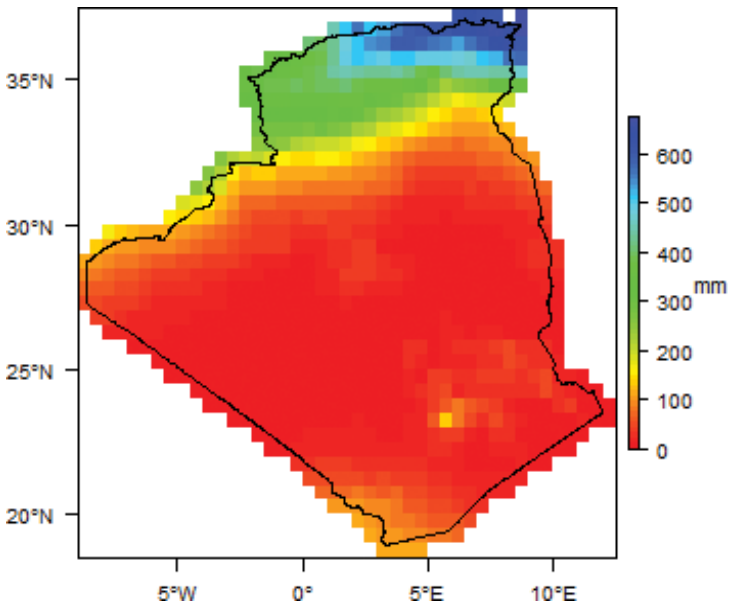

Figure 5. Annual precipitation in Algeria [17].

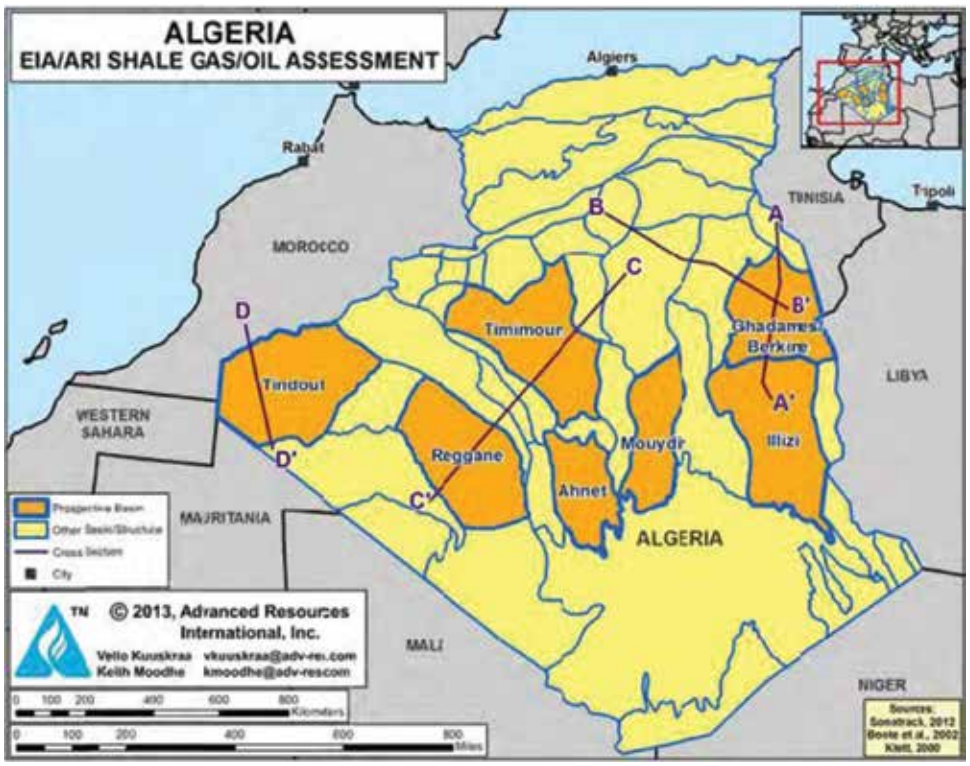

Figure 6. Location of shale gas basins in Algeria [14].

Algerians concerned for their water resources have already staged demonstrations and sit-ins. Their concerns range from water availability to pollution from fracking. Algerians living in areas above shale gas reserves rely on sole source aquifers, that is, aquifers that are their only source of drinking water, so their fears are well justified.

Another country where concerns over water availability (**Figure 7**) for hydrofracking are real and justified is Mexico. Mexico is the eleventh most populous country on earth, with over nearly 125 million people. Mexico has the second largest economy in Latin America after Argentina. Petroleum was discovered in Mexico in the nineteenth century, and production and export began in the 1890s. Petroleum has played a major part in the economy since at least 1980 and currently contributes about 35% of the country's GDP (CIA). It is estimated that Mexico has nearly 600 trillion cubic feet of shale gas, the sixth largest in the world.

Mexico is an arid country with large and growing water shortage issues. The Sonoran Desert and the Chihuahuan Desert are both found in the northern part of the country. The water shortage in 2012 led to failure of pasture land and the starvation of some 350,000 heads of cattle in the northern state of Chihuahua [18].

In some areas development of Mexico's shale gas resource (**Figure 8**) could be limited by water availability, or water already allocated to irrigation and human needs could be in danger of being diverted. Mexico's shale gas is found in the Burgos Basin and Sabinas Basin in the relatively dry north and in the Tampico and Veracruz basins along the Gulf of Mexico (shaded in orange) (**Figure 8**). The Burgos is an extension of the Eagle Ford Formation that has been so successfully developed in Texas (**Figure 8**). The western portion is the La Casita area shown on straddles the Chihuahuan desert.

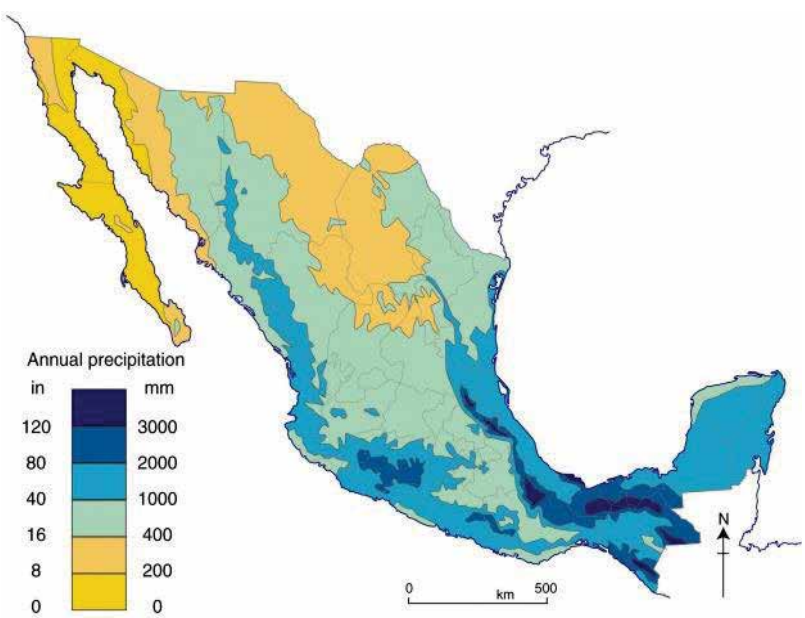

Figure 7. Annual precipitation in Mexico [19].

http://dx.doi.org/10.5772/intechopen.72327

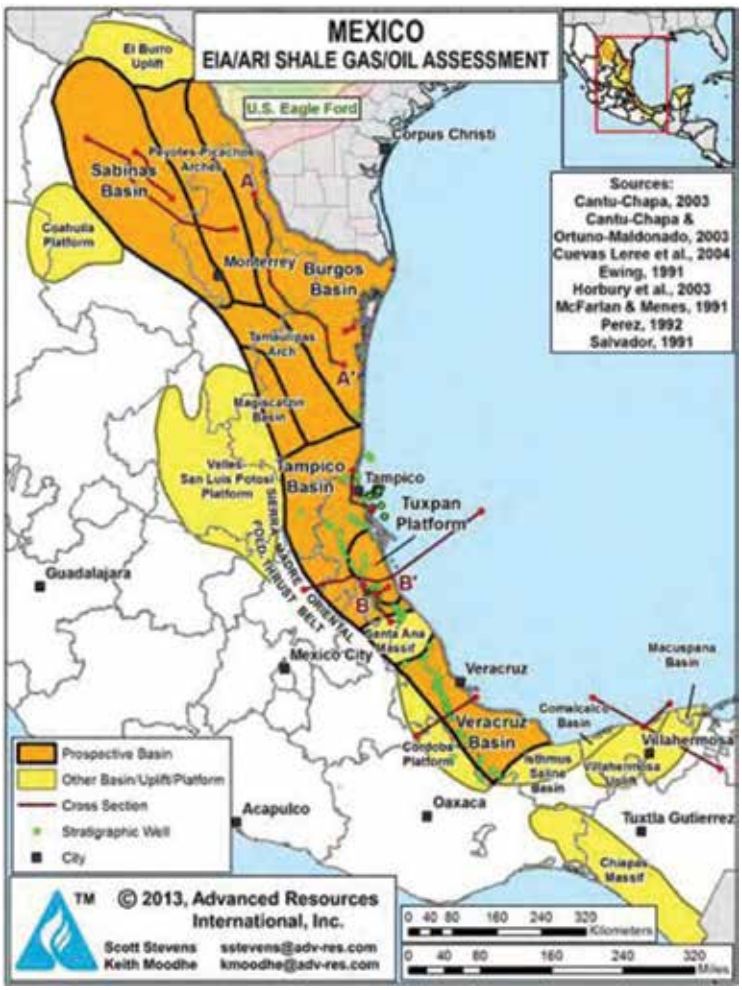

Figure 8. Location of shale gas basins in Mexico [14].

The Burgos and Sabinas lie below the watershed of the Rio Grande, a river system that drains one-tenth of the US territory and 40% of Mexico. The flow of the Rio Grande is used entirely for irrigation and dries entirely during the summer months [9]. Agriculture in the area is increasingly dependent on groundwater pumping, and fields are being abandoned due to salt buildup. Less than 500 cubic meters of water per person per year is available in the Rio Grande watershed. Clearly, supplying millions of liters of water for each hydrofracked well will have dire water resource consequences.

South Africa, located on the southern tip of the continent, is the 26th largest country in the world and the 25th most populous one. It is a developing country, with a GDP per capita near the world median [20]. Petroleum production has played little to no role in the county's economy to date. It has been estimated that the Karoo Basin hold as much as 13 trillion cubic feet of shale gas [21].

South Africa is a relatively dry country, with more than half of the country classified as hot desert, cold desert, hot semiarid, or cold semiarid. Demand exceeds reliable yield in 11 of

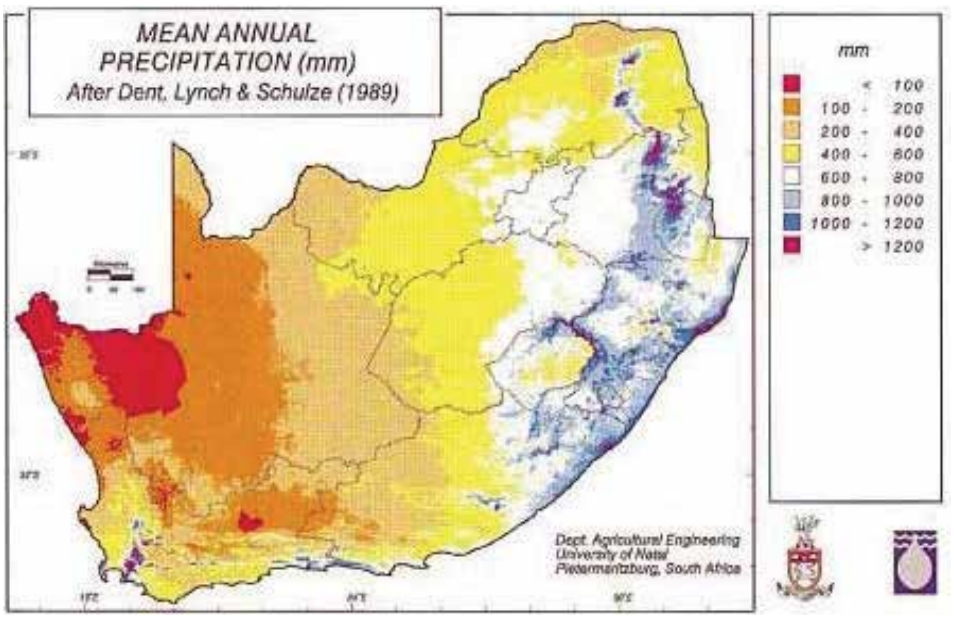

Figure 9. Annual precipitation in South Africa [22].

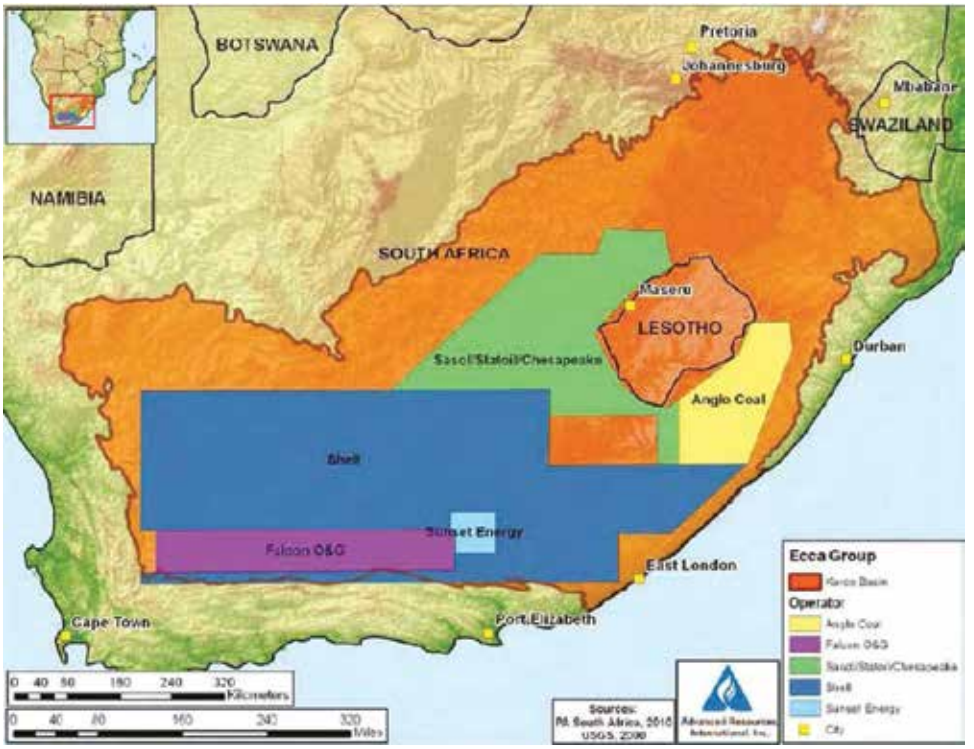

Figure 10. Location of shale gas basins in South Africa [14].

the country's 19 water management areas. The Orange and Limpopo watersheds cover the areas of potentially recoverable shale gas. These watersheds can supply only 500 to 1000 cubic meters of water per person on an annual basis. Nearly all groundwater in the shale gas areas is already under license for use. The proximity of the shale gas areas to low precipitation regions of South Africa can be seen in **Figures 9** and **10**.

South Africa already struggles to supply water to agriculture, domestic use, and industry. Growing population and an increase in standard of living will continue to increase the growth in demand. Much of the population in areas overlying South Africa's shale gas resources is fully dependent on groundwater.

6. Aquifers and water resources: hydrofracking's threat to water quality

Hydraulic fracturing may seem like a simple and straightforward process until one becomes aware of the complex chemistry of the fracking fluid and the necessary complexity based on the number of problems that must be overcome. One way to understand the chemical additives is to consider the problems that must be overcome to fracture thousands of feet of source rock located thousands of feet underground.

6.1. Problem 1: fracturing the rock

The main challenge of hydraulic fracturing is to create deep fractures in solid rock that is confined by the pressure associated with great depth. To accomplish this water is forced at high pressure through perforations in the well pipe. Pressures can be as high as 15,000 psi. In a horizontal well that is thousands of meters long, the fracking process is accomplished in multiple shorter sections.

This process uses vast quantities of water. In the USA it has been found that some wells use as little as 10,000 liters, but more typically wells are using in the range of 1 to 10 million liters, with some wells using more than 35 million liters. More important than the water use itself is the fact that the water use is consumptive, in that most of the water used to hydrofrack a well is lost within the fracked formation. The water that does return to the surface through the production well is too contaminated to be reused.

The water is only able to fracture rock if it is delivered at extremely high pressures. Pumps at the surface must not only pressurize the water but also deliver that pressure vertically and then horizontally through thousands of feet of pipe to the portion of the formation being fractured. This involves overcoming the frictional resistance to flow. This could not be accomplished without chemical friction reducers. Currently, organic polymers are most often used, but historically petroleum distillates were the friction reducer of choice.

6.2. Problem 2: keeping the fractures open

Hydrofracking generally is used on deep targets, usually at least a kilometer below the ground surface. If hydrofracking was done with water alone, the newly created fractures would

collapse as soon as the applied pressure decreased due to the weight of the overlying rock. Hydrofrackers use proppants to prop the fractures open. Proppants need to be strong enough not to fracture or be crushed during the fracking process or during the producing life of the well. By far the most common proppant used in the USA to date is so called "white" sand. White sand is high-purity silica sand with few other minerals. This gives the sand its light color and relatively uniform chemical and physical properties. Prior to use the sand is washed and sieved to produce a more uniform size distribution. Multiple sizes are used, with smaller particles injected first to infiltrate farthest into the newly fractured bedrock and larger sand particles used near the end of the process to better match the larger aperture near the well. The volume of sand used in the hydrofracking industry is considerable. The US Geological Survey reports that sand and gravel production in the USA more than doubled between 2010 and 2014, with more than 70% of the total 2014 sand production being used by the hydrofracking industry! [23].

Sand is not the only proppant. Ceramic proppants of various formulations allow for a more uniform manufactured proppant with specific beneficial properties. Ceramic proppant can be manufactured with properties that make them better than sand, such as higher sphericity, more uniformity of size, and more crush resistant. Formations hydrofracked with ceramic proppants have higher conductivity than those propped with sand. Many other materials have been used as proppants including resin-coated sand, resin-impregnated crushed walnut shell, and thermoplastics.

Proppants by their nature are inert and nonpolluting, but not without environmental impact. The landscape of rural Wisconsin is being transformed by mines that provide roughly 9000 truckloads of fracking sand per day [24].

6.3. Problem 3: keeping everything in solution

Sand or ceramic proppants are more than twice as dense as water. Gelling agents and crosslinking polymers are added to the fracking fluid to increase the water's density and help keep the proppants suspended. Various guar formulations are the typical gelling agents. This is the same plant-based material seen as an emollient on processed food. Other plant-based gelling agents are used as well.

6.4. Problem 4: keeping the propped fractures open for flow

The polymers and organic material described in Sections 6.1 and 6.3 keep proppants in solution, adjust the water's density, and decrease friction, making fracking possible. These same chemicals can then restrict the flow of natural gas out of the formation by clogging the newly created fractures and lowering the conductivity of the fractured rock. Therefore, an additional additive breaks these chemicals up into smaller molecules that will not clog the fractures. These "breakers" are usually enzymes that cut the organic chemicals into smaller pieces.

6.5. Problem 5: preventing corrosion, scale, etc.

Additional chemical additives include pH adjusters, corrosion inhibitors, clay stabilizers, scale inhibitors, and metal precipitation inhibitors that are added to the hydrofracking fluid. In general these prevent mineral precipitates and particulates from clogging fractures and inhibiting flow in the well.

http://dx.doi.org/10.5772/intechopen.72327

6.6. Problem 6: preventing bacterial proliferation

Many of the additives in hydrofracking solution, including the breaker, surfactant, gelling agent, cross-linkers, surfactants, and friction reducers, are organic chemicals. All of these are substrates for microorganisms to feed on. Proliferation of microorganisms creates biomass. The biofilm on surfaces made up of living and dead microbes can lower porosity and gas permeability by lowering the fracture aperture. This is the same effect seen in bioremediation of aquifers where the stimulation of the native flora choke off conductivity. Biocide is added to fracking fluid to prevent this counterproductive effect.

Among all the chemicals used to formulate hydrofracking fluid, it is the biocides that are of most concern for water quality. Fewer than 20 biocides have been identified as more or less commonly used in the hydrofracking industry. Among the most common are glutaraldehyde, dibromonitrilopropionamide (DBNPA), tetrakis(hydroxymethy)phosphonium sulfate, and chlorine dioxide [25]. These biocides are toxic to microorganism, and some are quite toxic to aquatic fauna. They have low toxicity for mammals. Although they are not acutely toxic to mammals, some are toxic during long-term exposure or possess carcinogenicity or mutagenicity.

How do these hydrofracking chemicals get into the hydrosphere, and how do they become a threat to water resource quality? Chemicals must be transported to the site by rail or truck so accidents are of course a threat to surface water quality. Hydrofracking fluids are generally mixed on site and stored in railroad tank cars or in lined storage lagoons. It is not uncommon for lagoons lined with geotextile to leak at the geotextile seams or from punctures, so this could be a threat to shallow aquifers.

Once fully mixed hydrofracking fluid is injected into the target formation. Fluids travel first down through the vertical well and then into the horizontal portion being hydrofracked. Improperly cased and grouted wells could leak into shallow aquifers during high-pressure injection of the fracking fluid. Hydrofracking opponents in the USA have claimed that hydrofracking of shale gas formations can cause fractures to extend upward from the target shale formation, allowing fracking fluid to reach freshwater aquifers above. This is likely not a realistic fear. Freshwater aquifers are generally found within a few hundreds of meters of the ground surface. Shale gas formations that could be subject to hydrofracking are generally found thousands of meters below the ground, and the pressures used to hydrofrack are incapable of creating fractures of the length that would be required to reach a freshwater aquifer. It is possible however for hydrofracking fluid to flow upward through existing faults or abandoned wells.

There have been wide ranges reported, but between a quarter and half of the hydrofracking fluid injected to break the shale returns to the surface as flow-back subsequent to the frack. This hydrofracking fluid wastewater returns to the surface to the wellhead where it is collected. Wastewater can be treated onsite, treated offsite, treated and reused as hydrofracking fluid, or disposed of in a deep brine aquifer. This presents a number of additional opportunities for pollution of surface water or aquifers.

Hydrofracking wastewater that is treated offsite or treated and reused as hydrofracking fluid must be transported and so again poses the threats associated with transporting chemical-laden water. Wastewater treated onsite and then disposed of to a surface water body may not be sufficiently treated and could still contain some chemicals not removed by the

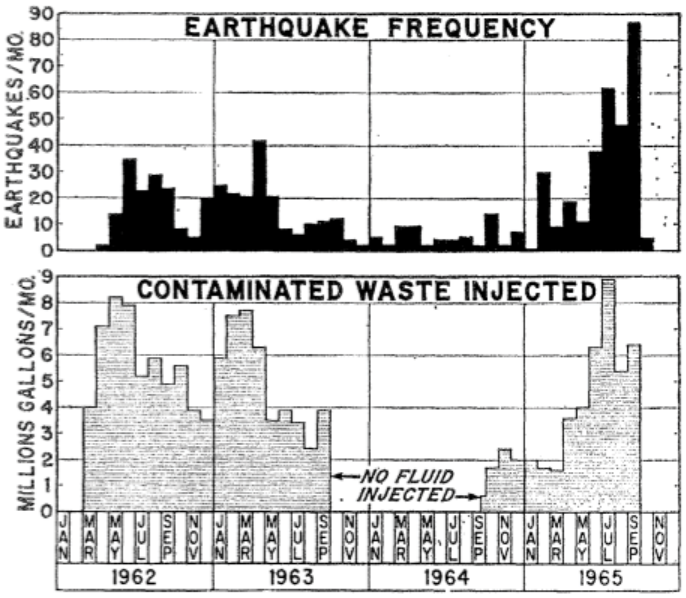

Figure 11. Correlation between the number of earthquakes and the volume of fluid injected [26].

treatment process. Injecting wastewater into a deep brine aquifer again presents the hazard of leakage from improperly cased or grouted wells.

Hydraulic fracturing operations cause earthquakes. The USGS has reported a sharp increase in the number of potentially damaging earthquakes, those with a magnitude of three or larger in the Central and Eastern USA due to hydrofracking operation. There has been a 50-fold increase in M3+ quakes from an average of roughly 20 per year to over a thousand in 2015.

The realization that high-pressure injection of fluids into the deep subsurface can cause earthquakes is not new. In 1967 David Evans, a consulting geologist in Colorado, noted a correlation between injection volumes at a US Army hazardous waste injection well located at the Rocky Mountain Arsenal and earthquake frequency. His figure showing the correlation (**Figure 11**) became a staple of college-level geology textbooks. It was determined that the injection of wastes into the nearly 4000 feet deep well decreased frictional resistance to faulting. "The mechanism by which the fluid injection triggered the earthquakes is the reduction of frictional resistance to faulting, a reduction which occurs with increase in pore pressure" [26]. Disposal of waste fluids by injection into a deep well has triggered earthquakes near Denver, Colorado [26].

It should be obvious to all readers that the injection of millions of gallons of highly pressurized hydrofracking fluid into each well contributes to the notable increase in induced seismicity reported by the US Geological Survey. Less obvious is the reinjection of brine wastewater that is produced from the formation along with the hydrocarbons after hydrofracking.

7. Conclusion

So, should we hydrofrack? On the positive side of the ledger, we need resources for an energy-hungry world. Although the Paris accords require countries to limit greenhouse gas emissions worldwide, fossil fuel consumption will continue to increase for decades. Also, on the positive side is that as we increase shale gas usage we have the opportunity to decrease the usage of coal for electricity production. Also, on the positive side of the ledger is the fact that shale gas production and export provide hard currency for exporting countries, some of which are in the developing world.

There are also significant considerations on the negative side of the ledger. It is an unassailable fact that hydrofracking will consumptively use vast volumes of freshwater, and a great deal of that usage will occur in regions already short on water resources. Pollution of water resources both in surface water and in aquifers due to hydrofracking is a reality. If we could hydrofrack the world's shale gas resource without human error, without equipment failure, and without any shortcuts taken to increase profits, then our freshwater resources would likely be safe from chemical pollution due to fracking!

Also, on the negative side of the ledger is the fact that methane is a significantly more potent greenhouse gas than carbon dioxide. Methane leaks during drilling, production, transportation, processing, distribution, and usage, and the effect these will have on the environment should be considered. Climate change caused by methane leaks will affect precipitation, surface water availability, and ultimately the recharge of our aquifers.

We will develop our shale gas resource through the marriage of horizontal drilling and high-volume hydrofracking. The shale gas is simply too valuable and too tempting to leave in the ground. It is reasonable to accept that hydrofracking will have a negative effect on water availability and water quality.

Author details

Abdullah Faruque[1]* and Joshua Goldowitz[2]

*Address all correspondence to: aafite@rit.edu

1 Civil Engineering Technology, Rochester Institute of Technology, New York, USA

2 Environmental Sustainability Health and Safety, Rochester Institute of Technology, New York, USA

References

[1] Shooters – A "Fracking" History. American Oil and Gas Historical Society [Internet]. 2017. Available from: https://aoghs.org/technology/hydraulic-fracturing/ [Accessed: October 22, 2017]

[2] Nelson PH. Pore-throat sizes in sandstones, tight sandstones, and shales. The American Association of Petroleum Geologists (AAPG) Bulletin. March 2009;**93**(3):329-340. DOI: 10.1306/10240808059

[3] Kilian L. The impact of the shale oil revolution on U.S. oil and gasoline prices. Review of Environmental Economics and Policy. July 1, 2016;**10**(2):185-205. DOI: 10.1093/reep/rew001

[4] Klett TR, Cook TA, Charpentier RR, Tennyson ME, Le PA. U.S. Geological Survey Assessment of Reserve Growth Outside of the United States. Scientific Investigations Report 2015-5091. U.S. Geological Survey, Reston, Virginia. DOI: 10.3133/sir20155091.pdf. Available from: https://pubs.usgs.gov/sir/2015/5091/sir20155091.pdf [Accessed: October 22, 2017]

[5] Hydraulically fractured wells provide two-thirds of U.S. natural gas production. U.S. Energy Information Administration (USEIA). Today in Energy, May 5, 2016. [Internet]. 2016. Available from: https://www.eia.gov/todayinenergy/detail.php?id=26112 [Accessed: October 22, 2017]

[6] Shale oil and shale gas resources are globally abundant, U.S. Energy Information Administration (USEIA), Today in Energy, February 1, 2014. [Internet]. 2014. Available from: https://www.eia.gov/todayinenergy/detail.php?id=14431 [Accessed: October 22, 2017]

[7] Ki-moon B. The Human Right to Water and Sanitation – The United Nations Media Brief. Available from: http://www.un.org/waterforlifedecade/pdf/human_right_to_water_and_sanitation_media_brief.pdf [Accessed: October 22, 2017]

[8] Reig P, Luo T, and Proctor J N. Global Shale Gas Development: Water Availability and Business Risks. Available from: http://www.wri.org/sites/default/files/wri14_report_shalegas.pdf [Accessed: October 22, 2017]

[9] Pearce F. When the Rivers Run Dry: Water – The Defining Crisis of the Twenty-First Century. Boston, MA, USA: Beacon Press; 2006. 336 p. ISBN-13: 978-0-8070-8573-8

[10] Lin A. Understanding China's New Mandatory 58% Coal Cap Target. Natural Resources Defense Council (NRDC). March 17, 2017. Available from: https://www.nrdc.org/experts/alvin-lin/understanding-chinas-new-mandatory-58-coal-cap-target [Accessed: October 22, 2017]

[11] Rechtschaffen D. How China's Growing Deserts Are Choking The Country. [Internet]. September 18, 2017. Available from: https://www.forbes.com/sites/danielrechtschaffen/2017/09/18/how-chinas-growing-deserts-are-choking-the-country/#7ec9bea95d1b [Accessed: October 22, 2017]

[12] Yu M, Weinthal E, Patino-Echeverri D, Deshusses MA, Zou C, Ni Y, Vengosh A. Water availability for shale gas Dvelopment in Sichuan Basin, China. Environmental Science & Technology. 2016;**50**:2837-2845. DOI: 10.1021/acs.est.5b04669

[13] Lee J, West J. Deep Inside the Wild World of China's Fracking Boom: US companies are salivating over the biggest shale gas resources in the world. What could possibly go wrong?

Mother Jones September/October 2014 Issue. Available from: http://www.motherjones.com/environment/2014/09/china-us-fracking-shale-gas/ [Accessed: October 22, 2017]

[14] EIA/ARI World Shale Gas and Shale Oil Resource Assessment. Technically Recoverable Shale Gas and Shale Oil Resources: An Assessment of 137 Shale Formations in 41 Countries Outside the United States. U.S. Energy Information Administration and U.S. Department of Energy. Arlington, VA, USA: Advanced Resources International, Inc. June 2013. Available from: https://www.adv-res.com/pdf/A_EIA_ARI_2013%20World%20Shale%20Gas%20and%20Shale%20Oil%20Resource%20Assessment.pdf

[15] Mackenzie K. Is Chinese (and Polish) shale gas hot air? MacroBusiness. July 10, 2013. [Internet]. 2016. Available from: https://www.macrobusiness.com.au/2013/07/is-chinese-and-polish-shale-gas-hot-air/ [Accessed: October 22, 2017]

[16] Jian-chun G, Zhi-hong Z. China vigorously promoting shale gas exploration, development. Oil & Gas Journal, 2012;**110**(3):60-65. Available from: http://www.ogj.com/articles/print/vol-110/issue-3/exploration-development/china-vigorously-promoting.html

[17] Chabour N, Mebrouk N, Hassani MI, Upton K, Dochartaigh BO. Hydrogeology of Algeria from Earthwise. British Geological Survey. [Internet]. 2016. Available from: http://earthwise.bgs.ac.uk/index.php/Hydrogeology_of_Algeria [Accessed: October 22, 2017]

[18] Estevez D. Fracking: Could Mexico's Water Scarcity Render Its Energy Sector Reforms Self-Defeating? [Internet]. June 11, 2014. Available from: https://www.forbes.com/sites/doliaestevez/2014/06/11/fracking-could-mexicos-water-scarcity-render-its-energy-sector-reforms-self-defeating-2/#7731174a54ea [Accessed: October 22, 2017]

[19] Rhoda R, Burton T. Geo-Mexico: The Geography and Dynamics of Modern Mexico. Ladysmith, BC, Canada: Sombrero Books; 2010. 288 p. ISBN 10:0973519134. ISBN 13: 9780973519136

[20] CIA World Factbook, South Africa. [Internet]. Available from: https://www.cia.gov/library/publications/the-world-factbook/geos/sf.html [Accessed: October 22, 2017]

[21] Kock MOD, Beukes NJ, Adeniyi EO, Cole D, Gotz AE, Geel C, Ossa FG. Deflating the shale gas potential of South Africa's Main Karoo basin. South African Journal of Science. September/October 2017;**113**(9/10):12 pages. Available from: http://www.sajs.co.za/system/tdf/publications/pdf/SAJS-113-9-10_DeKock_ResearchArticle.pdf?file=1&type=node&id=35846&force=

[22] Stewart TJ. Thirsting for Consensus: Multicriteria decision analysis helps clarify water resources planning in South Africa. OR/OM Today – April 2003. [Internet]. Available from: http://www.orms-today.org/orms-4-03/consensus.html [Accessed: October 22, 2017]

[23] Mineral Commodity Summaries 2015. U.S. Geological Survey. DOI: 10.3133/70140094. Available from: https://minerals.usgs.gov/minerals/pubs/mcs/2015/mcs2015.pdf [Accessed: October 22, 2017]

[24] Younger S. For National Geographic. July 4, 2013. Sand Rush: Fracking Boom Spurs Rush on Wisconsin Silica. Available form: https://news.nationalgeographic.com/news/energy/2013/07/130703-wisconsin-fracking-sand-rush/ [Accessed: October 22, 2017]

[25] Kahrilas GA, Blotevogel J, Stewart PS, Borch T. Biocides in hydraulic fracturing fluids: A critical review of their usage, mobility, degradation, and toxicity. Environmental Science & Technology. 2014;**49**:16-32. DOI: 10.1021/es503724k

[26] Healy JH, Rubey WW, Griggs DT, Raleigh CB. The Denver earthquakes. Science. September 27, 1968;**161**(3848):1301-1310. Available from: http://coloradogeological-survey.org/wp-content/uploads/docs/ERC/THE%20DENVER%20EARTHQUAKES-HEALY%20AND%20OTHERS%201968.pdf

Aquifers: The Fluid

Chapter 4

The Discharge-Storage Relationship and the Long-Term Storage Changes of Southern Taiwan

Hsin-Fu Yeh

Additional information is available at the end of the chapter

http://dx.doi.org/10.5772/intechopen.73163

Abstract

In this study, the water balance concept is used to understand the relationship between discharge and storage in a basin. Three low flow analysis models developed by Brutsaert, Vogel and Kroll, and Kirchner are used to select recession curves that are parameterized using lower envelope, linear regression, and binning methods to characterize basin hydrological behavior. Furthermore, the lowest annual groundwater storage, which is analyzed according to trend, slope, and a change point test, is used to assess the long-term storage properties of southern Taiwan and is also quantified. The water balance concept is used to assess the impact of discharge on groundwater storage that is affected by the different low flow analysis models. This can lead to a more clear understanding of the relationship between groundwater storage and discharge. After statistical tests of trend, it was determined that Chaozhou Station, which has a significant decreasing trend of the lowest groundwater storage, should implement precautionary measures such as an underground reservoir, an artificial recharge, and a collection gallery in the Donggang River Basin.

Keywords: recession curve, low flow analysis, groundwater storage

1. Introduction

Salt water accounts for 97% of the global distribution of water resources, but only 3% of the fresh water, which is approximately 22% of all water on Earth, is stored as groundwater as a main obtainable resource [1]. Nevertheless, over the past half century, global warming has caused a rise in sea level that has resulted in changes in groundwater [2]. Groundwater depletion, which causes land subsidence, salt water intrusion, the necessity to irrigate agriculture, and reductions in food security, is becoming more severe year by year [3–5]. Globally, groundwater storage is much greater than that of atmospheric water and soil water. Because of

significant differences in the storage of water resources, determining a method by which to assess groundwater storage is a very important issue [6].

Recently, Taiwan has been affected by climate change, which is resulting in distinct wet and dry seasons with stronger rainfall intensity in the wet season and a lack of rain in the dry season [7]. Variations in Taiwan's topography and uneven distribution of rainfall, with more in the mountains than in the plains and more in the northern than in the southern areas, are causing uneven distribution of water resources in time and space. Taiwan's annual average rainfall is up to 2500 mm, which is approximately 2.5 times more than the annual global average rainfall. Nevertheless, Taiwan is still facing a surface water shortage problem in the dry season. In southern Taiwan, which is the most serious area, the ratio of wet season rainfall and dry season rainfall is as high as 9:1 [8]. Therefore, in this study, the southern area is set as the study area to discuss what groundwater resource problems this area will be facing in the future. The water balance concept is used to explore the storage-discharge relationship, and a low flow analysis is used to assess the lowest groundwater storage in southern Taiwan. The assessment results can be provided to water resource agencies to assist with water resource management plans.

Low flow analysis, which is a hydrological method widely used to estimate hydraulic parameters, is used to characterize basin characteristics and assess groundwater storage trends. Brutsaert and Nieber [9] analyzed six basins in the Finger Lakes region of upstate New York using the lower envelope fitting method to characterize recession curves in order to estimate specific yield. Szilagyi et al. [10] pointed out that complexity of basin shape, hydraulic conductivity heterogeneity, and gently sloping impermeable layers do not affect the estimation of hydraulic conductivity and mean aquifer depth. Field-based estimates of these hydraulic parameters using a low flow analysis are a beneficial method for evaluating discharge data that are not easily obtained, mainly in low population density area [11].

Watershed properties such as hydrology, geology, and topography affect streamflow regimes [12]. Thus, through knowing the main factors dominating streamflow recession characteristics, it is possible to understand drainage systems. Zecharias and Brutsaert [13] selected 19 basins in the Allegheny Mountains of the Appalachian Plateaus to investigate streamflow recession curve characteristics, and their results showed that recession time is affected by mean basin slope, drainage density, and the ratio of the hydraulic conductivity and the specific yield. Vogel and Kroll [14] evaluated Massachusetts basin characteristics, and their result showed that recession time is highly correlated with basin area and basin slope. Brutsaert [15] suggested that streamflow recession time is highly correlated with basin area, basin elevation, and stream length. Kirchner [16] used a single-equation rainfall-runoff model to select streamflow data in order to estimate recession time from the headwaters of the Severn and Wye rivers at Plynlimon in mid-Wales. Sánchez-Murillo et al. [17] suggested that geology affects the length of recession time. Metamorphic and sedimentary rocks result in longer recession time. Low flow in flat basalt landscapes recesses rapidly. Knowing the dominating factors related to recession characteristics makes it easier to understand their effects on subsurface properties.

Recently, several studies analyzed annual groundwater storage trends in order to assess water supply availability in the future. Sugita and Brutsaert [18] researched perennial groundwater storage and low flow trends in the Kanto region. If the water demand remained constant, there

was no sign of danger to water supply shortages. Hughes et al. [19] found that precipitation and changes in groundwater storage have a close connection. When annual precipitation is above the threshold, groundwater storage will increase and vice versa. Zhang et al. [20] selected 17 catchments to assess perennial groundwater storage trends. The groundwater storage showed different trends over the various shorter periods, and strong consistencies in the trends existed across most catchments. These results suggest that short-term climate variability can significantly influence groundwater storage and that it will be affected by large-scale hydro-climate factors. A better insight into how groundwater storage has been changing will be critical in evaluating sustainable water resource management plans. The objectives of this study are (1) to discuss the relationship between discharge and storage and (2) to assess groundwater storage dynamics using low flow analysis to assess what water resource problems southern Taiwan will be facing.

2. Methodology

2.1. Water balance concept

In a catchment, a hydrological system can be represented with the mass conservation equation:

$$\frac{dS}{dt} = P - E - Q \tag{1}$$

where S [LT^{-1}] is the unit area water stored in the catchment; P [LT^{-1}] is the rate of precipitation; E [LT^{-1}] is the evapotranspiration rate; and Q [LT^{-1}] is the unit area discharge.

Assuming that discharge is only related to storage, $f(S)$ can be expressed as the storage-discharge relationship

$$Q = f(S) \tag{2}$$

Assuming that Q is an increasing single-valued function of S since storage-discharge function is invertible

$$S = f^{-1}(Q) \tag{3}$$

The discharge change rate through time is yielded by combining Eqs. (1) and (2)

$$\frac{dQ}{dt} = \frac{dQ}{dS}\,\frac{dS}{dt} = \frac{dQ}{dS}\,(\,P - E - Q\,) \tag{4}$$

Q is assumed to be an increasing single-valued function of S. Additionally, S cannot be directly measured, and thus $\frac{dQ}{dS}$ can be defined as a function of Q

$$\frac{dQ}{dS} = f'(S) = f'\left(f^{-1}(Q)\right) = g(Q) \tag{5}$$

$g(Q)$ refers to the streamflow sensitivity function because it expresses the sensitivity of discharge to changes in storage [16]. Because S cannot be directly measured in the catchment, combining Eqs. (4) and (5) to yield Eq. (6) solves the measurement problem of S, where discharge only has to be expressed as changes in storage

$$g(Q) = \frac{dQ}{dS} = \frac{\frac{dQ}{dt}}{\frac{dS}{dt}} = \frac{\frac{dQ}{dt}}{P - E - Q} \tag{6}$$

In a catchment, when the precipitation and evapotranspiration are much smaller than discharge, the relationship between discharge and groundwater storage can be most accurately expressed

$$g(Q) = \frac{dQ}{dS} \approx \frac{-\frac{dQ}{dt}}{Q} \mid_{P \ll Q, E \ll Q} \tag{7}$$

Finally, the relationship between discharge and storage is derived from Eq. (7)

$$\int dS = \int \frac{dQ}{g(Q)} \tag{8}$$

2.2. Low flow analysis

In the water balance conceptual method, Eq. (8) represents the relationship between discharge and storage. Brutsaert [21], Vogel and Kroll [14], and Kirchner [16] used low flow analysis models to select recession curves and the same method has been used in this study to characterize southern Taiwan's hydrological behaviors in order to quantify the lowest groundwater storage and to assess southern Taiwan whether facing a groundwater shortage problem in the future.

2.2.1. The Brutsaert (2008) model

Low flow is a period without precipitation. In these periods, the hydrologic water flow system in the river is only related to the groundwater drainage from the aquifer in the catchment. As exponential decay type function is more commonly used to describe low flows

$$\dot{Q} = \dot{Q}_0 \, e^{-\frac{t}{K}} \tag{9}$$

where $\dot{Q}$ is defined as volume of flow rate in the river [L^3 T^{-1}]; $\dot{Q}_0$ is the value of flow rate at arbitrarily chosen time such as t = 0 [L^3 T^{-1}]; and K, which is defined as the characteristic of time scale in the catchment, is also referred as the storage coefficient [T].

A power law function is used to describe the relation between the change in the flow rate and the discharge characterized hydrologic behavior in this research (e.g., Brutsaert and Nieber [9])

$$\frac{d\dot{Q}}{dt} = -a \, \dot{Q}^b \tag{10}$$

in which a and b are constants [−]. These constants can be characterized to display catchment hydrologic behavior [22].

Precipitation, evapotranspiration, and artificial input events are excluded in the low flow conditions when groundwater storage is only related to the water flow in the river. Furthermore, mass conservation law of hydrologic system can display as the following integral function:

$$S = -\int_t^{\infty} Q\, dt \tag{11}$$

where S and Q are defined as Eq. (1). Substitution of Eq. (9) in Eq. (11) derives following relationship between groundwater storage and drainage from the catchment

$$S = KQ \tag{12}$$

According to Eq. (12), the temporal trend of catchment groundwater storage can be obtained from the trend of discharge in the river as the following function:

$$\frac{dS}{dt} = K\frac{dQ}{dt} \tag{13}$$

Because daily flow varies, in this study, the annual lowest 7-day daily mean flow is used to replace daily flow to reduce uncertainty

$$\frac{dS}{dt} = K\frac{dQ_{L7}}{dt} \tag{14}$$

where Q_{L7} is the annual lowest 7-day daily mean flows [LT^{-1}].

The long-term temporal trend of catchment groundwater storage is significant because it reveals whether the catchment will face a water shortage problem in the future.

Obtaining the trend in the catchment groundwater storage requires the characteristics of time scale K. In this study, a lower envelope was adopted, which is defined as roughly 5% data points below the logarithmic plot of change of flow rate data against the flow rate. In order to delete the effectiveness of precipitation, the criteria for the selection of streamflow data are as follows [21]:

a. Changes of flow rate are zero and positive, and sudden anomalous data should be eliminated.

b. Three data points after the changes in the flow rate are zero and positive, and four data points after major events should be eliminated.

c. Two data points before the changes in the flow rate are zero and positive should be eliminated.

d. When there is suddenly a higher value of change in the flow rate in a dry period, it should be eliminated.

2.2.2. The Vogel and Kroll (1992) model

Vogel and Kroll [14] assumed discharge to be linearly related to storage. Eq. (15) is a well-known base flow equation

$$\dot{Q} = \dot{Q}_0 K_b^t \tag{15}$$

where K_b is base flow recession constant [−]. Eq. (16) is derived by Eq. (9) by comparing the Brutsaert (2008) model

$$K = -\frac{1}{lnK_b} \tag{16}$$

Vogel and Kroll's model used a linear regression to define the characteristics of time scale K to represent average basin hydrological behavior. The Vogel and Kroll model has criteria for selection of the streamflow data as follows:

a. A recession range is between a 3-day moving average beginning to decrease and a 3-day moving average beginning to increase.

b. Delete 30% of the front total recession length.

Only accept $\dot{Q}_t \geq 0.7\dot{Q}_{t-1}$.

2.2.3. The Kirchner (2009) model

Kirchner [16] suggested that when evapotranspiration, precipitation, aquifer recharge, and leakage are much smaller than discharge, they can be neglected. At this time, discharge is directly related to changes in storage as shown in Eq. (17) below:

$$\frac{dS}{dt} = -\dot{Q} \tag{17}$$

The power law equation proposed by Brutsaert and Nieber [9] is used to represent hydrological low flow analysis. Kirchner's model for streamflow criteria is simpler than the other available alternatives. It only requires the streamflow recession segment.

2.3. Trend test

2.3.1. Mann-Kendall test

Mann-Kendall (MK) [23, 24] test is nonparametric method developed from Kendall's tau (τ). It can be used to test the relationship between two sets of data. The advantages of this method are that the extreme values and missing data problems will not seriously affect the certification value. The MK test assesses the trend in a series via comparing the value of the series before and after to determine whether the series exhibits a specific degree of trend. The null hypothesis given that if there is not significant trend in the series, test statistic S is defined as:

$$Sign\ \left(X_j - X_i\right) = \begin{cases} +1 & , \quad X_j - X_i > 0 \\ 0 & , \quad X_j - X_i = 0 \\ -1 & , \quad X_j - X_i < 0 \end{cases} \quad , \quad S = \sum_{i=1}^{n-1} \sum_{j=i+1}^{n} Sign\left(X_j - X_i\right) \tag{18}$$

where $\{X_1, X_2, X_3,\ldots, X_n\}$ is streamflow data, which are arranged in accordance with time $\{T_1, T_2, T_3,\ldots, T_n\}$, n is the number of data. When n is close to infinity, the probability of the S distribution curve will present as a normal distribution with a mean of 0. In addition, when n is more than 10, the variance of S can be substituted into the following approximate solution:

$$\sigma^2 = \frac{n(n-1)(2n+5)}{18} \tag{19}$$

In this study, long-term streamflow data are likely to be repeated in the data series; thus, Kendall modified the approximated solution Eq. (19) to Eq. (20)

$$\sigma^2 = \frac{1}{18}\left[n(n-1)(2n+5) - \sum_{u=1} u(u-1)(2u+5)\right] \tag{20}$$

where u is the duplicate value number of the data series.

Finally, the normalized statistical test S values become the Z value, as follows:

$$Z = \begin{cases} \dfrac{S-1}{\sigma} & , S > 0 \\ 0 & , S = 0 \\ \dfrac{S+1}{\sigma} & , S < 0 \end{cases} \tag{21}$$

When Z is a positive value, this indicates that the series is exhibiting an increasing trend; in contrast, when the value is negative, it indicates that the series has decreased. At this time, the obtained Z value should be tested by a significance test to assess whether the series is significant. Assuming, a significance level of α, if $|Z| \geqq Z_\alpha$, the null hypothesis is rejected, which represents that the series has a significant trend; whereas, the series has no significant trend. In the study, the significance level is set as α = 0.05. When $|Z| \geqq 1.96$, the series has a significant trend. When it is below this level, there is no significant trend.

2.4. Slope test

2.4.1. Theil-Sen slope

The Theil-Sen slope [25] is used to estimate the magnitude of the trend slope. The Theil-Sen slope estimation method is different from the slope values calculated using a linear regression, because it selects the median value, and therefore, the properties are less affected by extreme values. Thus, it is often used with the MK test. Slope β is defined as follows:

$$\beta = Median\left(\frac{X_j - X_i}{j-i}\right), \quad for\ all\ i < j \tag{22}$$

$$\begin{aligned} X(t) &= \beta\ t + C \\ X(t) &= X_1 \sim X_n\ , \quad t = 1 \sim n \end{aligned} \tag{23}$$

2.5. Change point test

2.5.1. Mann-Whitney-Pettit test

The Mann-Whitney-Pettit (MWP) test [26] can be used to search for significant change points in a data series. The definition of a change point is when a data series $\{X_1, X_2,\ldots, X_n\}$ has a change point X_t, order $\{X_1, X_2,\ldots, X_t\}$ is $F_1(X)$ and $\{X_{t+1}, X_{t+2},\ldots, X_n\}$ is $F_2(X)$, then $F_1(X) \neq F_2(X)$. The definition of $U_{t,n}$ is as shown in Eq. (24). If there is not a change point in the data series, $|U_{t,n}|$ on the function of time, t will continue to rise, and there will be no turning point. On the contrary, if there is a change point, $|U_{t,n}|$ on the function of time t, there will be a decreasing turning point. In the same data series, the turning point may occur several times on behalf of this data series, and there may be more than one change point

$$Sign\ \left(X_i - X_j\right) = \begin{cases} +1 & , \quad X_i - X_j > 0 \\ 0 & , \quad X_i - X_j = 0 \\ -1 & , \quad X_i - X_j < 0 \end{cases} \quad , \qquad U_{t,n} = \sum_{i=1}^{t} \sum_{j=t+1}^{n} Sign\ \left(X_i - X_j\right) \tag{24}$$

$$K_n = Max\ |U_{t,n}| \ , \quad 1 \leq t < n \tag{25}$$

To confirm that change points exist, Eq. (25) is used to calculate the extreme value of $|U_{t,n}|$ that is turning point as K_n. Eq. (26) is used to calculate the probability of a change point. In this study, $P = 0.95$ is set as the confidence level, where $P > 0.95$ judges that the time is a significant changing point

$$P = 1 - \exp\left(\frac{-6{K_n}^2}{n^2 + n^3}\right) \tag{26}$$

However, in some data series, a change point may not exist by itself; thus, Eq. (27) is used to calculate each year's $P(t)$ value. The $P(t)$ value is identified when it is greater than the confidence level

$$P(t) = 1 - \exp\left(\frac{-6|U_{t,n}|^2}{n^2 + n^3}\right) \tag{27}$$

3. Study area

The study area is set in southern Taiwan, including Chiayi, Tainan, Kaohsiung, and Pingtung area. The main basin includes the Bazhang River, the Jishuei River, the Cengwen River, the Yanshui River, the Erren River, the Gaoping River, the Donggang River, and the Linbian River (see **Figure 1**). The annual average temperature is between 22 and 26°C, and the annual average precipitation is about 2000 mm, with distinct wet and dry seasons. The precipitation is concentrated in the May to October high flow periods, and on the contrary, November to April is the low flow period, which causes the rivers to dry up in southern Taiwan [8]. Two

standards are used for the selection of the streamflow station. First, a streamflow station must provide long-term continuous measurement data; thus, selected stations have at least 40 years of daily flow data. Second, streamflow stations are unaffected by artificial structures such as dams. After screening, Taiwan's southern basin was determined to have six stations complying with the above two criteria. These stations are listed in **Table 1** and are located in **Figure 1**.

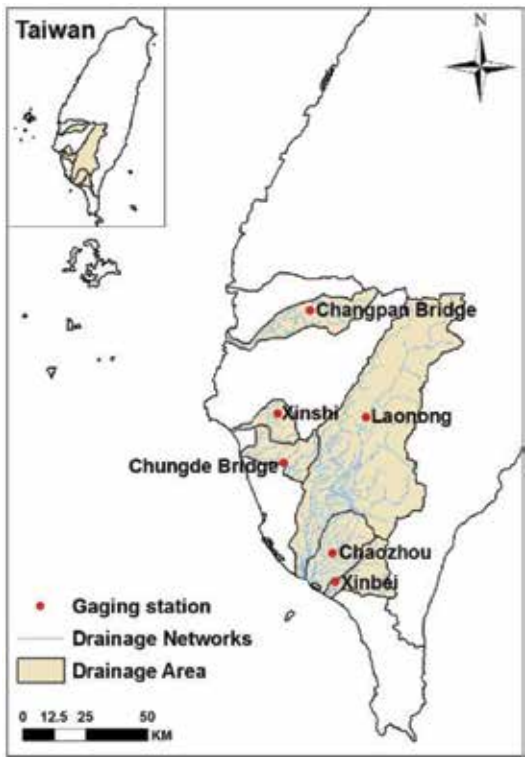

Figure 1. The location of streamflow gaging station.

Basin	Station	Stream order	Average elevation (m)	Length of main stream (m)	Average slope (m/m)	Slope of main stream (m/m)	Area (km^2)
Bazhang River	Changpan Bridge	4	309	22,547	0.31	0.05	98.34
Yanshui River	Xinshi	4	49	29,402	0.14	0.06	143.4
Erren River	Chungde Bridge	4	89	38,553	0.36	0.25	138.3
Gaoping River	Laonong	5	1833	99,211	0.70	0.08	803.0
Donggang River	Chaozhou	5	233	28,848	0.25	0.06	178.5
Linbian River	Xinbei	5	692	36,815	0.49	0.10	311.4

Table 1. The characteristics of the study basins of streamflow gaging station [8].

4. Results and discussions

4.1. The water balance conceptual method for assessing basin storage-discharge relationship

In this study, the water balance method is used to discuss the relationship between discharge and storage in six catchments in southern Taiwan using three low flow models from Brutsaert [21], Vogel and Kroll [14], and Kirchner [16] to select streamflow data. However, the groundwater storage cannot be measured directly at the catchment; thus, the streamflow sensitivity function (Eq. (6)) is used to assess the sensitivity of discharge to changes in storage.

First, the storage-discharge relationship in southern Taiwan according to the Brutsaert model is discussed. The results show that the most sensitivity is at the Chungde Bridge Station, and the least is at Chaozhou Station. The order of sensitivity is as follows: Chungde Bridge at the Erren River, Changpan Bridge at the Bazhang River, Laonong at the Gaoping River, Xinbei at the Linbian River, and Chaozhou at the Donggang River. However, the Xinshi catchment cannot exhibit the relationship between storage-discharge because the process of selecting streamflow data using the Brutsaert model is more complex than other alternatives. Thus, the streamflow data for Xinshi Station, which cannot reveal the storage-discharge relationship, are less than that for the other stations (**Figure 2(a)**). According to Eq. (8), when the discharge sensitivity to changes in groundwater storage is high as indicated by the slope of the storage-discharge relationship, the recession time is shorter. The time of the order of recession is Chaozhou at the Donggang River, Xinbei at the Linbian River, Laonong at the Gaoping River, Changpan Bridge at the Bazhang River, and Chungde Bridge at the Erren River as shown in **Figure 3(a)**. However, Xinshi Station cannot reveal the storage-discharge relationship, which causes the relationship between discharge and time to be inaccurate as well.

The results for the Vogel and Kroll model show that the Chungde Bridge station cannot display the storage-discharge relationship because the $Q_t \geq 0.7Q_{t-1}$ selection criteria resulted in discontinuous selected data. **Figure 2** shows that for the same changes in discharge, the Kirchner model has higher storage variations and shorter recession periods.

4.2. Low flow analysis

In this study, low flow analyses of the Brutsaert [21], Vogel and Kroll [14], and Kirchner [16] models are fitted by lower envelope, linear regression, and binning to parameterize streamflow recession curve and discuss the relationship between parameters (e.g., hydrological characteristic constants and recession time) and topography factors. Stream order, average elevation, length of main stream, average slope, slope of main streamflow, and basin area are selected and shown in **Table 1** to analyze the correlation between hydrological characteristic constants and recession time (K).

In order to ensure that low flow is a period without precipitation, thus, the Brutsaert [21], Vogel and Kroll [14], and Kirchner [16] models have their own selection procedure criteria for streamflow data. **Figure 4** shows that different models will affect the selection of streamflow

http://dx.doi.org/10.5772/intechopen.73163

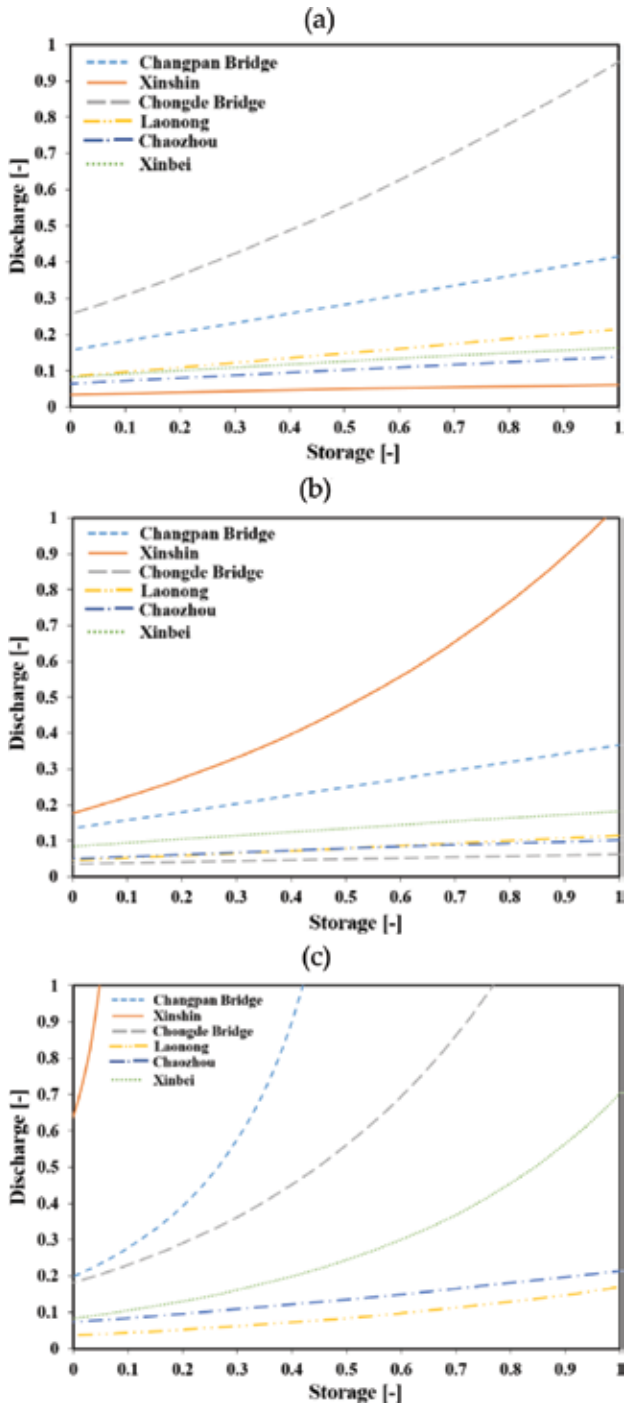

Figure 2. Water balance conceptual method for storage-discharge relationship in six catchments in southern Taiwan. (a) Brutsaert (2008), (b) Vogel and Kroll (1992) and (c) Kirchner (2009).

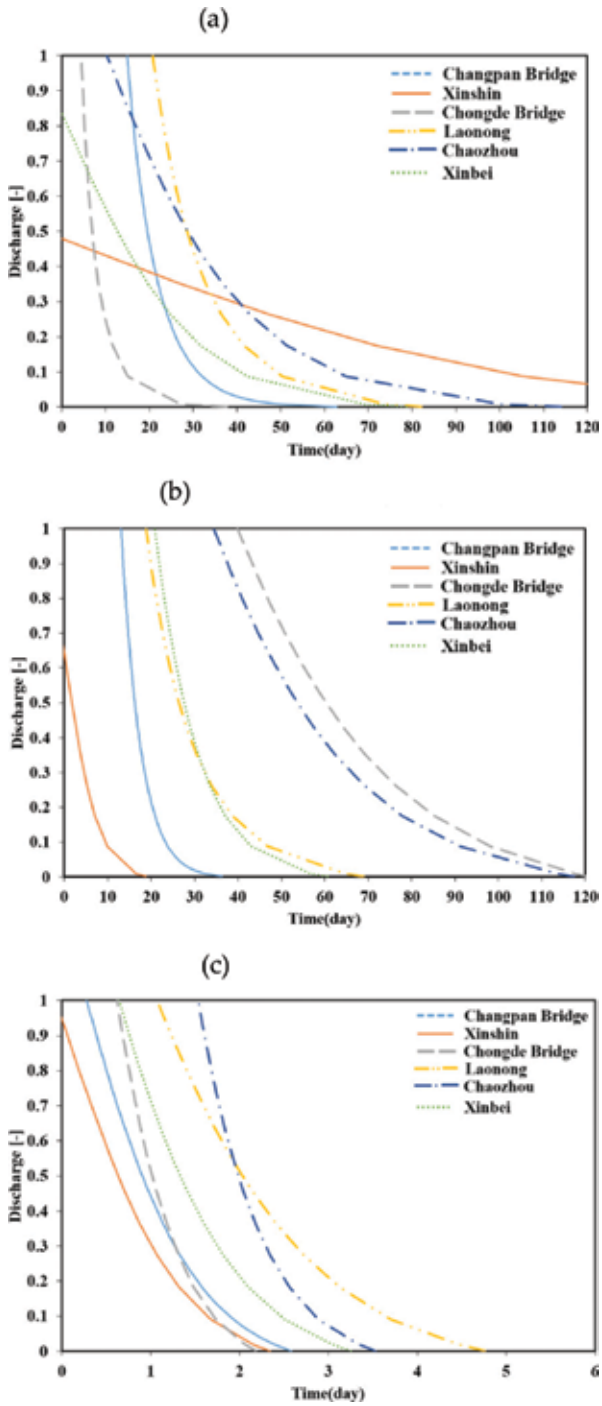

Figure 3. Discharge and recession time relationship in six catchments in southern Taiwan. (a) Brutsaert (2008), (b) Vogel and Kroll (1992) and (c) Kirchner (2009).

data points; thus, the streamflow data points of the Kirchner model are approximately 40 times than the Brutsaert model. Those results in assessing the basin hydrology characteristics that are more subjective.

Table 2 shows that the characteristic constant *a* order is binning > linear regression > lower envelope. Generally, the characteristic constant *a* using the binning and linear regression has higher values due to the fact that the regression line is moved upward when compared to the lower envelope fit line. **Table 3** shows that the recession time order is lower envelope > linear regression > binning. This indicates the inverse relationship between the characteristic constant *a* and recession time. The six basins with the distribution of recession time show that the binning fitting method exhibits the most quickly recessions, with ranges from 3 to 22 days. The lower envelope fitting method had the longest recessions, with ranges from 32 to 127 days. Because the average value will be influenced by the outlier median is more suitable for representing recession time. It can be noted in **Figure 5** that lower envelope fitting with the

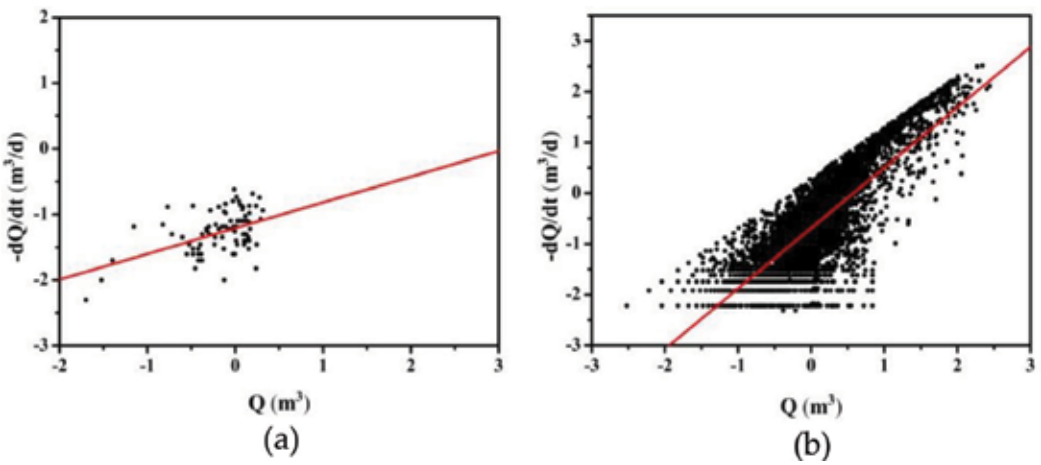

Figure 4. Fitted method by linear regression in Xinshi station. (a) Brutsaert (2008) and (b) Kirchner (2009).

	Lower envelope			Linear			Binning		
Basin	**BRU**	**VOG**	**KIR**	**BRU**	**VOG**	**KIR**	**BRU**	**VOG**	**KIR**
Changpan Bridge	0.016	0.018	0.026	0.064	0.099	0.218	0.067	0.077	0.321
Xinshi	0.026	0.016	0.022	0.062	0.099	0.204	0.068	0.115	0.334
Chungde Bridge	0.029	0.013	0.031	0.084	0.110	0.244	0.085	0.096	0.355
Laonong	0.008	0.010	0.022	0.033	0.011	0.079	0.047	0.068	0.065
Chaozhou	0.012	0.018	0.012	0.044	0.034	0.071	0.046	0.060	0.082
Xinbei	0.020	0.019	0.017	0.057	0.054	0.180	0.061	0.076	0.248

Table 2. Characteristic constant ***a*** for three extraction procedures (BRU, VOG, and KIR) and three different fitted models (lower envelope, linear, and binning).

	Lower envelope			Linear			Binning		
Basin	**BRU**	**VOG**	**KIR**	**BRU**	**VOG**	**KIR**	**BRU**	**VOG**	**KIR**
Changpan Bridge	61	57	39	16	10	5	15	13	3
Xinshi	39	63	46	16	10	5	15	9	3
Chungde Bridge	35	75	32	12	9	4	12	10	3
Laonong	127	102	45	30	90	13	21	15	14
Chaozhou	85	57	83	23	29	14	22	17	12
Xinbei	50	53	60	17	19	6	16	13	4

Table 3. Recession time for three extraction procedures (BRU, VOG, and KIR) and three different fitted models (lower envelope, linear, and binning) (day).

Brutsaert model obtained a median of 55.5 days; the Vogel and Kroll model obtained a median of 60 days, and the Kirchner model obtained a median of 45.5. **Figure 6** shows a characteristic constant a range from 0.008 up to 0.355. **Figure 7** shows that the characteristic constant b varies from 0.678 to 1.432 without outliers.

In the results of the correlation between recession curve and topography factors, the Vogel and Kroll model, which is fitted using a linear regression, is the most suitable result for characterizing southern Taiwan basin hydrological behavior. The recession time is highly correlated with average elevation, length of main stream, and basin area as shown in **Table 4**. According to Tague and Grant [27], a higher characteristic hydrology constant a represents rapid recession. In this study, only the characteristic hydrology constant a from the Vogel and Kroll model as fitted using a linear regression is found to be highly correlated with the slope of the main stream as shown in **Table 5**. There is a high correlation the between characteristic hydrology constant b and average slope according to the Vogel and Kroll model, which is fitted using a linear regression, as shown in **Table 6**. According to above results indicating that the Vogel and Kroll model as fitted using a linear regression is the most optimal result to represent

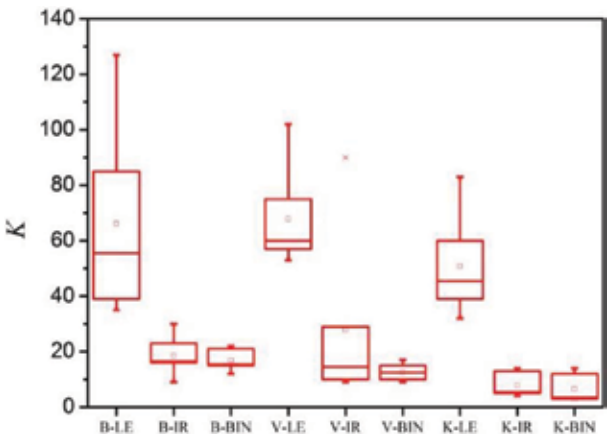

Figure 5. The distribution of recession time for three extraction procedures and three different fitted models.

http://dx.doi.org/10.5772/intechopen.73163

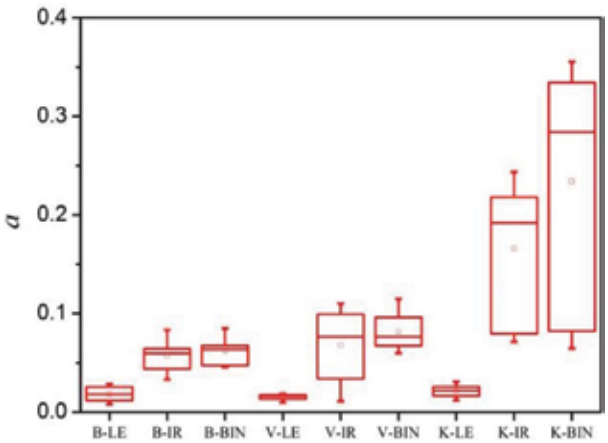

Figure 6. The distribution of characteristic constant ***a*** for three extraction procedures and three different fitted models.

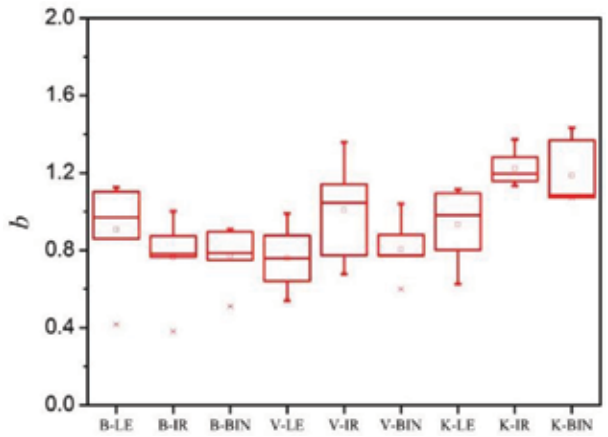

Figure 7. The distribution of characteristic constant ***b*** for three extraction procedures and three different fitted models.

southern Taiwan basin characteristics, the Vogel and Kroll model is used to quantify the lowest groundwater storage in southern Taiwan.

4.3. The trend test of lowest groundwater storage

The optimal results of the Vogel and Kroll model as fitted using a linear regression is shown in Section 4.2. It is used to quantify the lowest groundwater storage in southern Taiwan. In the trend test results shown in **Table 7**, Changpan Bridge, Chungde Bridge, and Xinbei Station exhibit the most significant increasing trend. Chaozhou Station exhibits a significant decreasing trend. Xinshi Station has an increasing trend. Laonong Station has a decreasing trend. **Figure 8** shows the perennial basin slope test indicating that the increasing trend range for

Fitting method	Model	Stream order	Average elevation (m)	Length of main stream (m)	Average slope (m/m)	Slope of main stream (m/m)	Area (km^2)
Lower envelope	Brutsaert	0.666	0.841	0.784	0.662	−0.381	0.828
	Vogel and Kroll	0.168	0.753	0.927	0.685	0.259	0.818
	Kirchner	0.734	0.302	0.272	0.161	−0.342	0.337
Linear regression	Brutsaert	0.738	0.797	0.707	0.546	−0.571	0.799
	Vogel and Kroll	0.633	0.942	0.948	0.794	−0.181	0.965
	Kirchner	0.780	0.551	0.520	0.370	−0.384	0.583
Binning	Brutsaert	0.802	0.549	0.456	0.325	−0.569	0.561
	Vogel and Kroll	0.793	0.461	0.290	0.392	−0.436	0.403
	Kirchner	0.753	0.682	0.685	0.514	−0.281	0.721

Table 4. The correlation between recession time and topography factors.

Fitting method	Model	Stream order	Average elevation (m)	Length of main stream (m)	Average slope (m/m)	Slope of main stream (m/m)	Area (km^2)
Lower envelope	Brutsaert	−0.712	−0.708	−0.542	−0.528	0.594	−0.646
	Vogel and Kroll	−0.032	−0.626	−0.852	−0.573	−0.367	−0.710
	Kirchner	−0.761	−0.107	0.067	0.052	0.621	−0.116
Linear regression	Brutsaert	−0.785	−0.723	−0.601	−0.462	0.655	−0.723
	Vogel and Kroll	−0.719	−0.569	−0.385	−0.279	0.821	−0.555
	Kirchner	−0.835	−0.591	−0.533	−0.392	0.456	−0.622
Binning	Brutsaert	−0.817	−0.571	−0.410	−0.330	0.709	−0.556
	Vogel and Kroll	−0.760	−0.498	−0.300	−0.519	0.303	−0.408
	Kirchner	−0.867	−0.671	−0.605	−0.515	0.378	−0.689

Table 5. The correlation between characteristic constant a and topography factors.

changes in the lowest groundwater storage ranges from 33.5% to 2.7 times, and the decreasing trend ranges from −16.3% to −96.9%.

In this study, the change point is primarily set from 1983 to 2004 as shown in **Figure 9**. The lowest groundwater storage is smaller than before the change point at Chaozhou Station and greater than before the change point at Changpan Station, Chungde Station, and Xinbei Station. The lowest groundwater storage before the change point is 0.65 mm, and after the change point, it is 4.07 mm. The difference between before and after is up to 5.3 times than that of the Xinbei Station. The change point differences before and after are approximately 2.4, 1.4 and −56.9% at Changpan Station, Chungde Station, and Chaozhou Station, respectively. Xinshi Station and Laonong have no change point.

In the southern Taiwan basin, the lowest groundwater storage test results show that a significant change point occurred in the 1980s and after 2000. According to Hsu et al. [28], after the

Fitting method	Model	Stream order	Average elevation (m)	Length of main stream (m)	Average slope (m/m)	Slope of main stream (m/m)	Area (km^2)
Lower envelope	Brutsaert	0.202	0.471	0.403	0.677	0.294	0.364
	Vogel and Kroll	0.492	0.817	0.580	0.698	−0.553	0.701
	Kirchner	0.385	−0.086	−0.344	0.091	−0.166	−0.225
Linear regression	Brutsaert	0.431	0.649	0.547	0.784	0.116	0.549
	Vogel and Kroll	0.779	0.855	0.633	0.741	−0.529	0.773
	Kirchner	0.583	0.268	0.224	0.038	−0.534	0.287
Binning	Brutsaert	0.360	0.592	0.431	0.737	0.033	0.457
	Vogel and Kroll	0.014	0.316	0.067	0.130	−0.757	0.165
	Kirchner	0.691	0.652	0.677	0.483	−0.251	0.694

Table 6. The correlation between characteristic constant ***b*** and topography factors.

Basin	Gaging station	Trend test	Slope estimator	The lowest groundwater storage variable (%)	Change point	The lowest groundwater storage average		Variable of change point (%)
						Before	After	
Bazhang River	Changpan Bridge	3.40	0.046	192.4	1989	0.826	2.767	235.0
Yanshui River	Xinshi	0.92	0.007	33.5	—	—	—	—
Erren River	Chungde Bridge	2.25	0.022	158.0	2004	0.481	1.176	144.55
Gaoping River	Laonong	−0.64	−0.28	−16.3	—	—	—	—
Donggang River	Chaozhou	−3.92	−0.457	−96.9	2000	26.322	11.345	−56.9
Linbian River	Xinbei	5.34	0.057	272.6	1989	0.647	4.069	528.9

Table 7. The lowest groundwater storage trend test in the southern basins of Taiwan.

1980s, the average global temperature increased rapidly, resulting in abnormal weather phenomena. Additionally, Lu et al. [29] pointed out that after the 1980s, the temperature increased significantly by about twice than the century before. These studies show that there was a change in Taiwan's climate in the 1980s, thus suggesting that the impact of climate change on Taiwan's hydrological conditions caused a significant change point to occur in the 1980s. Fan et al. [30] indicated that the frequency of extreme rainfall events related to typhoons increased from 2000 to 2009, occurring once on an average 3–4 years between 1970 and 1999 and an average once every year after 2000. According to the research of Tsuang et al. [31], an annual average of 3.3 typhoons occurred in the twentieth century. However, in the research of Tu et al. [32], typhoon frequency increased up to an annual average of 5.7, causing significant increases in rainfall and affecting changes in groundwater storage.

In this study, the Brutsaert [21], Vogel and Kroll [14], and Kirchner [16] models are fitted using lower envelope, linear regression, and binning methods to parameterize the recession curve.

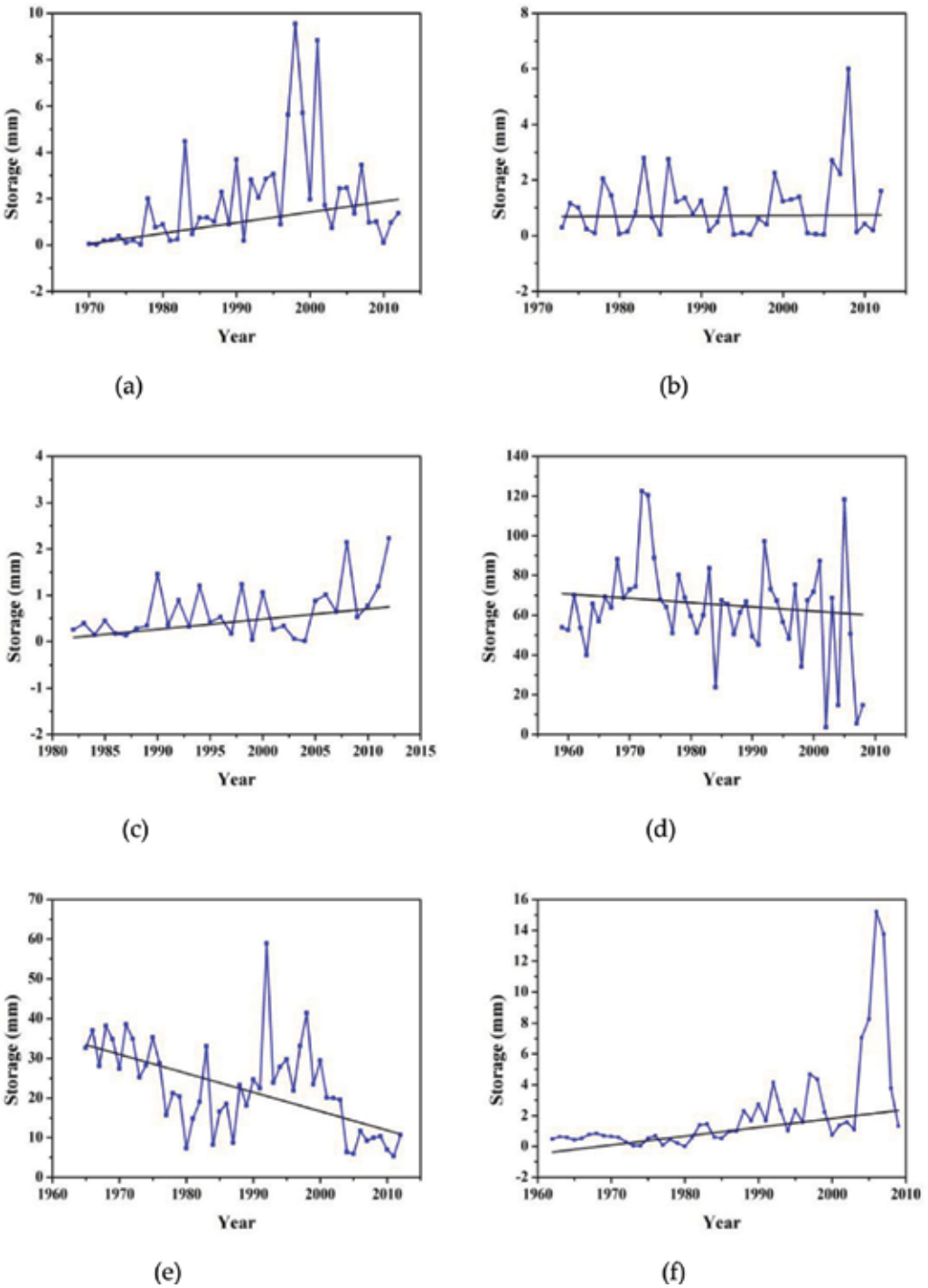

Figure 8. Annual trends in the minimum groundwater storage value for each study basin. (a) Changpan Bridge, (b) Xinshi, (c) Chungde Bridge, (d) Laonong, (e) Chaozhou, and (f) Xinbei.

http://dx.doi.org/10.5772/intechopen.73163

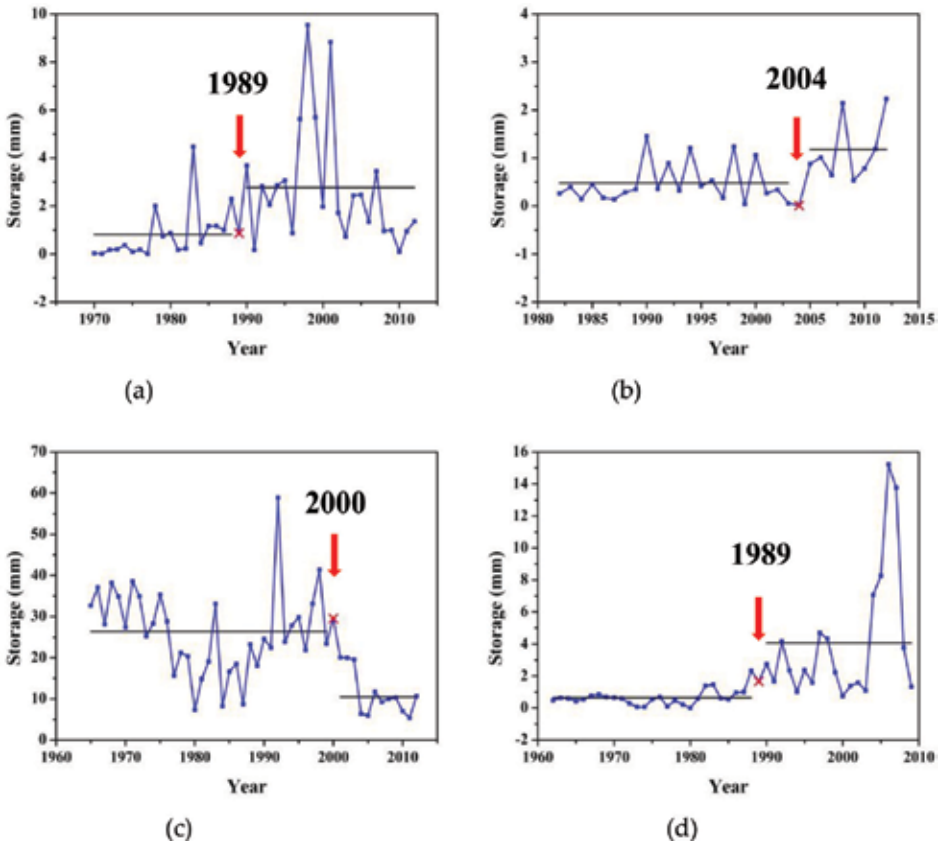

Figure 9. The lowest groundwater change point in the southern Taiwan. (a) Changpan Bridge, (b) Chungde Bridge, (c) Chaozhou, and (d) Xinbei.

The results show that the Vogel and Kroll model is the most optimal model to describe hydrological behavior in southern Taiwan. Thus, it is selected to quantify the lowest groundwater storage in the six basins. According to the trend, slope, and change point tests, the lowest groundwater storage exhibits a decreasing trend at the Laonong and Chaozhou stations. Most notably, Chaozhou Station exhibits a significant decreasing trend. In the future, shortage problem of Chaozhou station has a greater probability of facing low groundwater storage than the other basins under consideration. Moreover, in the study, the storage-discharge relationships in southern Taiwan are assessed using the water balance concept. All of the above hydrological studies in the long-term in southern Taiwan can be provided to water resources authority as a reference for water resource management planning.

5. Conclusions

This study examined the discharge-storage relationship and the changes in the lowest groundwater storage in six selected southern Taiwan basins over the last 40 years using observed daily

streamflow. The method is based on the water balance concept and low flow analysis, where precipitation and evapotranspiration in the natural river system are ignored, causing the base flow to be directly controlled by groundwater storage. Therefore, the observed streamflow can be used to assess the discharge-storage relationship and quantify the catchment groundwater storage. The results from this study show that the methods are valid for evaluating the discharge-storage relationship and long-term groundwater storage trends.

The water balance concept method indicated that different low flow analysis models will affect the sensitivity of discharge and groundwater storage. The Kirchner model is the most sensitive model. Thus, the recession time in this model was shown to be significantly shorter than that of the others under consideration. To summarize, the Vogel and Kroll model as fitted using a linear regression is most the optimal model by which to represent the hydrological characteristics in southern Taiwan. Overall, the lowest groundwater storage exhibited a significant decreasing trend at Chaozhou Station. The assessment results can be provided to water resource agencies to assist with water resource management plans.

Acknowledgements

The authors are grateful for the support of the Research Project of the Ministry of Science and Technology (MOST 106-2116-M-006-012).

Author details

Hsin-Fu Yeh

Address all correspondence to: hfyeh@mail.ncku.edu.tw

Department of Resources Engineering, National Cheng Kung University, Tainan, Taiwan

References

[1] Pimentel D, Berger B, Filiberto D, Newton M, Wolfe B, Karabinakis E, Clark S, Poon E, Abbett E, Nandagopal S. Water resources: Agricultural and environmental issues. Bioscience. 2004;**54**:909-918

[2] Pokhrel YN, Hanasaki N, Yeh PJF, Yamada TJ, Kanae S, Oki T. Model estimates of sea-level change due to anthropogenic impacts on terrestrial water storage. Nature Geoscience. 2012;**5**:389-392

[3] Wada Y, van Beek LPH, van Kempen CM, Reckman JWTM, Vasak S, Bierkens MFP. Global depletion of groundwater resources. Geophysical Research Letters. 2010;**37**:L20402

[4] Famiglietti JS, Lo M, Ho SL, Bethune J, Anderson KJ, Syed TH, Swenson SC, Linage CR, Rodell M. Satellites measure recent rates of groundwater depletion in California's Central Valley. Geophysical Research Letters. 2011;**38**:L03403

[5] Döll P, Schmied HM, Schuh C, Portmann FT, Eicker A. Global-scale assessment of groundwater depletion and related groundwater abstractions: Combining hydrological modeling with information from well observations and GRACE satellites. Water Resources Research. 2014;**50**:5698-5720

[6] Werner AH, Gleeson T. Regional strategies for the accelerating global problem of groundwater depletion. Nature Geoscience. 2012;**5**:853-861

[7] Hsu HH, Chen CT, Lu MM, Chen YM, Chou C, Wu YC. Climate Change in Taiwan: Scientific Report 2011. New Taipei City, Taiwan: National Science and Technology Center for Disaster Reduction; 2011

[8] Hydrological Year Book of Water Resources Agency. Taipei: Ministry of Economic Affairs; 2013

[9] Brutsaert W, Nieber JL. Regionalized drought flow hydrographs from a mature glaciated plateau. Water Resources Research. 1977;**13**:637-643

[10] Szilagyi J, Parlang MB, Albertson JD. Recession flow analysis for aquifer parameter determination. Water Resources Research. 1998;**34**:1851-1857

[11] Mendoza GF, Steenhuis TS, Walter MT, Parlange JV. Estimating basin-wide hydraulic parameters of a semi-arid mountainous watershed by recession-flow analysis. Journal of Hydrology. 2003;**279**:57-69

[12] Tague C, Grant GE. Groundwater dynamics mediate low-flow response to global warming in snow-dominated alpine regions. Water Resources Research. 2009;**45**:W07421

[13] Zecharias YB, Brutsaert W. Recession characteristics of groundwater outflow and base flow from mountainous watersheds. Water Resources Research. 1988;**24**:1651-1658

[14] Vogel RM, Kroll CN. Regional geohydrologic-geomorphic relationships for the estimation of low-flow statistics. Water Resources Research. 1992;**28**:2451-2458

[15] Brutsaert W. Is Mongolia's groundwater increasing or decreasing? The case of the Kherlen River basin. Hydrological Sciences Journal. 2008;**53**:1221-1229

[16] Kirchner JW. Catchments as simple dynamical systems: Catchment characterization, rainfall-runoff modeling, and doing hydrology backward. Water Resources Research. 2009;**45**:5577-5596

[17] Sánchez-Murillo R, Brooks ES, Elliot WJ, Gazel E, Boll J. Baseflow recession analysis in the inland Pacific Northwest of the United States. Hydrogeology Journal. 2015;**23**:287-303

[18] Sugita M, Brutsaert W. Recent low-flow and groundwater storage changes in upland watersheds of the Kanto region, Japan. Journal of Hydrologic Engineering. 2009;**14**: 280-285

[19] Hughes JD, Petrone KC, Silberstein RP. Drought, groundwater storage and declining stream flow in southwestern Australia. Geophysical Research Letters. 2012;**39**:L03408

[20] Zhang L, Brutsaert W, Crosbie R, Potter N. Long-term annual groundwater storage trends in Australian catchment. Advances in Water Resources. 2014;**74**:156-165

[21] Brutsaert W. Long-term groundwater storage trends estimated from streamflow records: Climatic perspective. Water Resources Research. 2008;**44**:W02409

[22] Stoelzle M, Stahl K, Weiler M. Are streamflow recession characteristics really characteristic? Hydrology and Earth System Sciences. 2013;**17**:817-828

[23] Kendall MG. Rank Correlation Methods. London, England: Charles Griffin; 1975

[24] Mann HB. Non-parametric test against trend. Econometrica. 1945;**13**:245-259

[25] Sen PK. Estimates of the regression coefficient based on Kendall's tau. Journal of the American Statistical Association. 1968;**63**:1379-1389

[26] Pettit AN. A non-parametric approach to the change point problem. Journal of the Royal Statistical Society, Series C. 1979;**28**:126-135

[27] Tague C, Grant GE. A geological framework for interpreting the low-flow regimes of Cascade streams, Willamette River Basin, Oregon. Water Resources Research. 2004;**40**: W04303

[28] Hsu HH, Lo TT, Hung CW, Hung CC, Li MY, Chen YL, Huang WK, Lu MM, Sui CH. Climatic natural variability and interdecadal variation. Atmospheric Sciences. 2012;**40**: 249-295

[29] Lu MM, Cho YM, Lee SY, Lee CT, Lin YC. Climate variations in Taiwan during 1911–2009. Atmospheric Sciences. 2012;**40**:297-322

[30] Fan JC, Yang CH, Chang SC, Huang HY, Guo JJ. Effects of climate change on the potential of the landslides in the Basin of Kaoping Stream. Journal of Chinese Soil and Water Conservation. 2013;**44**:335-350

[31] Tsuang BJ, Chen HH, Wu MC, Liu CC. Regional climatic change in Taiwan. Journal of the Chinese Institute of Environmental Engineering. 1996;**6**:131-150

[32] Tu JY, Chou C, Chu PS. The abrupt shift of typhoon activity in the vicinity of Taiwan and its association with western north Pacific-East Asian climate change. American Meteorological Society. 2009;**22**:3617-3627

Chapter 5

Recharge and Turnover of Groundwater in Coastal Aquifers with Emphasis on Hydrochemistry and Isotopes

Gunnar Jacks and Satheesachandran Thambi

Additional information is available at the end of the chapter

http://dx.doi.org/10.5772/intechopen.73301

Abstract

Coastal aquifers are globally subject to considerable stress. The population density is often high in coastal areas, and in addition, the coastal plains often have good agricultural soils demanding irrigation. While a portion of the irrigation can be provided by rivers, local groundwater is also used adding to the water requirement. Many coastal aquifers are large with a slow turnover of the groundwater and recharge is difficult to assess. This review is aimed at giving an overview of the hydrochemistry with an emphasis of giving insight into the groundwater recharge and the sustainability of the groundwater quality. The past climate history has given an imprint of hydrochemistry of especially coastal aquifers.

Keywords: groundwater, aquifer, coastal, recharge, hydrochemistry, isotopes

1. Introduction

About 1 billion out of 7 billion people in the world live in coastal areas and rely on coastal aquifers for their water supply and irrigation [1]. A simple calculation of the water requirement can be done by assessing that the population density is 2000/km^2, a figure taken from the Kerala coast in SW India. With the proposed population density, each person has an area of 500 m^2 to reside on. The water need is dominated by the water requirement for food production and varies from 2500 l/day and person in developing countries to 5000 l/day in industrialized countries [2]. The water use in households is in the order of less than 200 l/day and person. If using the figure 2700 litres per day and person for total water demand, then this would be equal to a water requirement of around 2000 mm/year or of the same

order as the yearly rainfall in the actual area. Thus, even in rather rainfall-rich areas, coastal aquifers are subject to a considerable stress.

Coastal plains are often underlain by thick sediments, and they are complex intercalations of finer and coarser sediments formed under different climatic conditions. Looking back on the recent past climatic history, just a few thousands of years back, there have been large variations in sea level and locally, there have been considerable tectonic movements.

This review will be focused on using the hydrochemistry of the groundwater and isotopes to decipher the groundwater exchange in coastal aquifers. This approach is especially useful in coastal aquifers where salt water intrusion could complicate the picture. In view of the authors' experience, there will be a focus on South and Southeast Asia, however, with some examples from other regions such as Europe.

2. Groundwater recharge

Groundwater recharge can occur in different ways:

- recharged locally by rainwater
- recharged from coastal plain rivers
- being a mixture of intruded saltwater and freshwater

Local groundwater is in many places not sufficient to recharge the aquifers. There are many aquifers in semiarid areas that are overused. Examples are common in S and SE Asia. Megacities with groundwater supply have in several places salinity problems resulting from land subsidence like in Bangkok and Jakarta [3]. In view of the climate change foreseen, there will be increase in sea levels that will affect the balance between groundwater and seawater. Ericson et al. [4] have evaluated 40 deltas regarding the effective sea level rise (ESLR), which in their evaluation is a combined effect of sea level rise and subsidence of the deltas. The Bengal delta in Bangladesh and India is experiencing an ESLR rate as high as 25 mm/year, while the Mississippi delta in USA has a rate of around 10 mm/year. The sea level rise as such is in the order of 3.3 mm/year, and the rate is expected to increase in the coming decades [5]. Ericson et al. [4] estimate that by 2050, about 8.6 M people are at risk due to ESLR. Local conditions such as tectonic movements and land subsidence due to excessive groundwater extraction thus play a large role in the risk of saline intrusion into costal aquifers in coming years [3]. The shoreline displacements may have a variety of reasons such as neo-tectonic movements but also anthropogenic activities such as deforestation and increased erosion [6].

Fog water condensation is a rare mechanism of groundwater recharge, but it may play a limited role under specific conditions. An example is the Al-Qara Mountain behind the Salalah Plain in Oman [7]. The browsing of a large population of camels has caused the degradation of mountain forest and decrease in recharge. The local precipitation is 100 mm, and the fog collection now adds just 10 mm to the recharge.

http://dx.doi.org/10.5772/intechopen.73301

3. Groundwater recharged from rivers

This is a common case. To trace the river water into the aquifer is of interest to assess the recharge. In this case, isotope investigations may be of good use. In some cases, the river water has a specific composition not only regarding water chemistry but also regarding isotopes of some elements. This could be traced in the aquifer mirroring where the river is recharging the aquifer.

With a past history of saline groundwater being refreshed by recharge, there are cases with elevated chloride ratio that could be interpreted as salt water intrusion. If the recharge occurs in a located area giving kind of a piston flow, a sequence of defined water types could be observed. These water types range from a typical fresh water of Ca-HCO_3 type via a Na-HCO_3 type to a brackish mixed type of water. The Na-HCO_3 type is formed by ion exchange, the Na-saturated aquifer material from the saline period, picks up calcium from the fresh recharged water and releases sodium into the groundwater. This is observed in a Tertiary aquifer on the Kerala coast in India [8] and in the Tertiary and Cretaceous aquifers in Tamil Nadu [9] (**Figure 1**).

If the recharge area is scattered, not creating piston flow of recharge, mixtures of water types are found [10, 11].

Elevated chloride levels in the local Kerala Tertiary aquifer [8] were in places caused by diffusion of chloride from intercalated clay beds. Drilling and sampling of sediments, sand, and intercalated clay showed that the pore water in the clay contained elevated salinity with chloride that diffused into the surrounding coarser sediments (**Figure 2**).

This could also be seen by plotting the $\delta^{18}O$ ratio in the water versus chloride. There was no mixing line toward sea water composition, but the $\delta^{18}O$ ratios remained constant irrespective of the chloride concentration (**Figure 3**) (**Table 1**).

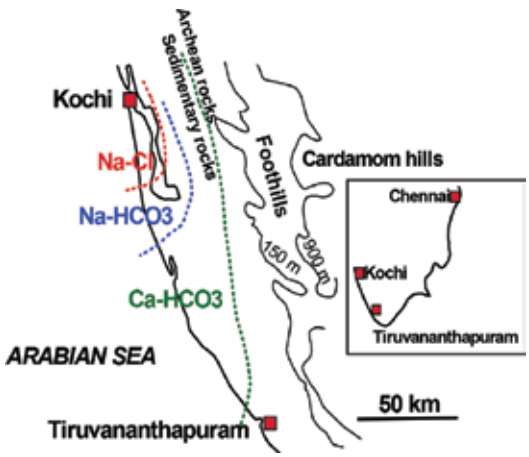

Figure 1. Water types in the Kerala Tertiary coastal aquifer resulting from flushing by recharge before the Last Glacial Maximum. The Precambrian, under-laying the Tertiary strata, are faulted in the SE-NW direction, which also guides the recharge in the same direction.

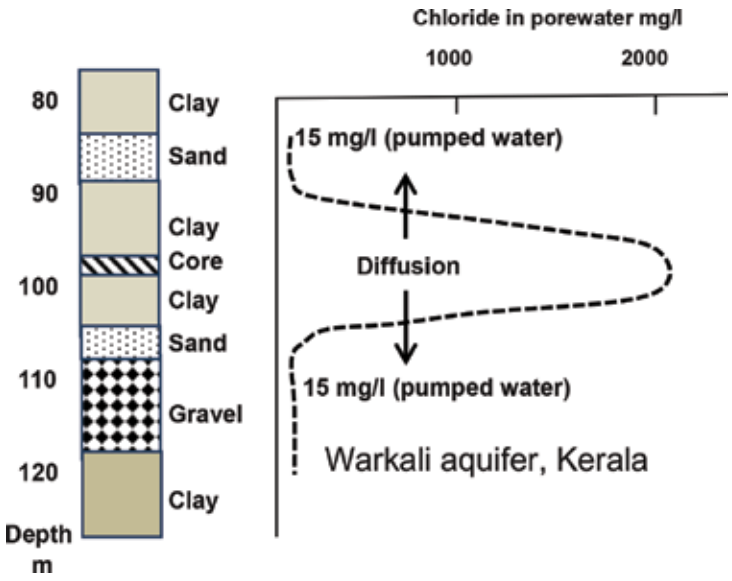

Figure 2. Residual pore water chloride in a clay layer dating back from a previous saline period was found in the Kerala coastal aquifers. The pore water was extracted from the core in the center of the clay layer.

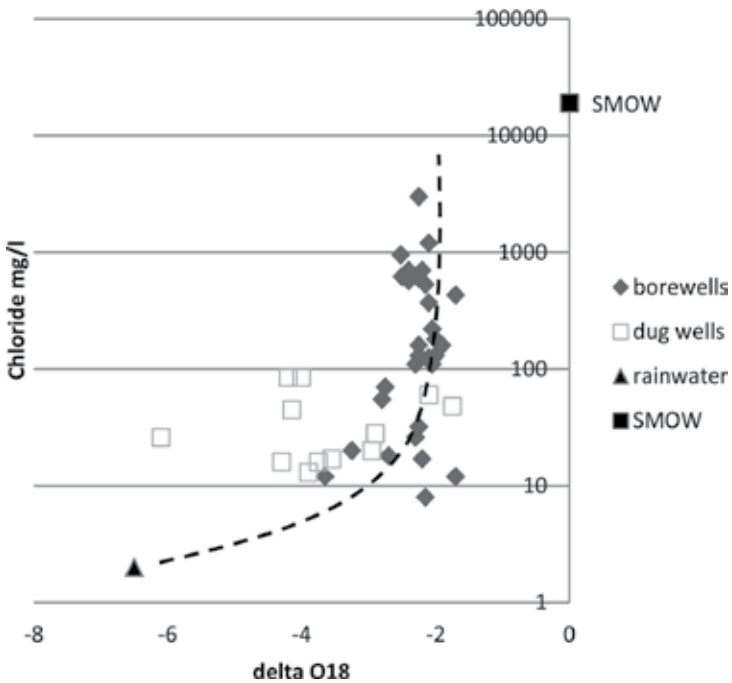

Figure 3. $\delta^{18}O$ ratios in groundwater plotted versus chloride. Data from Kerala coastal aquifers. There is no mixing in of sea water, but the increase of chloride above about 80–100 mg/l is likely to come from pore water in clay layers as is seen in **Figure 2**.

Sample	δD (‰)	$\delta^{18}O$ (‰)	Chloride (mg/l)
1	−44.20	−7.46	4.9
2	−43.85	−7.14	10.0
3	−44.52	−7.36	146
4	−44.83	−7.83	995
5	−48.12	−7.04	76
6	−47.12	−7.75	60.1
7	−43.10	−9.30	1220
8	−46.15	−8.35	392
9	−44.82	−8.22	819
10	−44.32	−8.46	191
SMOW	0.00	0.00	19,345

Table 1. δD and $\delta^{18}O$ in groundwater in Mati Plain in Albania have no relationship with chloride concentration showing that sea water intrusion is not the source of chloride.

The groundwater in Mati coastal plain in the northern Albania serves as water source for about 400,000 people, and there was a concern that this pumping rate may cause salt water intrusion [12]. In the catchment, there are several abandoned and active copper mines and the sulfate in river has an isotopic ratio typical of sulfides. This could be traced over large areas of plain showing that the recharge from the river is good. Close to the seaside, there were elevated chloride and sulfate levels that could be of old sea water origin. The $\delta^{34}S$ ratio was 24‰, thus well over the sea water ratio at 21‰. This can be explained by sulfate reduction in the intercalated clay layers (**Figures 4** and **5**). Thus, sea water intrusion is not a current threat.

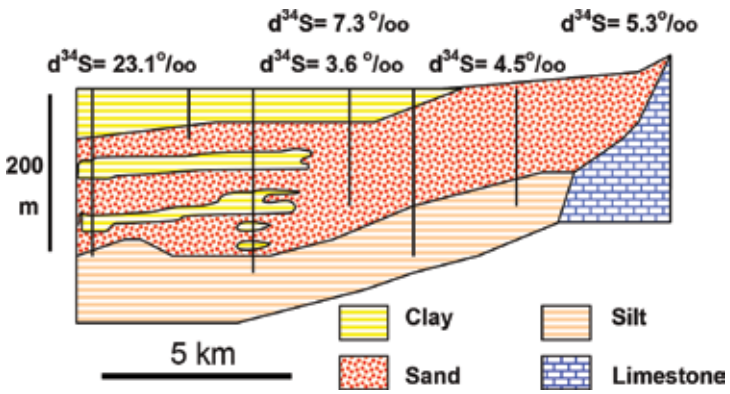

Figure 4. Cross section of the Mati Plain aquifer in Albania with $\delta^{34}S$ ratios in groundwater [12]. In the plain, the $\delta^{34}S$ ratios are mirroring recharge from river Mati, which has a $\delta^{34}S$ ratio mirroring sulfide oxidation in mining areas in the catchment. The left well, close to the seaside, has a $\delta^{34}S$ ratio above the sea water, likely to be caused by sulfate reduction in clay layers.

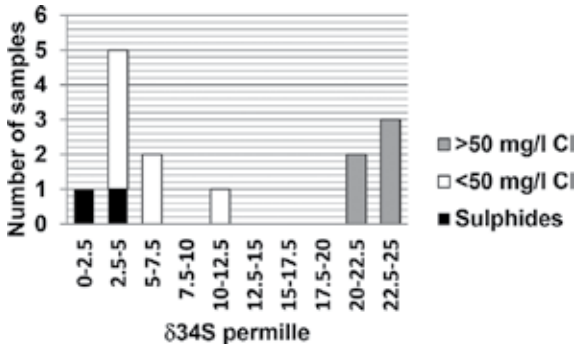

Figure 5. Staple diagram with $\delta^{34}S$ ratios in groundwater indicating recharge from the river Mati with sulfate having sulfide origin from oxidation of waste rock from copper mines [12]. The high $\delta^{34}S$ ratios in sea near wells are above the sea water ratio (21‰), which indicates sulfate reduction in intercalated clay layers. The black bars are samples from copper mine waste in the catchment.

4. Measures to halt sea water intrusion

Where sea water intrusion is already a fact, there are measures to halt it. First of all, groundwater extraction should be diminished. While there are no visible signs of sea water intrusion in the Kerala Tertiary aquifers, there is a gradual development of surface water utilization for the larger towns in the coastal plain, which is a good measure to protect the coastal aquifers. On the Indian east coast, this is more difficult as the river flows are lesser there. Ballykraya and Ravi [13] describe the creation of a barrier by artificial recharge near the coast. A similar measure has been taken in the Salalah plain by well recharge of treated waste water along the coast line [14, 15]. A new approach, which could be more efficient, is when fresh water recharge into the nonsaline part of the coastal aquifer is combined with pumping of saline water near the shoreline [16].

5. Effects of past climate change

The last glaciation has implied large variations in sea level, in the order of 125 m. Several areas that were under the sea level in preglacial time were drained from the sea during the Last Glacial Maximum (LGM).

This could enhance the recharge with fresh water. A Tertiary aquifer on the Kerala coast in SW India has groundwater dates varying between 23 and 34 kA BP (kA BP = kilo-annum, thousands of years before present) [8] and should thus have been recharged just before LGM. This is reasonable as the head for recharge was large, 60–80 m. However, just before LGM, the recharge has obviously been interrupted. In this case, the paleoclimatic conditions seem to have promoted the recharge during a wet SW monsoon which just before LGM was interrupted by a dry monsoon (**Figure 6**).

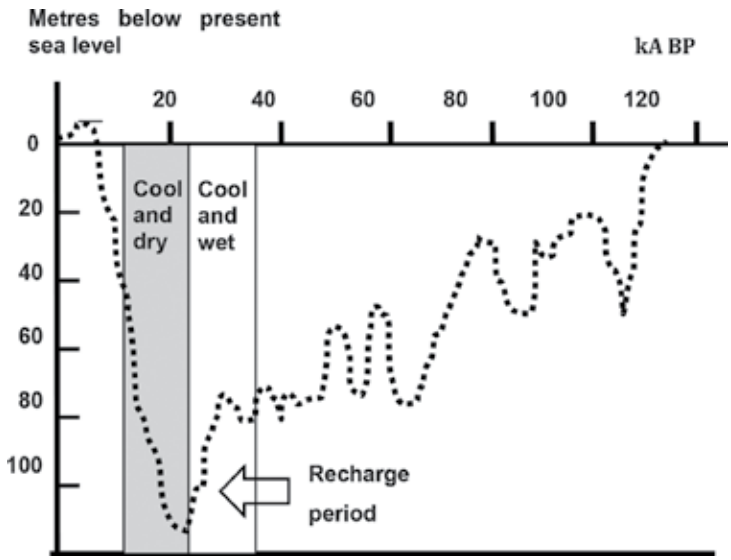

Figure 6. Sea water levels during the last glacial period. The SW monsoon had, as per the abundant paleoclimatological data published, a wet period before LGM followed by a dry period after the LGM.

Other aquifers on the Indian east coast has groundwater of a similar age and the same period and mechanisms of recharge may apply [9, 17]. The paleoclimatic data from India are abundant from both marine sediments as well as local pockets on current land illustrating the variations in the strength of the SW monsoon [18–23].

The past climate change has, in several aquifers near sea, formed a sequence of Ca-HCO_3 → Na-HCO_3 → Na-Ca-Cl types of groundwater formed by flushing of an initially formed saline/brackish aquifer by fresh water [24, 25]. This could be seen laterally in Kerala (**Figure 1**). The direction of the recharge flow is from SE toward NW directed by the topography of the underlying Precambrian, which is likely to be intersected by faults in the same direction. The same zonation is seen depth-wise for instance in the Mekong river delta and in the Red River delta in Vietnam [26].

A secondary effect of flushing is that the softening effect of the process creates Na-HCO_3 type of groundwater (**Figure 7**) which tends to mobilize fluoride [27–30]. Where the recharge is less of a "piston flow" process, there will be more mixed forms of groundwater types. This is often the case on the Indian SE coast where the sedimentology is more intricate [10, 11].

Another effect of the last glaciation is the common occurrence of arsenic in groundwater in Holocene sediment, for instance not only in the Bengal delta [31–36] but also in other coastal plains in S and SE Asia [37–39] like in the Mekong river delta, the Red River delta, and the Irrawaddy river delta. When the sea level was lowered before Last Glacial Maximum (LGM) at around 18 kA before present, the sediments were subject to erosion and redeposition and this lowered the organic matter content [39]. Contrarily, after LGM, the sea level rose and created abundant wetlands rich in organic matter [40]. These sediments become easily anoxic with reduction of ferric oxyhydroxides and mobilization of arsenic into groundwater [41].

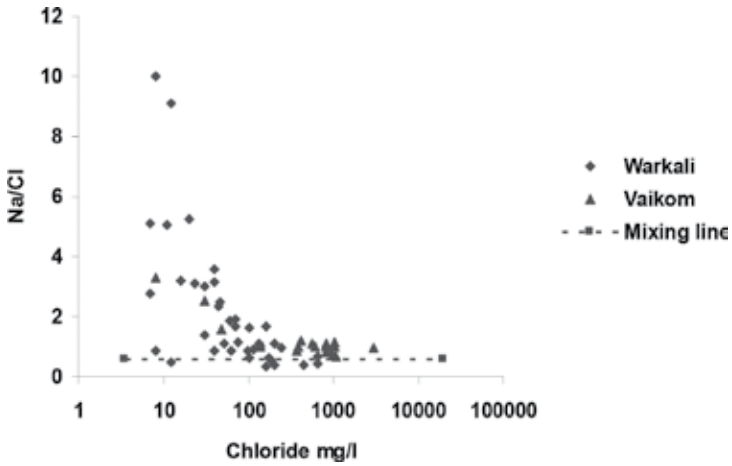

Figure 7. Na/Cl ratios versus chloride, showing the mobilization of sodium during the late stage of fresh water flushing. When the fresh water stage is approached, there is mobilization of sodium creating a Na-HCO_3 type of water often with elevated levels of fluoride.

6. Conclusions and summary

Coastal aquifers and their recharge is a crucial issue for approximately 1 billion people who are living on coastal plains globally. Due to high population density and high water demand for domestic and more so for food production, there is a high stress on the water resources. There are modeling tools that can be used to assess the sustainability of the groundwater in coastal aquifers, but in addition, hydrochemistry and isotopes may be a substantial help in the assessment, especially in costal aquifers where a possible sea water intrusion adds to the complexity. Dating, mostly by ^{14}C methodologies gives reliable results adding to the assessments of the groundwater turnover [42]. For aquifers that that have a past memory of salinity, there may be a good relationship between age and chloride levels, chloride which is retained in parts of the aquifer where groundwater turnover is slower (**Figure 8**). Chloride in this case, as is shown in **Figure 2**, is not derived from salt water intrusion. For shorter turnover rates, tritium is used especially after the bomb tests in the 1960s has faded out [43].

Elevated salt content in coastal aquifers could have many sources in addition to salt water intrusion. A common case is found in coastal aquifers that consist of sand and gravel intercalated with clay layers. As the groundwater turnover is slow, often in the range of thousands of years, there might still be more or less saline pore water in the clay layers that continue to diffuse into the coarser material (**Figure 8**). In some, there is sulfate reduction in the clay due to elevated organic matter content and this is mirrored as elevated $\delta^{34}S$ ratios.

The often intricate mixtures of water and dissolved salt in coastal aquifers could be interpreted by suitable isotopes such as δD, $\delta^{18}O$, $\delta^{34}S$, if different sources of the isotope ratios can be traced back to the source of the water. A good example is $\delta^{34}S$ on a coastal aquifer in Albania where there were two main sources, sulfide-related sulfate from mines and sulfate in the groundwater formed by sulfate reduction in intercalated clay layers in the aquifer. A common feature often formed by flushing in postglacial time of formerly saline aquifers is the

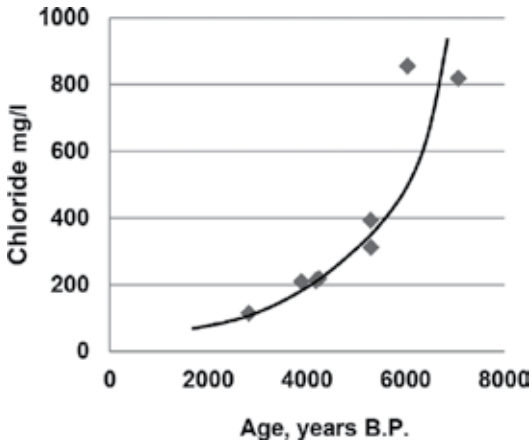

Figure 8. Age of groundwater in the Mati plain aquifer related to the chloride levels [12]. The slow turnover rate has left portion of the aquifer with elevated chloride levels.

appearance of specific water such as $NaHCO_3$ formed by ion exchange. At the end of the flushing period, there is a pronounced increase in the Na/Cl ratio formed by the uptake of calcium in the fresh water recharge and release of sodium at adsorption sites from the saline period.

Abbreviations

^{18}O	$^{18}O/^{16}O$ for oxygen isotopes
ESLR	Effective sea level rise
ka BP	Thousands of years before present
LGM	Last Glacial Maximum
SMOW	Surface mean ocean water
SW monsoon	Southwest monsoon
$\delta^{34}S$	$^{34}S/^{32}S$ ratio for sulfur isotopes
δD	Isotopic ratio for hydrogen isotopes ($^{2}H/H$ or deuterium/common hydrogen)

Author details

Gunnar Jacks[1]* and Satheesachandran Thambi[2]

*Address all correspondence to: gunnjack@kth.se

1 Royal Institute of Technology (KTH), Stockholm, Sweden

2 Central Groundwater Board of India, Thiruvananthapuram, Kerala, India

References

[1] Walton B. Here comes the sea: The struggle to keep the ocean out of California's coastal aquifers. http://www.circleofblue.org/2015/world/here-comes-the-sea-the-struggle-to-keep

[2] Chapagain AK, Hoekstra AY. Water footprints of nations. UNESCO-IHE, Inst. for water education. Main report. Vol. 1. 75 pp

[3] Onodera S, Saito M, Sawano M, Hosono T, Taniguchi M, Shimada J, Umezawa Y, Lubis RF, Buapeng S, Delinom R. Effects of intensive urbanization on the intrusion of shallow groundwater into deep groundwater: Examples from Bangkok and Jakarta. Science of the Total Environment. 2008;**404**:401-410

[4] Ericson JP, Vörösmarty CJ, Dingman SL, Ward LG, Meybeck M. Effective sea-level rise and deltas: Causes of change and human dimension implications. Global and Planetary Change. 2006;**50**:63-82

[5] Chen X, Zhang X, Church JA, Watson CS, King MA, Monselesan D, Legresy B, Harig C. The increasing rate of global mean sea-level rise during 1993-2014. Nature Climate Change. 2017;**7**:492-495

[6] Fouache E, Vella C, Dimo L, Gruda G, Mugnier J-L, Denèfle M, Monnier O, Hortyat M, Huth E. Shoreline displacement since Middle Holocene in the vicinity of the ancient city Apollonia (Albania, Seman and Vjosa deltas). Quaternary International. 2010;**216**:118-128

[7] Shammas M. Impact of the AlQara mountain fogwater forest on groundwater recharge in the Salalah paain. Sultanate of Oman. Ecohydrology and Hydrobiology. 2007;**7**(1):37-49

[8] Jacks G, Thambi DSC. Hydrochemistry of the Kerala coastal aquifers. In: A. Mukherjee, editor. Groundwater in Asia. Berlin: Springer Verlag; 2018. in print

[9] Sukhija BS, Varma VN, Nagabushanam P, Venkat Reddy D. Differentiation of palaeomarine and modern seawater intruded in coastal groundwaters of Karaikal and Tanjavur, India based on inorganic chemistry organic biomarker fingerprints and radioactive dating. Journal of Hydrology. 1996;**174**:173-201

[10] Thilagavathi R, Chidambaram S, Prasanna MV, Thivya C, Singaraja C. A study on groundwater geochemistry and water quality in layered aquifer systems of Pondicherry region, Southeast India. Applied Water Science. 2012;**2**:253-269

[11] Sonkamble S, Chandra S, Ahmed S, Rangarajan R. Source speciation resolving hydrochemical complexity of coastal aquifers. Marine Pollution Bulletin. 2014;**78**:118-129

[12] Kumanova X, Marku S, Fröjdö S, Jacks G. Recharge and sustainability of a coastal aquifer in northern Albania. Hydrogeology Journal. 2013;**22**:883-892

[13] Ballykraya PN, Ravi R. Natural fresh-water ridge as barrier against sea-water intrusion in Chennai city. Journal of the Geological Society of India. 1998;**52**(3):279-286

[14] Shammas M, Jacks G. Seawater intrusion in the Salalah plain aquifer, Oman. Environmental Geology. 2007;**53**(3):575-587

[15] Shammas M. The effectiveness of artificial recharge in combatting seawater intrusion in Salalah coastal aquifer, Oman. Environmental Geology. 2008;**55**:191-204

[16] Abdoulhalik A, Ahmed A, Hamill GA. A new physical barrier system for seawater intrusion control. Journal of Hydrology. 2017;**549**:416-427

[17] Sukhija BS, Venkat Reddy D, Nagabushanam P. Isotopic finger prints of palaeoclimates during the last 30 000 years in deep confined groundwater of southern India. Quaternary Research. 1998;**50**:252-260

[18] Jayalahshmi K, Nair KM, Kumar H, Santosh M. Late Pleistocene-Holocene palaeoclimate history of the southern Kerala basin, southwest India. Gondwana Research. 2004;**7**(2): 585-594

[19] Juyal N, Chamyal IS, Bhandari S, Bhushan R, Singhvi AK. Continental record of the southwest monsoon during the last 130 kA: Evidence from the southern margin of the Thar desert, India. Quaternary Science Reviews. 2006;**25**:2632-2650

[20] Juyal N, Pant RK, Basaviah N, Bhushan R, Saini NK, Yadava MG, Singhvi AK. Reconstruction of the Last Glacial to early Holocene monsoon variability from relict lake sediments of the Higher Central Himalya, Uttarakhand, India. Journal of Asian Earth Sciences. 2009;**34**:437-449

[21] Agrawal S, Sanyal P, Sarkar A, Jaiswal MK, Dutta K. Variability of Indian monsoonal rainfall over past 100 kA and its implication for C_3-C_4 vegetational change. Quaternary Research. 2012;**77**:159-170

[22] Kumaran KPN, Limaye RB, Punekar SA, Rajaguru SN, Jashi SV, Karlekar SN. Vegetation response to South Asian Monsoon variations in Konkan, western India during late Quaternary: Evidence from fluvio-lacustrine archives. Quaternary International. 2013; **286**:3-18

[23] Huang C, Wei G, Ma J, Liu Y. Evolution of the Indian summer monsoon during the interval 32.7-11.4 kA BP: Evidence from the Baoxiu peat, southwest China. Journal of Asian Earth Sciences. 2016;**131**:72-80

[24] Agerstrand T, Hansson G, Jacks G. Effect on groundwater composition of sequential flushing with fresh and saline water. In: Proc. of the 7th Salt Water Intrusion Meeting, Uppsala, Sweden 1981. http://www.swim.site.nl/pdf.swim07html

[25] Mercado A. The use of hydrogeological patterns in carbonate sand and sandstone aquifers to identify intrusion and flushing of saline water. Ground Water. 1985;**23**(5):635-645

[26] Kim J, Kim K, Thao NT, Batsaikhan B, Yun S. Hydrochemical assessment of freshening saline groundwater using multiple end members model: A study of the Red River aquifer, Vietnam. Journal of Hydrology. 2017;**549**:703-714

[27] Jacks G, Bhattacharya P, Chaudhary V, Singh KP. Controls on the genesis of some high-fluoride groundwaters in India. Applied Geochemistry. 2005;**20**:221-228

[28] Dhaniya Raj, Shaji E. Fluoride contamination in groundwater resources of Alleppey, southern India. Geoscience Frontiers. 2016. DOI: http://dx.doi.org/10.1016/j.gsf.2016.01.002

[29] Berger T, Mathurin FA, Drake H, Åström M. Fluoride abundance and controls in fresh groundwater and bedrock fractures in an area with fluoride rich granitoid rocks. Science of the Total Environment. 2016;**560-570**:948-960

[30] Jacks G. Chapter 15 in Four Decades of Groundwater Research in India. In: Thangarajan M. editor. Fluoride in Groundwater—Mobilization, Trends and Remediation. UK, England: CRC Press

[31] Ghosh D, Routh J, Dario M, Bhadury P. Elemental biomarkers characteristics in a Pleistocene aquifer vulnerable to arsenic contamination in the Bengal Delta Plain, India. Applied Geochemistry. 2015;**62**:87-98

[32] Acharyya SK, Lahiri S, Raymahashay BC, Bhowmik A. Arsenic toxicity of groundwater in parts of the Bengal basin and Bangladesh. The role of Quaternary stratigraphy and Holocene sea-level fluctuation. Environmental Geology. 2000;**39**:1127-1137

[33] Acharyya SK. Arsenic levels in groundwater from Quaternary alluvium in the Ganga Plain and the Bengal Basin, Indian Subcontinent: Insights into influence of statigraphy. Gondwana Research. 2005;**8**(1):55-66

[34] Al Lawati WM, Rizoulis A, Eiche E, Boothman C, Polya D, Lloyd JR, Berg M, Vasquez-Aguilar P, van Dongen BE. Characterization of organic matter and microbial communities in contrasting arsenicrich Holocene and arsenic-poor Pleistocene aquifers, Red River Delta, Vietnam. Applied Geochemistry. 2012;**27**:315-325

[35] Hossein M, Bhattacharya P, Frape SK, Jacks G, Islam MM, Rahman MM, von Brömssen M, Hasan MA, Ahmed KM. Sediment colour tool for targeting arsenic-safe aquifers for the installation of shallow drinking water tubewells. Science of the Total Environment. 2014;**493**:615-625

[36] Kulkarni HV, Mladenov N, Johanneson KH, Datta S. Contrasting dissolved organic matter quality in groundwater in Holocene and Pleistocene aquifers and implications for influencing arsenic mobility. Applied Geochemistry. 2017;**77**:195-205

[37] Hoang TH, Bang S, Kim K-W, Nguyen MH, Dang DM. Arsenic in groundwater and sediment in the Mekong river delta, Vietnam. Environmental Pollution. 2010;**158**:2648-2658

[38] Norrman J, Sparrenbom C, Berg M, Nguyen MH, Dang DM. Arsenic in groundwater and sediments in the Mekong river delta, Vietnam. Applied Geochemistry. 2015;**61**:248-258

[39] Stuckey JW, Sparks DL, Fendorf S. Delineating the convergence of biogeochemical factors responsible for arsenic release to groundwater in South and Southest Asia. Advances in Agronomy. 2016;**140**:43-74

[40] Jacks G, Thambi DSC. Groundwater memories of past climate change—Examples from India and the Nordic countries. Advances in Agronomy. 2017;**3**:49-57

[41] Bhattacharya P, Chatterjee D, Jacks G. Occurrence of arsenic in groundwater in alluvial aquifers from delta pklains, eastern India: Options for safe drinking water supply. International Journal of Water Resources Development. 1997;**13**:79-92

[42] Pearson FJ, Hanshaw BB. Sources of dissolved carbonate species in groundwater and their effects on carbon 14 dating. In: Isoptope Hydrology. Vienna: IAEA. 1970. pp. 271-285

[43] Kralik M. How to estimate mean residence times for groundwater. Progress in Earth and Planetary Science. 2015;**13**:301-306

Chapter 6

Hydrochemical Investigation and Quality Assessment of Groundwater in the BouHafna-Haffouz Unconfined Aquifers, Central Tunisia

Hatem El Mejri, Amor Ben Moussa,
SarraBel Haj Salem and Kamel Zouari

Additional information is available at the end of the chapter

http://dx.doi.org/10.5772/intechopen.72173

Abstract

Multivariate statistical techniques were applied to improve the understanding of the aquifers hydrodynamic and to identify the natural and anthropogenic processes that control the BouHafna and Haffouz groundwater quality. Some other parameters, such as sodium adsorption ratio (SAR), percent sodium (%Na), residual sodium carbonate (RSC), and permeability index (PI), were used to examine the suitability of groundwater for irrigation applications. Groundwater samples are classified into Ca-Mg-HCO_3 and Ca-Mg-SO_4 water-type. The statistical investigation permits to identify three different groups. The first group reflects the influence of water-rock interaction in relation with the dissolution of evaporatic minerals, the cation exchange process with phyllosilicates and the dedolomitization. The second and third groups, including the weakly mineralized groundwater samples, suggest, firstly, that the return flow of irrigation waters has a small, but not negligible contribution to the groundwater contamination, and secondly, the reduction of nitrate (NO_3) to nitrogen gas (N_2). Furthermore, it has been demonstrated that the majority of the groundwater samples are suitable for irrigation uses.

Keywords: Central Tunisia, statistical techniques, water-rock interaction, dissolution, cation exchange, suitable, irrigation uses

1. Introduction

In most parts of Central Tunisia, and particularly in Haffouz and BouHafna regions, groundwater has played a fundamental role in shaping the social and economic development.

Due to rapid demographic growth and agricultural progress, exploitation of groundwater has increased dramatically to provide drinking water to rural community, support irrigation, and maintain ecosystems. During the past 30 years, the exponential increase in water abstraction from Haffouz and BouHafna aquifers has caused ground water depletion, a term often defined as long-term water-level declines, and an increase in salinity of groundwater pumped from wells situated mainly downstream. On the other hand, recent changes in agricultural land use and irrigation may result in groundwater contamination throughout agricultural fertilizers and pesticides applied to fields. Therefore, information about irrigation groundwater quality is critical to the understanding of necessary management changes for long-term productivity [1]. Proper assessment of groundwater sustainability requires understanding and quantification of human effects on water resources using analysis, application of management practices, and revision.

Within this framework, a combined hydrogeological and hydro-chemical data were examined, using statistical methods, to determine (i) natural and anthropogenic processes that control the groundwater mineralization; (ii) the origin of different water bodies and their sources of recharge; and (iii) to assess the suitability of groundwater for agricultural purposes.

2. General features

The Haffouz study areas, which make up part of the Kairouan plain in Central Tunisia, cover about 1192 Km^2 and lie between longitudes 39G 55′ and 39G 70′ north and latitudes 7G 88′ and 8G 33′ east (**Figure 1**). This region is bounded by Ouesselat and Jebil Mountains in the north, the Trozza Mountain in the south, and the plain of El Ala in the west. The altitude of the study area ranges from 200 m a.m.s.l. at Haffouz plain to 997 m at Trozza Mountain. The study area has a semi-arid climate with mild, wet winters and warm, dry summers [2]. The average monthly temperature varies between a minimum of 10.15°C measured in January and a maximum of 33.07°C measured in August. It receives an annual rainfall ranging between 300 and 500 mm/year. The annual total evaporated exceeds 1720 mm Piche [3].

The drainage network consists of several nonperennial Wadis such as Mourra, 55 Zabbes, and MsilahWadis that drain toward the Merguellil Wadi, the most important Wadi of the Kairouan plain [2] (**Figure 5**).

2.1. Geological setting

Several geologic studies [4–11] have focused on the stratigraphy, structure, and surficial and subsurface deposits characteristics in the study district. As shown in the geologic map and in the lithostratigraphic column, the geological formations, which outcrop in the study area, are represented by sedimentary series ranging from the Trias to the Quaternary (**Figures 1** and **2**). The Trias deposits, which outcrop in Cherichira Mountain, consist mainly of an alternation of gypsum, clay, and carbonate levels [6]. The Cretaceous units that outcrop in the foot of Trozza

http://dx.doi.org/10.5772/intechopen.72173

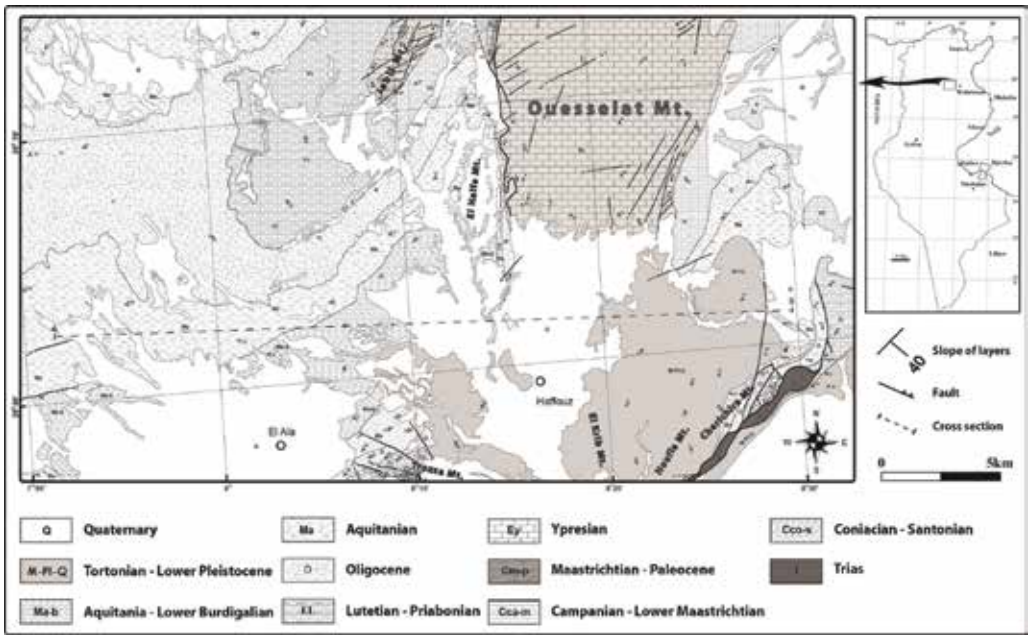

Figure 1. Location and geological map of the study areas.

Mountain are constituted of the Yprisian limestone of AlagAbiod and El Metlaoui formations. These formations are covered by the Lutetian limestone and clay of Cherahil and Souar formations, respectively. On the Lutetian deposits, the sandy and sandstone units of the Oligocene repose with an average thickness of about 350 m. These deposits belong to the Fortuna formation out crop in the central part of the study area. The Miocene deposits are represented by thick calcareous and clayey layers, which correspond to A in Grab and Mahmoud formations, respectively. These formations are overlaid by the sandy clay of the Beglia Formation and the clay Saouaf Formation. The Quaternary sediments that are represented by sand, clay, and conglomerate deposits occur in the plains of El Ala and Haffouz and in the Merguellil Wadi depression.

Structurally, the BouHafna basin is bordered to the east by the major fault of Ouesselat Mountain and corresponds to a syncline structure, which consists of the sandy deposits of Fortuna Formation. However, the Haffouz region, which is limited by the faults F1 in the east and F2 in the west, corresponds to a Graben structure filled by the sand, sandstone, sandy clay, and clay of Mio-plio-quaternary (**Figure 3**).

2.2. Hydrogeological setting

The BouHafna aquifer is lodged in the sand and sandstone deposits of the Oligocene. This aquifer, which is unconfined overall the basin, has a thickness varying largely from 50 to

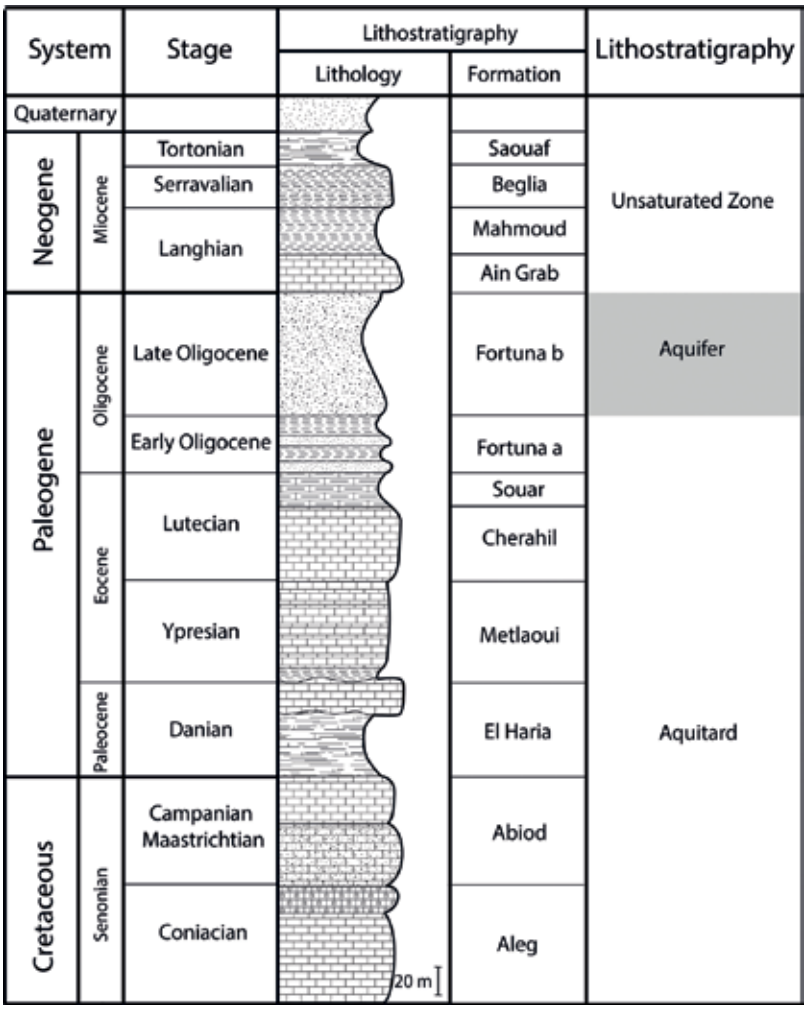

Figure 2. Simplified lithostratigraphic column of the study areas.

300 m. The bedrock of this aquifer is constituted of the Lutetian marly deposits of Souar Formation (**Figure 3**). Nevertheless, the Haffouz unconfined aquifer is constituted of the Mio-Plio-82 Quaternary detrital deposits with a thickness of about 1000 m.

The piezometric map (**Figure 4**) shows that the general directions of groundwater flow are N-S, NW-SE, and W-E in the case of BouHafna aquifer, and they are oriented NW and NE in the case of Haffouz aquifer. This may indicate that the recharge of BouHafna aquifer occurs in the Western part of the basin and in the pediment of Ouesselat and Jebil Mountains, where the Oligocene sediments outcrop largely. For the Haffouz region, rainwater infiltrates and recharges the aquifer, locally, in the pediment of Ouesselat Mountain. The hydraulic gradient of BouHafna and Haffouz aquifers varies from 0.009 to 0.003, highlighting the importance of localized recharge in the pediment of mountains, in the northern part, and the linear recharge by the Merguellil Wadi, in the southern part of the region. This variation of hydraulic gradient can also be explained by the lateral variation of lithology caused by abundance of clayey layer, especially in the south of this aquifer.

http://dx.doi.org/10.5772/intechopen.72173

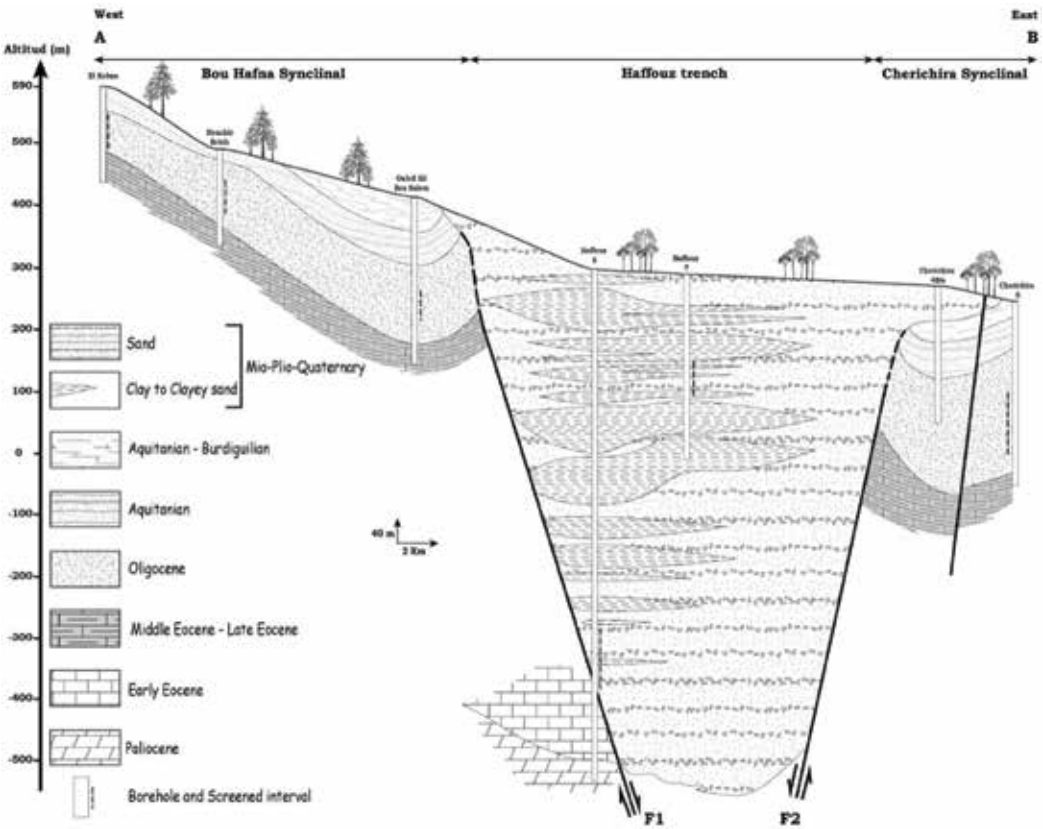

Figure 3. Hydrogeological cross section of Haffouz and BouHafna aquifers.

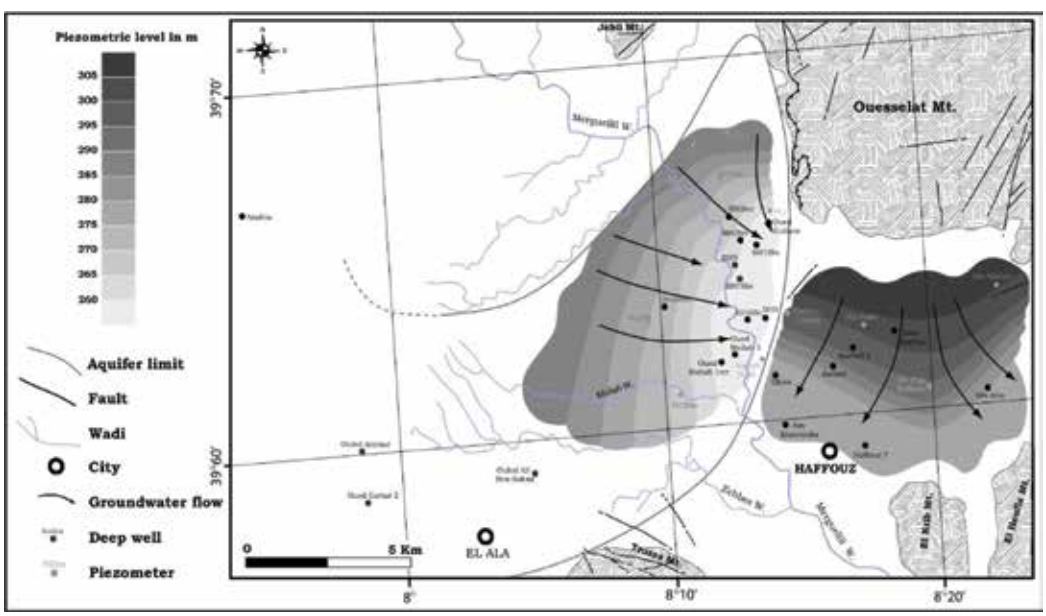

Figure 4. Piezometric and sampling map of Haffouz and BouHafna aquifers [12, 13].

3. Sampling and analytical methods

A total of 22 boreholes were sampled for chemical analysis, 15 samples collected from the BouHafna aquifer and 7 samples from the Haffouz aquifer. The physicochemical parameters such as Temperature (T°C), pH, and electrical conductivity (EC) were measured directly in situ using portable meters. Groundwater samples were analyzed for major ions in the laboratory of Radio-Analyses and Environment of the school of engineers of Sfax, Tunisia. Major cation concentrations were determined by Waters Ion chromatograph using IC-PakTM CM = D columns. Major anion concentrations were measured using a Metrohm ion chromatograph equipped with CI SUPER-SEP columns. The analysis of bicarbonate was undertaken by titration to the methyl orange endpoint.

4. Results and discussion

4.1. In situ measurements interpretation

The physicochemical parameters and overall hydrochemical data of Haffouz and BouHafna groundwater samples are presented in **Table 1**. Groundwater temperature values are relatively homogenous and vary from 19.9 to 25.3°C. The pH measurements range between 7.39 and 7.73 for Haffouz aquifer and between 7.01 and 7.74 for BouHafna aquifer. This may indicate a neutral to slightly alkaline pH but suitable for drinking and agricultural purposes. Electrical conductivity (EC) values, which vary in a wide range between 422 and 1623 μS/cm, are probably related to the signification variation of the TDS values that range from 203 to 1188 mg/l, respectively.

Aquifer	Well	Cl	NO3	SO4	HCO3	Na	K	Mg	Ca	pH	TDS (mg/l)	EC (µs/cm)	T°C
		(mg/l)											
Haffouz	AK	50,00	1,50	50,00	219,00	27,40	2,12	13,20	73,50	7,53	400,00	520,10	19,90
	AZ	42,00	1,90	60,00	219,00	35,70	2,05	12,60	69,05	7,73	464,00	510,10	20,00
	DH	57,00	0,70	60,20	235,00	39,10	2,55	21,50	79,30	7,53	400,00	834,00	20,10
	JA	24,62	4,06	28,86	213,50	37,98	2,72	22,52	34,00	7,49	240,00	484,00	21,70
	H 7	25,88	8,15	17,04	213,50	45,21	1,46	10,34	38,50	7,81	216,00	481,00	22,00
	DEB	20,81	8,49	11,31	213,50	20,75	1,06	9,86	46,10	7,46	203,00	422,00	21,60
	M 1	17,23	0,00	7,26	244,00	21,53	0,97	9,70	49,00	7,39	207,00	436,00	24,70
Bou Hafna aquifer	BH 4bis	57,75	17,46	151,92	250,10	38,50	2,05	31,07	85,00	7,47	579,00	939,00	23,90
	BH 8	71,21	12,67	161,51	208,60	51,50	2,45	38,51	75,00	7,11	516,00	945,00	24,10
	OM 1 ter	191,36	10,47	512,37	225,70	97,42	3,44	59,17	154,00	7,14	1188,00	1623,00	22,80
	BH 2 ter	75,35	9,07	213,18	268,40	58,38	3,78	41,74	117,44	7,31	655,00	1074,00	24,70
	OEG 2	57,40	8,56	51,79	195,60	39,57	1,82	19,23	51,10	7,01	337,00	596,00	22,40
	BH 7 bis	57,49	14,23	113,97	225,70	48,58	2,43	34,26	60,85	7,19	426,00	845,00	24,60
	EA	35,05	20,23	50,17	219,60	39,96	2,67	21,75	36,10	7,34	305,00	611,00	22,70
	AO	50,22	16,37	89,17	256,20	42,12	1,90	25,57	60,50	7,21	431,00	767,00	22,00
	BH 3 ter	96,89	9,01	383,54	231,80	109,42	4,01	60,07	105,00	7,14	1089,00	1594,00	24,40
	BH 9	49,86	12,41	95,70	244,00	46,94	2,12	28,54	55,65	7,22	386,00	733,00	22,60
	BH 1 bis	81,53	7,52	202,66	280,60	59,37	3,19	42,30	95,35	7,26	668,00	1085,00	25,30
	OABS	53,94	10,38	58,39	219,60	38,95	1,90	22,51	55,90	7,09	367,00	664,00	23,80
	OA	70,48	25,42	124,14	231,80	48,21	2,92	38,26	61,53	7,74	511,00	913,00	23,50
	OM 1	58,88	9,21	144,81	237,90	51,87	2,46	30,35	61,78	7,23	471,00	852,00	23,80
	OEG	65,95	31,10	61,23	268,40	59,23	1,58	17,72	64,50	7,41	449,00	819,00	22,50

Table 1. In situ measurement and geochemical data of groundwater samples.

http://dx.doi.org/10.5772/intechopen.72173

4.2. Water type

The data plotted in the Piper diagram [14] show that Haffouz and BouHafna groundwater samples have the same Ca-Mg-HCO_3water-type, except for some samples collected from BouHafna aquifer, which are distinguished by Ca-Mg-SO_4 water-type (**Figure 5**).

4.3. Correlation matrix

The correlation matrix of 12 parameters (Cl, NO_3, SO_4, HCO_3, Na, K, Mg, Ca, TDS, EC, pH, and T°C) was computed in order to calculate the contribution degree of each hydrochemical parameters to the groundwater mineralization [15, 16] (**Table 2**).

Overall groundwater samples display positive and strong correlations between Cl, SO_4, Na, Mg, and Ca versus TDS (>0.9), providing insight into the large contribution of these ions to BouHafna and Haffouz groundwater salinization. There is well positive correlation between Na and Cl (r = 0.84), indicating the same origin of these elements likely related to the halite dissolution. The strong and positive relationship between Ca and SO_4 (r = 0.98) suggests that these ions derive from the same origin probably in relation with the dissolution of gypsum and/or anhydrite. The moderate correlation between NO_3 and the majority of ions can be explained by an anthropogenic effect related to the pollution through return flow of irrigation water.

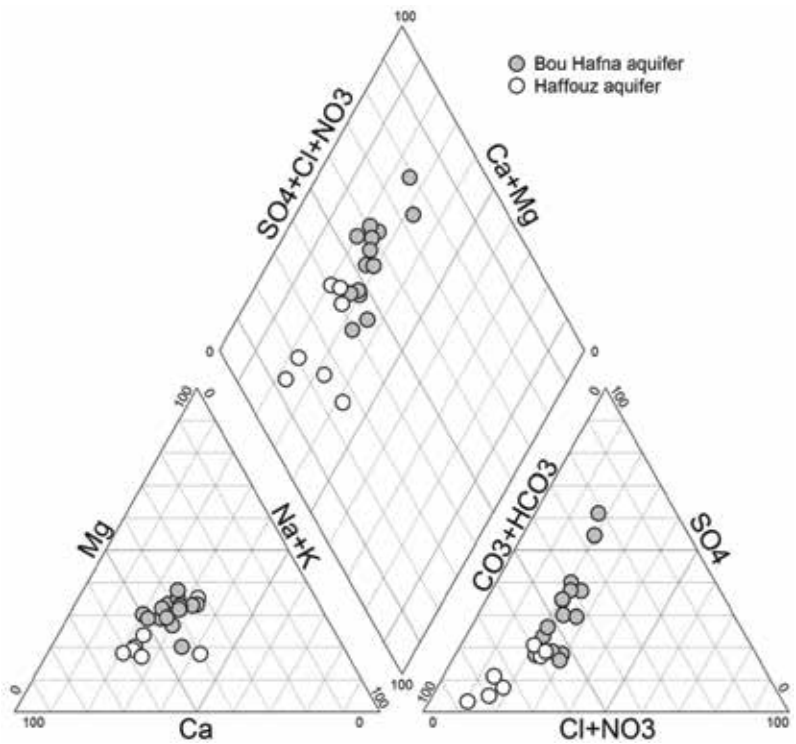

Figure 5. Piper diagram of Haffouz and BouHafna aquifers.

	Cl	NO_3	SO_4	HCO_3	Na	K	Mg	Ca	pH	TDS	EC	T°C
Cl	1,000											
NO_3	0,263	1,000										
SO_4	0,858	0,076	1,000									
HCO_3	0,322	0,276	0,203	1,000								
Na	0,839	0,209	0,902	0,207	1,000							
K	0,759	0,035	0,757	0,226	0,750	1,000						
Mg	0,882	0,199	0,924	0,271	0,874	0,865	1,000					
Ca	0,835	-0,055	0,891	0,363	0,720	0,676	0,772	1,000				
pH	-0,419	-0,050	-0,402	0,009	-0,402	-0,212	-0,443	-0,250	1,000			
TDS	0,900	0,098	0,976	0,260	0,906	0,766	0,901	0,908	-0,329	1,000		
CE	0,927	0,210	0,956	0,334	0,923	0,791	0,954	0,861	-0,407	0,961	1,000	
T°C	0,385	0,270	0,384	0,403	0,370	0,323	0,550	0,246	-0,502	0,320	0,454	1,000

Table 2. Correlation matrix of the 22 physicochemical parameters.

4.4. Principal component analysis

The principal component analysis (PCA), which is widely used in environmental studies, exhibits complex associations among several variables and individuals [17, 18]. Factors analysis was applied to the hydrochemical data set (Na, K, Mg, Ca, Cl, SO_4, HCO_3, NO_3, EC, and TDS) of BouHafna and Haffouz aquifers in order to precisely specify the main processes controlling the groundwater mineralization (**Figure 6a**). The PCA approach has preserved only the first two factors, which represent 74.63% of total samples variance (62.77% for F1 and 11.86% for F2). In the variables space, the F1 factor displays strong positive loadings for Na, K, Mg, Ca, Cl, SO_4, NO_3, and TDS. The strong correlations for the referred major ions suggest that the groundwater mineralization is acquired through water-rock interaction processes. The positive loading for NO_3 may reflect the influence of the return flow of irrigation water as a potential source of contamination related to the application of fertilizers. The F2 factor takes positive loadings for pH and negative loading for NO_3 and HCO_3. The inverse relationship between pH and NO_3 with respect to F2 factor lends support to the implication of the denitrification process in the groundwater salinization.

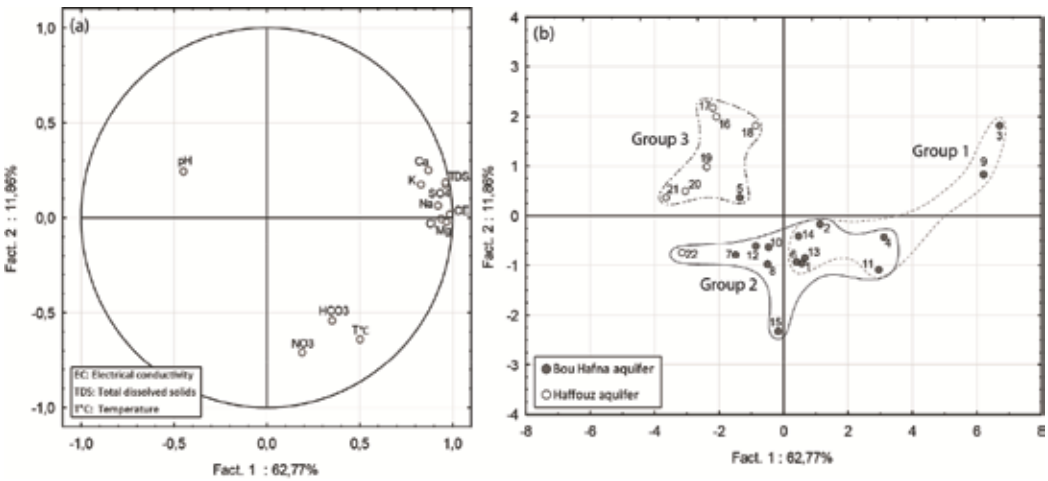

Figure 6. Variable space deduced from the geochemical PCA (a); cluster analysis main sample groups according to their scores for F1 and F2 (b).

The projection of the 22 samples on the same first factorial plan (F1, F2) permits to classify groundwater samples into three groups (**Figure 6b**). The first group, which lies in the positive side of the first factor (F1), is mainly represented by the BouHafna groundwater samples. This group is mainly influenced by natural processes of mineralization in relation with the dissolution of evaporatic minerals, dedolomitization, and cation exchange. These processes are summarized in the schematic model, which indicates that all groundwater samples display an undersaturation state with respect to gypsum and anhydrite, suggesting that dissolution of these minerals takes place there (**Figure 7**). Supplementary concentration of Ca^{2+}deriving from gypsum dissolution can cause calcite precipitation [19]. On the other hand, the decrease of bicarbonate concentration related to the precipitation of calcite causes the groundwater to be undersaturated with respect to dolomite and promotes the incongruent dissolution of this mineral known as dedolomitization [20–22].

The second group is mainly composed of BouHafna groundwater samples, which are strictly associated with intensive agricultural activities. This group, which plots in the negative side of the second factor (F2), is strongly associated with nitrate and highlights the considerable contribution of the return flow of irrigation waters to the contamination of groundwater. The third group comprises mainly the groundwater samples collected from the Haffouz aquifer. This group, which falls in the negative side of F1 and the positive side of F2, is extremely related to pH and negatively correlated with nitrate element. This position lends support to the predominance of denitrification processes, which corresponds to the biological reduction of nitrate (NO_3) to nitrogen gas (N_2).

4.5. Gibbs plot

Gibbs plot is used in the present investigation to confirm the significant role played by the natural hydrochemical processes already cited and their effect on groundwater quality [23]. Plot of (Na + K)/(Na + K + Ca) *versus* TDS shows that all the groundwater samples of the BouHafna and Haffouz aquifers fall in the field of water-rock interaction suggesting that the weathering of rocks is the major process that controls the groundwater mineralization in this region (**Figure 8**). Moreover, the plot of Cl/(Cl + HCO_3) *versus* TDS displays that groundwater

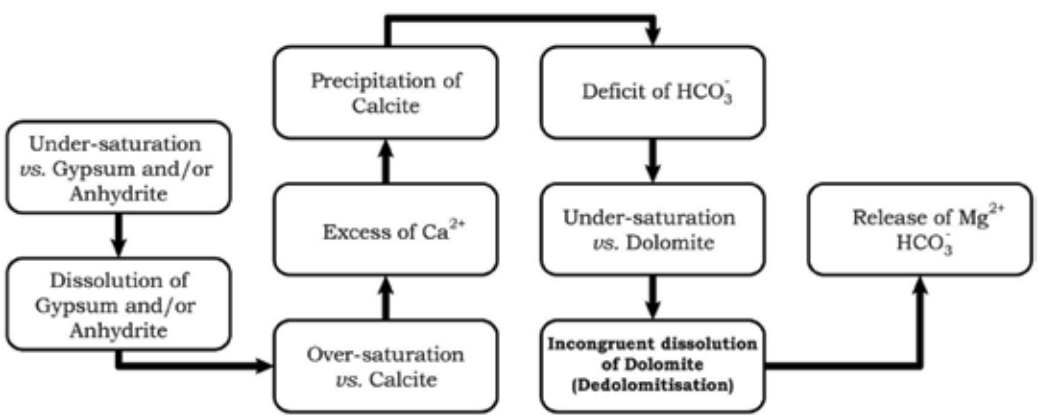

Figure 7. Schematic model showing the dedolomitization process.

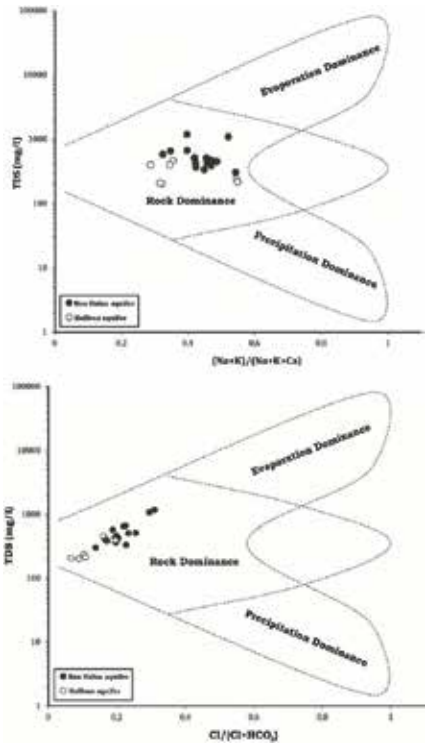

Figure 8. Gibbs plots explain groundwater geochemical process in the Haffouz and BouHafna regions.

samples fall on a linear trend on the field of rock dominance with a slight tendency toward the evaporation domain, highlighting the contribution of the evaporation process to the chemical composition of groundwater in the study area. In fact, for the Bouhafna groundwater samples, evaporation greatly increases the concentration of major ions resulted from chemical weathering, leading to higher salinity [24].

4.6. Suitability of groundwater for irrigation

Several parameters can be used to determine the suitability of groundwater for irrigation, that is, the electrical conductivity (EC), sodium adsorption ratio (SAR), and percent sodium.

The plot of analytical data on the Wilcox (1955) diagram shows that 83% of groundwater samples collected from the Haffouz aquifer belong to excellent category. All groundwater samples collected from the BouHafna aquifer, and only one sample of the Haffouz aquifer falls in the field of good to permissible (**Figure 9**). These very low to low SAR and low to medium salinity suggest that the studied groundwaters are suitable to moderately suitable for irrigation purposes without any threat of imposition of any hazard. Therefore, the application of these groundwaters in irrigation will be very advantageous as it will increase the agricultural yield.

http://dx.doi.org/10.5772/intechopen.72173

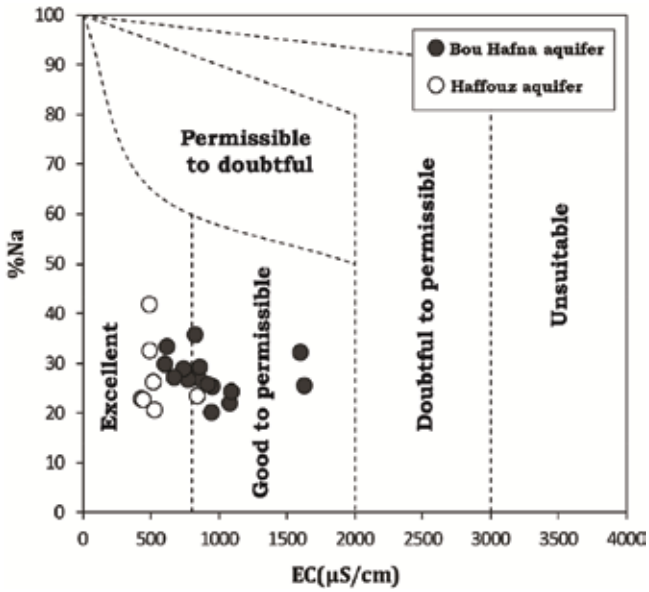

Figure 9. The quality of groundwater in relation to salinity and sodium hazard.

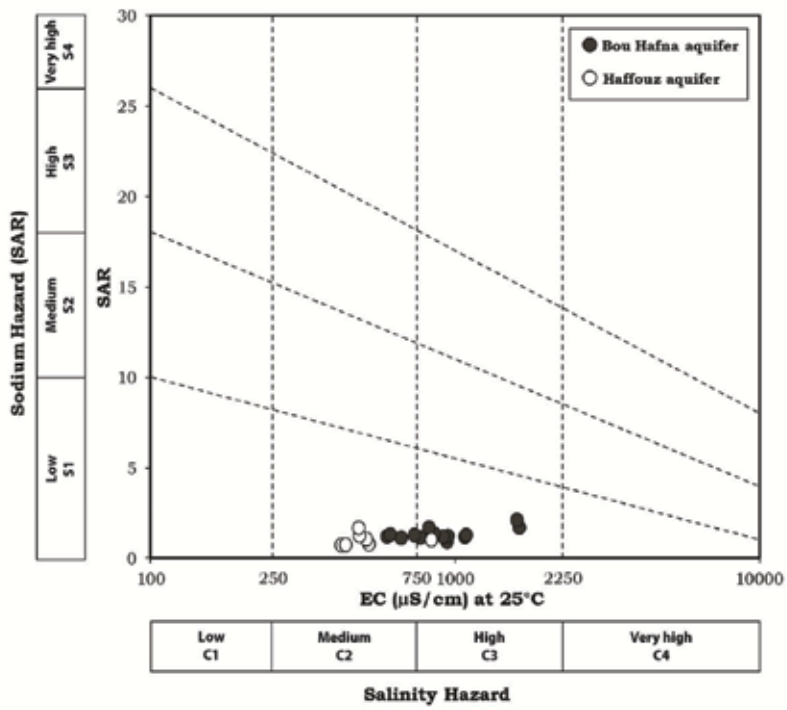

Figure 10. The quality of groundwater in relation to electrical conductivity and percent sodium (Wilcox diagram).

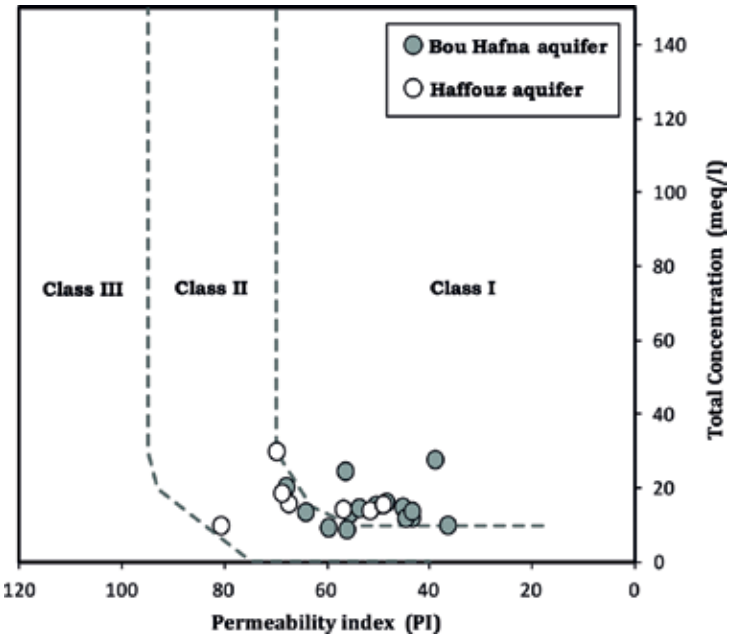

Figure 11. Doneen plot for Haffouz and BouHafna groundwater samples.

The correlation of sodium adsorption ratio (SAR) *versus* electrical conductivity shows that 55% of groundwater samples fall in the field of C3–S1, highlighting high salinity and low sodium in groundwater, which is suitable for the irrigation of all types of soil with little danger of exchangeable sodium. However, 45% of the samples fall in the field of C2–S1, reflecting low alkalinity hazard and medium salinity of groundwater. This may indicate that irrigation water can come from the referred groundwaters without danger of exchangeable sodium on all types of soils (**Figure 10**).

4.7. Permeability index (PI)

The permeability index (PI) parameter was used to assess the suitability of groundwater for irrigation. Indeed, the long-term irrigation with relatively enriched Na^+, Ca^{2+}, Mg^{2+}, and HCO_3^- groundwater can affect soil permeability [25]. Groundwater in the study area displays PI value ranging from 43 to 70% with an average value of 55% (PI greater than 25%) indicating that are good and suitable for irrigation purposes. Moreover, Doneen plot shows that groundwater samples in the study area fall in the fields of Class I and II, highlighting excellent to good permeability (**Figure 11**).

5. Conclusion

The hydrochemistry of BouHafna and Haffouz aquifer was investigated employing multivariate statistical approach in order to identify different processes that control groundwater

mineralization. This investigation reveals the predominance of Ca-Mg-HCO_3 and Ca-Mg-SO_4 water-types. These water facies are derived mainly from water-rock interaction processes, i.e., the dissolution of halite, gypsum, the dedolomitization, and the cation exchange. On the other hand, return flow of irrigation water has resulted in elevated nitrate concentrations in groundwater especially in the agricultural zones, which are characterized by an excessive use of fertilizer. Thus, it is important to protect the aquifers against overexploitation and groundwater quality deterioration related to the evaporate dissolution and agricultural contamination. For these reasons, in the BouHafna and Haffouz regions where groundwater resources are under the great development stress and environmental pressure, some preventive measures should be taken. These are (1) control the exploitation groundwater; (2) the definition of special groundwater resources protection zones; (3) control the potential processes and sources of salinization; and (4) improvement of diffuse source groundwater pollution.

Author details

Hatem El Mejri[1], Amor Ben Moussa[2,3]*, SarraBel Haj Salem[4] and Kamel Zouari[5]

*Address all correspondence to: amor_geologie@yahoo.fr

1 Laboratory "Water-Energy-Environment", ENIS, Tunisia

2 Research Laboratory of Environmental Science and Technologies, Tunisia

3 Laboratoire eau-membrane et biothechnologie de l'environnement, Tunisia

4 Higher Institute of Sciences and Technology of Environment of BorjCedria, Tunisia

5 Laboratory of Radio-Analyses and Environment, National School of Engineers of Sfax, University of Sfax, Sfax, Tunisia

References

[1] Bauder TA, Cardon GE, Waskam RM, Davis JG. Irrigation Water Quality-Cooperative Extension Agriculture. Colorado: Colorado State University; 2004

[2] Kingumbi A. Modélisation hydrogéologique d'un bassin affecté par 236 des changementsd'occupation. Cas du Merguellil en Tunisie centrale. Université de Tunis El Manar, Ecole Nationale d'ingénieurs de Tunis; 2006. Thèse de Doctorat en Génie Hydraulique

[3] EL Mejri H. Caractérisation hydrogéologique, hydro-chimique et isotopique des nappes Haffouz et Bou Hafna (Tunisie centrale). Master. Tunisie: Université de Sfax; 2010

[4] Abbes C. Etude préliminaire de la structure du Dj. Ouesselat (axe N-S Tunisie centrale); Rapport de DEA. Paris VI: Université de Pierre et Marie Curie, laboratoire de géologie structurale et géodynamique; 1979

[5] Ben Jemiaa M. Evolution tectonique de la zone de failles Trozza-Labeied (Tunisie centrale): Thèse de doctorat de 3éme cycle, université de Paris-Sud, Centre d'Orsay; 1986

[6] Burolet, Contribution à l'étude stratigraphique de la Tunisie centrale (Thèse, Alger). Ann. Mines et géol., N°18, Tunisie; 1956

[7] Castany G. Etude géologique de l'Atlas Tunisien oriental. Direction de 212 travaux publics. Annales des mines et de la géologie N 8. Tunisie; 1951

[8] Coiffait PE. Etude géologique de l'Atlas tunisien à l'Ouest de Kairouan (Tunisie centrale). Thèse Doc. 3ème cycle. Paris VI: Univ; 1974. p. 131

[9] El Ghali A. Néotectonique et évolution tectono-sédimentaire associées aux jeux de la faille deSbiba-Kairouan du crétacé supérieur à l'actuel (Tunisie centrale). Univ. Tunis II, Faculté de science Tunis; 1993. Thèse troisième cycle

[10] Rigane A. Les calcaires de l'Yprésien en Tunisie centro-septentrionale : cartographie, cinématique et dynamique des structures. Thesis. University of Franche-Compté; 1991. p. 214

[11] Yaïch C, Hooyberghs HJF, Durlet C, Renard M. Corrélation stratigraphique entre les unités oligo-miocènes de Tunisie centrale et le Numidien. Comptes Rendus de l'Académie des Sciences - Series. 2000;**331**:499-506

[12] El Mejri H, Ben Moussa A, Zouari K. The use of hydrochemical and environmental isotopic tracers tounderstand the functioning of the aquifer system in the BouHafna andHaffouz regions, Central Tunisia. Quaternary International. 2014;**338**:88-98

[13] El Mejri H, Ben Moussa A, Zouari K. The use of hydrochemical and environmental isotopic tracers to understand the functioning of the aquifer system in the BouHafna and Haffouz regions, Central Tunisia. Quaternary International. 2014;**338**:88-98

[14] Piper AM. A graphic procedure in the geochemical interpretation of water-analyses. Transactions of the American Geophysical Union. 1944;**25**:914-923

[15] Helena BB, Pardo M, Vega E, Barrado JM, Fernandez, Fernandez L. Temporal evolution of groundwater composition in an alluvial aquifer (Pisuerga River, Spain). Water Research. 2000;**34**(3):807-816

[16] Nair A, Abdalla G, Mohmed I, Premkumar K. Physicochemicalparameters and correlation coefficient of ground waters of north-east Liblya. Pollution Research. 2005;**24**(1):1-6

[17] Davis JC. Statistics and Data Analysis in Geology. NY: John Wiley & Sons Inc; 2002

[18] Guler C, Thyne GD, McCray JE, Turner AK. Evaluation of graphical and multivariate statistical method for classification of water chemistry data. Hydrogeology Journal. 2002;**10**(C4):455-474

[19] Jacobson AD, Wasserburg GJ. Anhydrite and the Sr isotope evolution of groundwater in a carbonate aquifer. Chemical Geology. 2005;**214**:331-250

[20] Appelo CAJ, Postma D. Geochemistry, Groundwater and Pollution. Rotterdam: A.A. Balkema; 1993. p. 536; ISBN 90-5410-106-7

[21] Ben Moussa A, Zouari K, Marc V. Hydrochemical and isotope evidence of groundwater salinization processes on the coastal plain of Hammamet-Nabeul, north-eastern Tunisia. Physics and Chemistry of the Earth. 2013;**36**:167-178

[22] Gomis Yagües V, Boluda-Botella N, Ruiz-Beviá F. Gypsum precipitation/dissolution as an explanation of the decrease of sulphate concentration during sea water intrusion. Journal of Hydrology. 2000;**228**:48-55

[23] Gibbs R. Mechanisms controlling worlds water chemistry. Science. 1970;**170**:1088-1090

[24] Chebbah M, Allia Z. Geochemistry and hydrogechemical process of groundwater in the Souf valley of low septentrional Sahara, Algeria. African Journal of Environmental Science and Technology. 2015;**9**(3):261-273

[25] Doneen LD. Notes on Water Quality in Agriculture. Davis: Water Science and Engineering, University of California; 1964

Chapter 7

Hydrogeology and Groundwater Geochemistry of the Clastic Aquifer and Its Assessment for Irrigation, Southwest Kuwait

Fawzia Mohammad Al-Ruwaih

Additional information is available at the end of the chapter

http://dx.doi.org/10.5772/intechopen.71577

Abstract

Al-Atraf field, is located southwest of Kuwait City, the groundwater is produced from the Kuwait Group aquifer. The objectives are to identify aquifer type and its characteristics. The major geochemical processes operating in the aquifer have to be revealed. In addition, to evaluate the groundwater quality and its suitability of drinking and agriculture usage, an investigation was carried out by estimating physiochemical parameters like pH, EC, TDS, TH, Na^+, K^+ Ca^{2+}, Mg^{2+}, Cl^-, HCO_3^-, SO_4^{2-}, total alkalinity, and SiO_2. Irrigation parameters like SAR, %Na, RSC, potential salinity, magnesium ratio, Kelly's ratio, permeability index, and chloro-alkaline index have been determined. The aquifer is confined and occupied by brackish groundwater mainly of NaCl type. Gibb's plot suggests that the chemical weathering of rock primarily controls the chemistry of the study area. WATEVAL program revealed that the main geochemical processes are silicate weathering, dissolution, precipitation, and reverse ion exchange. WATEQ4F indicates that the groundwater is oversaturated with respect to calcite and dolomite and undersaturated with respect to gypsum and anhydrite. The high total hardness and TDS identify the unsuitability of groundwater for drinking, while irrigation parameters indicate that this water cannot be used on soil without special management for salinity control and salt tolerance plants.

Keywords: Kuwait Group aquifer, saturation index, geochemical processes, Gibb's ratio, irrigation parameters

1. Introduction

The State of Kuwait is located at the northwestern side of the Arabian Gulf and occupies an area of about 18,000 km^2. Kuwait is bordered on the north and west by Iraq and on the south

by the Kingdom of Saudi Arabia. The climate is extremely hot and dry in summer and mild-to-cold in winter. The rainfall is scarce and limited to the period from October to May. The highest ever temperature recorded in Kuwait was 54°C on July 2016. The average annual precipitation recorded during the period 2001–2016 is 114.5 mm. It lies within an arid-semiarid zone lacking renewable surface water. The natural water resources are the brackish groundwater located in the Kuwait Group and the Dammam Formation aquifers, which have been utilized since 1953 on a small scale and for limited purpose, but with increasing population and growth of demands, the production of groundwater embarked on a wide scale project to provide consumers with it through a separate pipe network. This groundwater is used for blending with distilled water for fresh water production, irrigation and landscaping plus household purposes, livestock watering, and construction works. The present total output installed capacity of groundwater wells is around 145 MIGD, meanwhile the maximum consumption hit 114.6 MIGD. However, the demand for water in Kuwait is met from three sectors: desalination, brackish groundwater, and tertiary treated waste water.

The Al-Atraf field is one of the brackish groundwater fields and is located southwest of Kuwait between 29° 18⁻ to 29° 24⁻ north latitudes and 47° 31⁻ to 47° 38⁻ east longitudes. The area under study is about 87.75 km^2 and includes 83 water wells, producing groundwater from the Kuwait Group aquifer, where the nominal production capacity is 30 MIGPD. The salinity of the aquifer ranges from 3504 to 6366 mg/l, with an average value of 4441 mg/l.

1.1. Topography

The topography of Kuwait is generally flat, with a gentle rise from sea level at the coast to an elevation of about 270 m in the southwest corner of the country (**Figure 1**). Local relief is low except in the Jal-Az-Zor escarpment, the Ahmadi Ridge, the Wara Hill, and the Wadi Al-Batin [1]. The Jal-Az-Zor escarpment, about 60 km in length and 145 m in height above MSL, borders the northwestern shore of Kuwait Bay. It trends from Al-Atraf southwest to Bahra northeast. The Ahmadi Ridge parallels to the coastline south of Kuwait City and rises to a height of 137 m above MSL. The east and west slopes of the ridge are very gentle. Another elevation is the Wara Hill, located southeastern Kuwait and has a local relief of about 31 m. The Wadi Al-Batin is a major and shallow depression marking the western boundary of the country for a distance of 75 km with an average width of 6–8 km. The central part of Kuwait and the Neutral Zone are featureless with few wadis and little vegetation. Furthermore, small and shallow depressions exist throughout the northern, western, and central areas. The northern and the western parts of the country have a dense drainage pattern of small and shallow wadi systems, draining northeast toward the Iraq border and toward the shallow depressions near Al-Rawdhatain [2].

1.2. General stratigraphy

The surface of Kuwait is formed by sedimentary rocks and sediments ranging from Middle Eocene to Recent. The Dammam Formation represents the oldest exposed sedimentary rocks. The Recent deposits of fine-grained beach sands cover the southern coast of Kuwait and the Neutral Zone. The Cenozoic (Tertiary-Quaternary) sediments can be divided into two groups:

http://dx.doi.org/10.5772/intechopen.71577

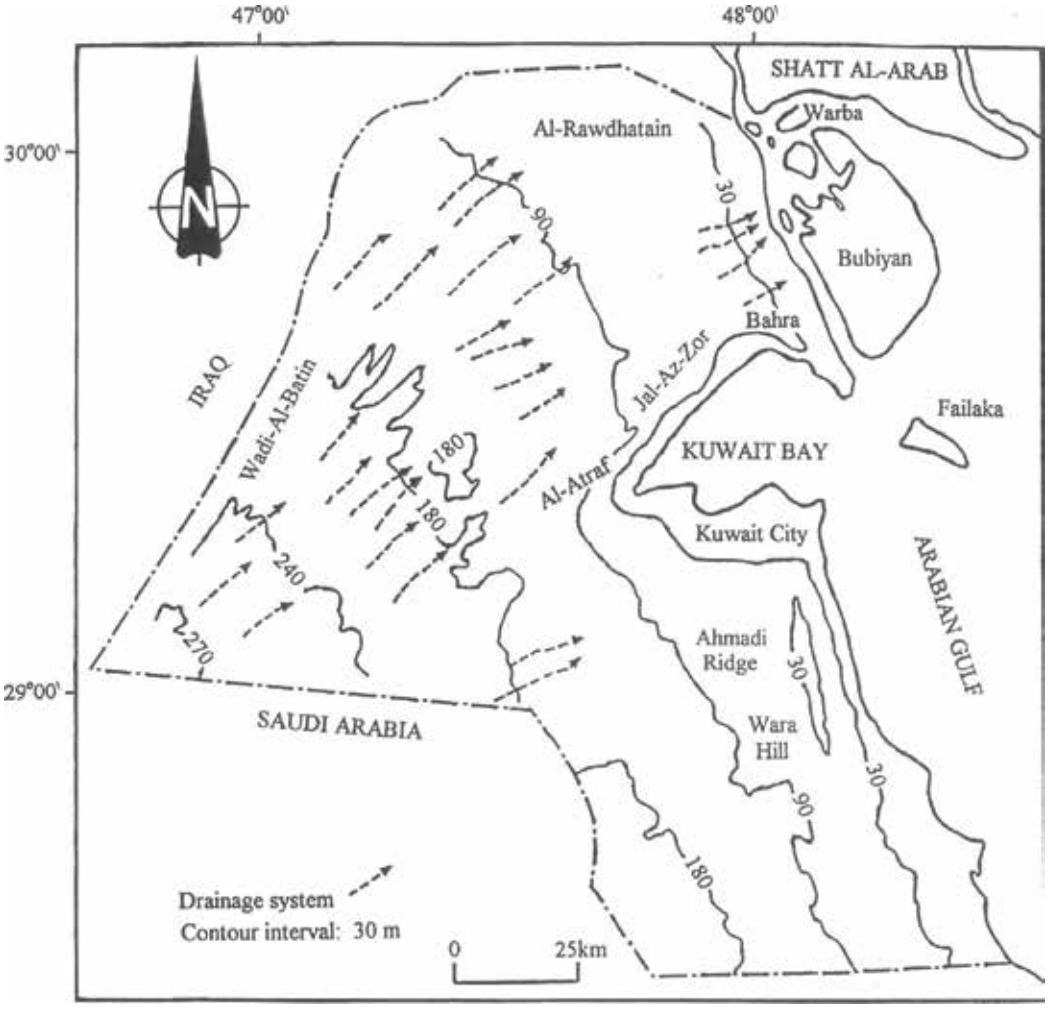

Figure 1. The topographic and the dominant northeast drainage patterns of Kuwait.

the Kuwait Group and the Hasa Group. The Mesozoic (Late Cretaceous) sediments are characterized by carbonate rocks [3]. A generalized lithostratigraphic subdivisions of Tertiary-Quaternary sediments in Kuwait with the groundwater conditions [4] is summarized and discussed below.

1.3. The Kuwait Group

The Kuwait Group consists of sand, gravel, sandstone, clay, silt, calcareous and gypseous cemented sandstones, and marl covering the entire surface of Kuwait and extending down to the top of the underlying Dammam Formation. The thickness of the Kuwait Group increases from 150 m in the southwest to about 400 m in the northeast. The Kuwait Group is relatively

dry in the extreme southwest and is almost saturated with water along the coast of the Arabian Gulf. In the north of Kuwait, the Kuwait Group can be divided into three formations based on the presence of an intermediate evaporite development. These divisions are Dibdibba, Lower Fars, and Ghar Formations, arranged from top to bottom. The undivided Kuwait Group extends under all of Kuwait with an extension eastwards beneath the Arabian Gulf. The Dibdibba Formation was named after the type locality Al-Dibdibba Plain, which extends from Basra to the northern part of Kuwait. The Dibdibba Formation is overlain by unconsolidated Recent and sub-Recent sediments of varying lithologies. The Lower Fars Formation ranges in thickness from 61 m in the west to more than 100 m in the eastern area into the offshore and it is absent in the south. It consists of fine to coarse-grained conglomeratic sandstone, variegated shale, and thin, fossiliferous limestone. The outcrop thickness of the Ghar Formation is only 33 m but it increases in subsurface and ranges from 195 to 250 m of marine to terrestrial, coarse-grained, unconsolidated sandstone with a few thin, sandy limestone, clay and anhydrite layers. At the base of the formation, above the eroded top of the Dammam Formation, is a brown, marly, coarse-grained sandstone with white, crystalline limestone resting unconformably over the Dammam Formation, and in gradational contact with the Lower Fars Formation.

2. Hydrogeology

The northeastern part of Arabian Peninsula is characterized by four major systems of aquifers. These are (1) The Paleozoic-Triassic System, (2) The Cretaceous System, (3) The Eocene System, and (4) The Neogene-Quaternary System. The last two aquifers contain usable water, while the other deeper aquifers have connate water. Thus, the principle aquifer system in Kuwait consists of the Kuwait Group and the Dammam Formation of the Hasa Group. Many hydrological and hydrochemical evidences indicate local hydraulic connection between the Kuwait Group and the Dammam Formation aquifers in which both aquifers are considered as one complex system forming the main potential aquifers in Kuwait. Basically, the saturated part of the Kuwait Group and the Dammam Formation aquifers are replenished by infiltration on the outcrop area of Hasa Group at the eastern-northeastern part of Saudi Arabia and groundwater is discharged in Shatt Al-Arab and the Arabian Gulf [5]. Potentiometric level maps of the Kuwait Group and the Dammam Formation aquifers indicate a direction of groundwater movement from southwest to northeast direction. Due to the variations of clay percentage and cementation degree, the Kuwait Group is divided into two aquifers separated by an aquitard formation of clay and sand. Accordingly, the Kuwait Group appears to be semi-confined aquifer with a free water surface in the uppermost horizons. The saturated thickness of the Kuwait Group aquifer gradually increases toward northeast direction, as related to the structure of the Dammam Formation, where the groundwater in the aquifer becomes very saline.

The Kuwait Group aquifer is hydraulically connected with the underlying Dammam Formation aquifer under natural hydrological conditions; the flow occurs in a dynamic equilibrium

http://dx.doi.org/10.5772/intechopen.71577

state, in SW-NE direction, to be discharged finally by seepage into Kuwait Bay and the Arabian Gulf [6]. The Kuwait Group aquifer gains part of its water by leakage from the Dammam Formation aquifer. The other sources of aquifer replenishment are the infiltration through the well-developed wadies and depression system, and lateral flow coming from Saudi Arabia. It is generally estimated that the hydraulic conductivity in the aquifer conjunctively decreases with depth by the increase of cementation degree. The hydraulic conductivity is relatively high in the upper saturated zones of the aquifer.

3. Objectives of the study

The main objectives of this piece of research are to identify the aquifer type and its characteristics, to reveal the geochemistry of the study area in order to recognize the prevailing and the major geochemical processes that control the quality of the groundwater. Moreover, to evaluate the suitability of groundwater for drinking and irrigation, physiochemical and irrigation parameters have been determined.

4. Methodology

Seventy-one groundwater samples have been collected and analyzed to determine physical parameters like pH, EC, TDS, total hardness (TH), total alkalinity, and SiO_2. In addition, the chemical parameters of the major cations and anions such as Ca^{2+}, Mg^{2+}, Na^{+}, K^{+}, HCO_3^{-}, SO_4^{2-}, and Cl^{-} expressed in mg/l were analyzed and converted to equivalent per million (e.p.m), and % e.p.m. [7]. Ion balance equation was applied to validate the accuracy of the chemical analyses where $\pm 5\%$ is acceptable [8]. The reaction error of all groundwater samples was less than the accepted limit of $\pm 10\%$ [9].

A speciation model has been used to determine the degree of saturation of groundwater with respect to some minerals using WATEQ4F program [10]. A mass-balance modeling WATEVAL computer program [11] is used to reveal the major geochemical reactions that control the geochemistry of the study area, along with the application of Gibb's ratio to assess the functional sources of dissolved chemical constituents, and to recognize the main processes governing the groundwater chemistry of the study area [12]. Hydrochemical facies interpretation is used to determine flow pattern and origin of chemical histories of groundwater by plotting the major cations and anions on the Piper diagram [13]. The assessment of groundwater for irrigation purposes based on different irrigation indices is carried out which includes sodium adsorption ratio (SAR), residual sodium carbonate (RSC), %Na. permeability index (PI), potential salinity (PS), salinity hazard, magnesium ratio (MgR), Kelly's ratio (KR), and chloro-alkaline index [14].

Wilcox diagram Wilcox [15] and Doneen permeability index [16, 17] have also been utilized for classification of groundwater for irrigation.

5. Analyses and evaluation of pumping test data

A pumping test is a tool to determine the hydraulic characteristics of water-bearing formations such as transmissivity, storage coefficient, and any relevant hydrogeological properties. Such a test is called an aquifer test.

Analytical methods were applied to determine the aquifer type and hydrogeological properties of the Kuwait Group aquifer of the study area. These methods are Theis type curve [18], Cooper and Jacob straight line method for confined aquifer [19], and Walton method for semi-confined aquifer [20]. In effect, the pumping test data analyses indicated that the Kuwait Group aquifer is confined to semi-confined aquifer as shown in **Figure 2** for the well AT-15 and **Figure 3** for the well AT-18. The aquifer transmissivity ranges between 62.03 and 320.51 m^2/day, where the estimated storage coefficient equals 7.5×10^{-4}. The flow net analysis shows that the groundwater flows from the southwest to the northeast. Recharge to the aquifer is primarily from subsurface flow from adjacent bed rocks and by leakage from the underlying Dammam Formation aquifer. The presence of an aquitard layer (i.e., sandy clay) that bounds the aquifer from the top acts as a semipermeable layer and can leak water into the aquifer in the direction of the hydraulic gradient.

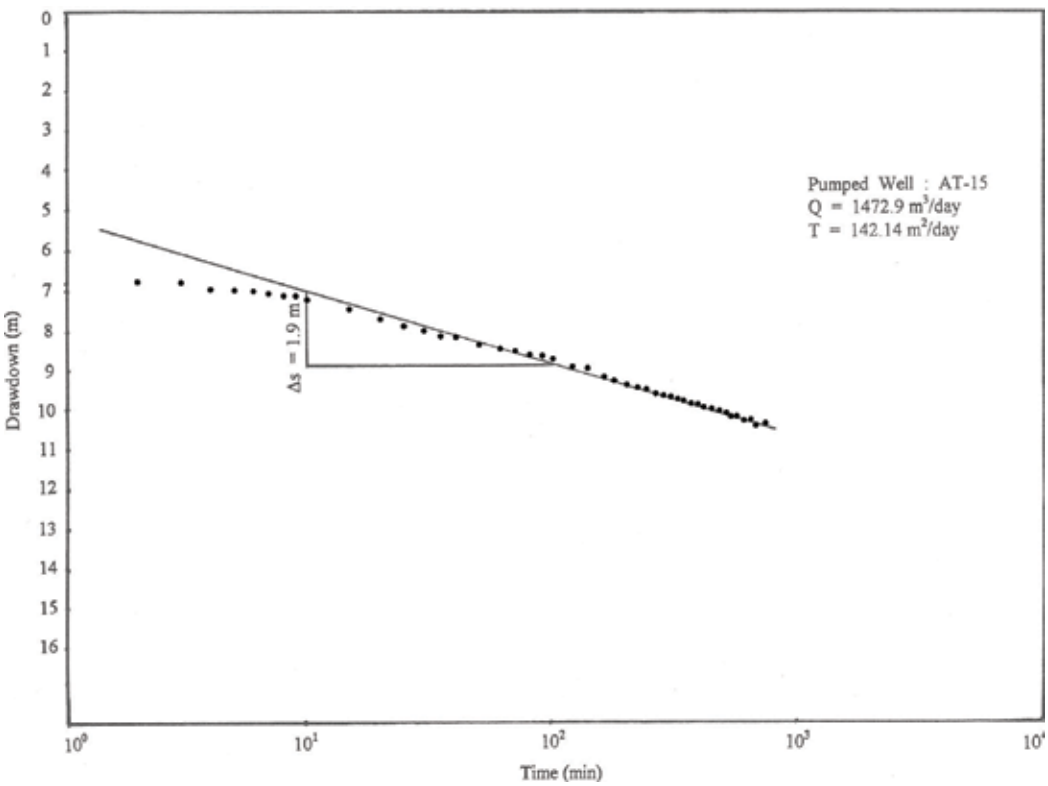

Figure 2. Time-drawdown curve of well no. AT-15, using Cooper and Jacob straight line method.

http://dx.doi.org/10.5772/intechopen.71577

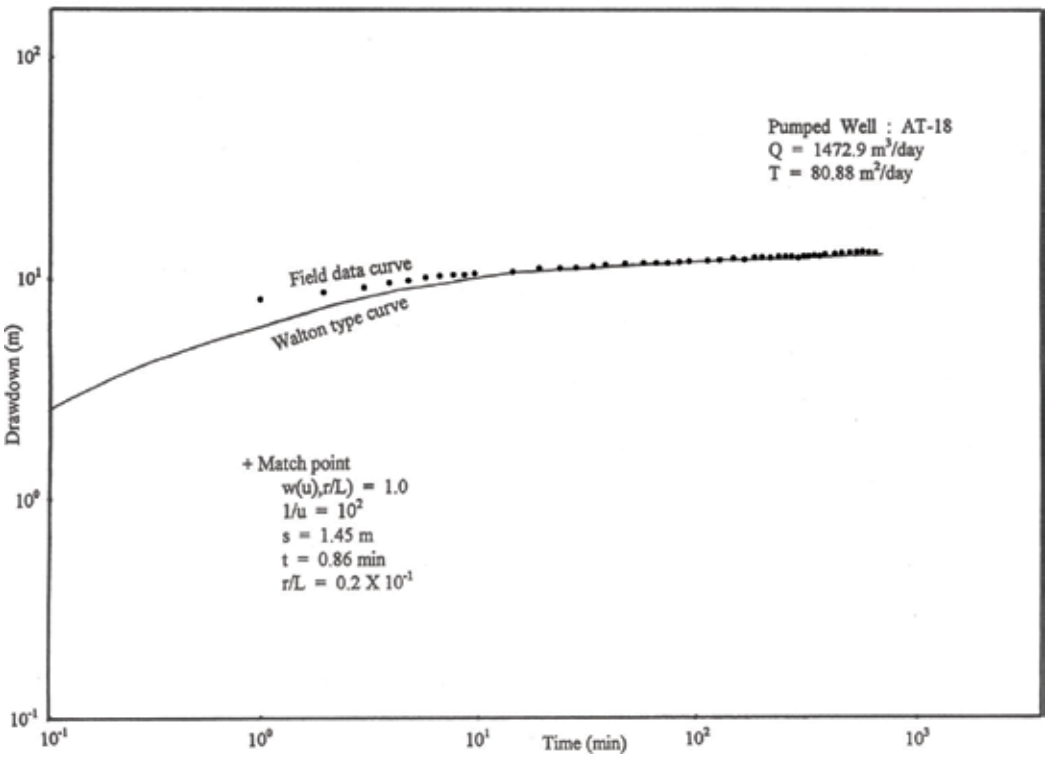

Figure 3. Time-drawdown curve of well no. AT-18, Walton method.

6. Mechanisms of controlling groundwater chemistry

It is important to study the relationship between the water chemistry and the aquifer lithology. Gibbs as mentioned in [12] suggested a diagram that represents the ratio of dominant anions and cations plotted against the value of TDS. These ratios can be divided into two formulas, the first ratio is for the cations $[(Na^+ + K^+)/(Na^+ + K^+ + Ca^{2+})]$ and the second ratio is for the anions $Cl^-/ (Cl^- + HCO^-_3)$ as a function of TDS. This diagram is widely used to evaluate the functional sources of dissolved constituents such as precipitation dominance, rock dominance, and evaporation dominance. The chemical analyses of the study area are plotted in Gibb's diagram as shown in **Figure 4**, and they showed that the predominant samples fall into the category of rock-water interaction field and few samples are located in evaporation-dominance field and precipitation-dominance field, which revealed that the chemical weathering of rock-forming minerals is influencing the groundwater quality by dissolution of rock through which there is circulation, while the data in the evaporation-dominance field indicate that the increasing ions of Na^+ and Cl^- are in relation with the increasing of the TDS, as evaporation will increase the concentration of total dissolved in groundwater.

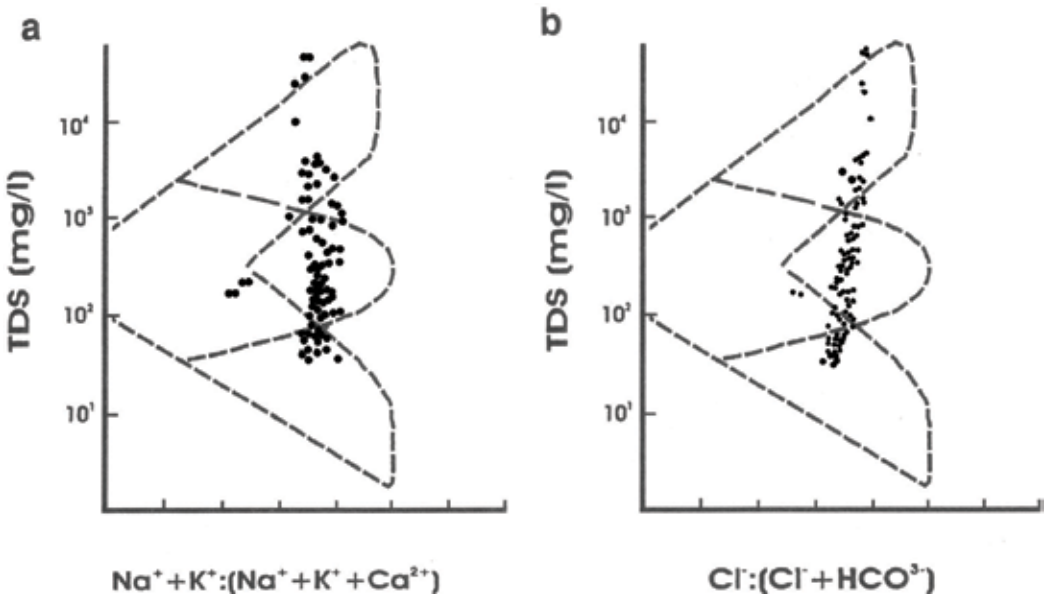

Figure 4. Gibbs plots represent groundwater chemistry and geochemical process in the study area.

6.1. Hydrochemical facies

Hydrochemical facies interpretation using Piper trilinear diagram is a useful tool for determining the flow pattern and origin of chemical histories of groundwater. The Piper trilinear diagram is presented in **Figure 5**. One principal hydrochemical water type has been delineated. The majority of the groundwater samples of the study area fall in Ca^{2+}– Na^{+} – Cl^{-} water type, where alkaline earth ($Ca^{2+} + Mg^{2+}$) exceeds the alkaline ($Na^{+} + K^{+}$) and strong acid (Cl^{-} and SO_4^{2-}) exceeds the weak acid (HCO_3^{-} and CO_3^{2-}), and non-carbonate hardness exceeds 50%.

6.2. Saturation index

Geochemical models are tools used to calculate chemical reaction in groundwater system such as dissolution and precipitation of solids, ion exchange, and sorption by clay minerals. In this study, the speciation model has been applied to the groundwater samples of Al-Atraf field to determine the saturation index (SI) of minerals. The SI for a given mineral measures the degree of saturation of that mineral with respect to the surrounding system. The degree of saturation index is defined as follows [21]:

$$\mathrm{SI} = \log \frac{\mathrm{K_{iap}}}{K_{sp}}, \tag{1}$$

where "iap" is the ion activity product of the dissociated chemical species in solution and "K_{sp}" is the solubility product of the mineral. When SI is <0, it indicates that the groundwater is undersaturated with respect to that particular mineral. When SI > 0, it means that the

http://dx.doi.org/10.5772/intechopen.71577

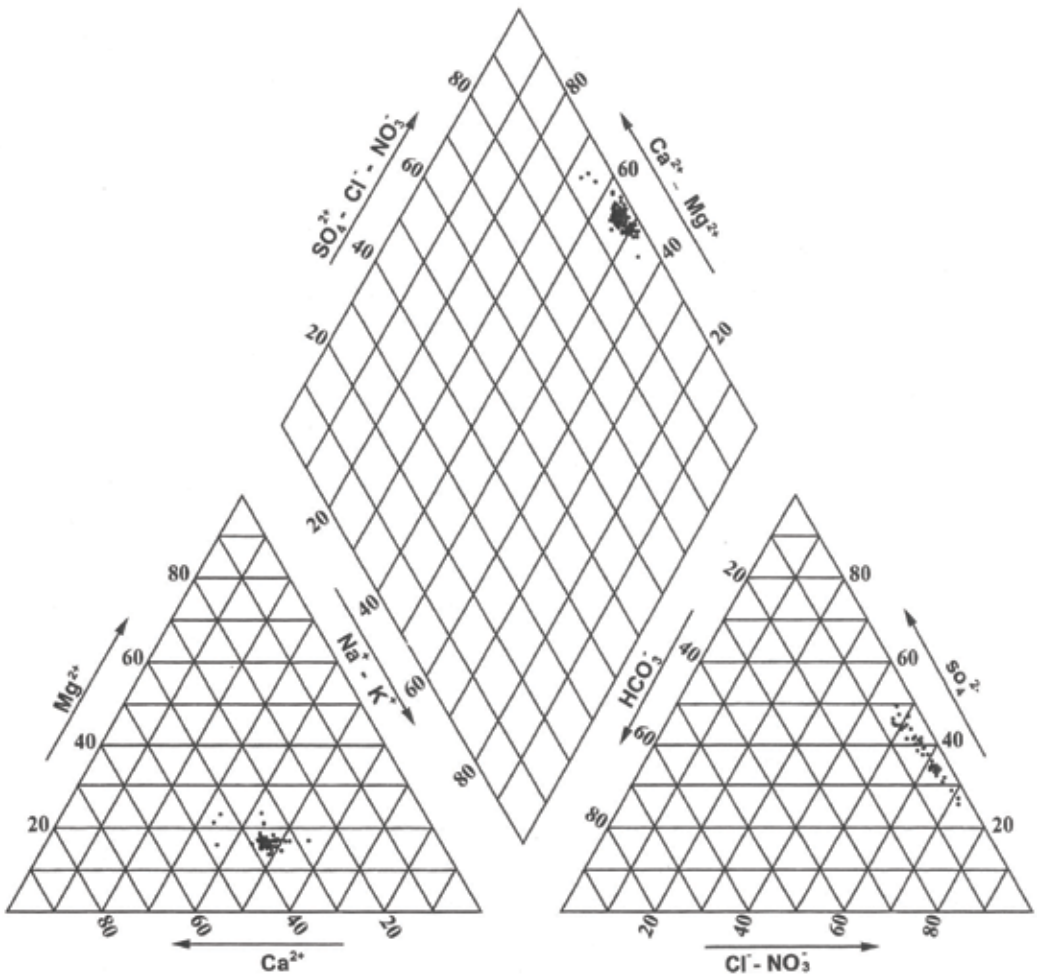

Figure 5. Piper trilinear diagram representing the chemical analysis of the study area.

groundwater is being saturated with respect to the mineral and incapable of dissolving more of the minerals. The oversaturation can also be produced by incongruent dissolution, common ion effect.

Table 1 shows the saturation indices of anhydrite, calcite, gypsum, dolomite, halite, and silica along with Pco_2. Nearly, all groundwater samples of the study area are undersaturated with respect to anhydrite, gypsum, halite, and silica and oversaturated with respect to calcite and dolomite.

The partial pressure of the carbon dioxide value (Pco_2) of the study area ranges between 1.32×10^{-3} and 8.23×10^{-3} atm., with an average value of 3.78×10^{-3} atm. This indicates that the groundwater of the Kuwait Group aquifer becomes charged with CO_2 during infiltration through the soil zones. According to Appelo et al. [22], when Pco_2 values range between $10^{-2.5}$

S.No.	PCO_2	Anhydrite	Cacite	Gypsum	Dolomite	Halite	Silica
	atm.	$CaSO_4$	$CaCO_3$	$CaSO_4.2H_2O$	$Ca\ Mg\ (CO_3)_2$	Na Cl	SiO2
1	2.13E-03	-0.13	0.40	-0.17	0.53	-4.38	-0.19
2	2.88E-03	-0.19	0.38	-0.23	0.49	-4.45	-0.16
3	2.56E-03	-0.19	0.42	-0.23	0.60	-4.47	-0.12
4	3.18E-03	-0.17	0.29	-0.21	0.34	-4.53	-0.19
5	3.97E-03	-0.15	0.26	-0.19	0.26	-4.40	-0.15
6	4.06E-03	-0.14	0.37	-0.18	0.50	-4.65	-0.33
7	3.05E-03	-0.16	0.47	-0.20	-0.27	-4.52	-0.14
8	3.48E-03	-0.17	0.33	-0.20	0.43	-4.50	-0.15
9	4.09E-03	-0.22	0.17	-0.26	0.10	-4.55	-0.24
10	5.47E-03	-0.23	0.22	-0.27	0.24	-4.74	-0.12
11	3.07E-03	-0.19	0.44	-0.23	0.62	-4.65	-0.15
12	8.12E-03	-0.30	-0.19	-0.34	-0.70	-4.68	-0.13
13	2.66E-03	-0.29	0.34	-0.33	0.37	-4.71	-0.23
14	3.69E-03	-0.24	0.40	-0.28	0.57	-4.91	-0.33
15	3.13E-03	-0.30	0.33	-0.34	0.28	-4.88	-0.33
16	2.43E-03	-0.33	0.25	-0.37	0.27	-4.80	-0.23
17	3.53E-03	-0.30	0.24	-0.34	0.26	-4.72	-0.27
18	5.36E-03	-0.32	0.15	-0.36	0.09	-4.79	-0.14
19	5.03E-03	-0.26	0.20	-0.30	0.17	-4.75	-0.18
20	1.32E-03	-0.22	0.80	-0.26	1.40	-4.81	-0.16
21	7.40E-03	-0.22	0.04	-0.26	-0.21	-4.86	-0.15
22	4.26E-03	-0.33	0.19	-0.37	0.11	-4.86	-0.23
23	4.47E-03	-0.30	0.20	-0.34	0.24	-4.82	-0.28
24	3.93E-03	-0.24	0.28	-0.28	0.24	-4.85	-0.18
25	8.23E-03	-0.02	0.25	-0.06	0.27	-5.27	-0.37
26	5.09E-03	-0.24	0.05	-0.28	-0.23	-4.62	-0.32
27	3.58E-03	-0.28	0.16	-0.32	0.04	-4.71	-0.25
28	4.91E-03	-0.28	0.15	-0.32	0.01	-4.86	-0.19
29	3.37E-03	-0.27	0.39	-0.31	0.52	-4.89	-0.22
30	2.23E-03	-0.41	0.11	-0.44	0.09	-4.69	-0.25
31	3.93E-03	-0.18	0.49	-0.22	0.75	-4.84	-0.31
32	3.18E-03	-0.18	0.27	-0.22	0.15	-5.09	-0.30
33	4.70E-03	-0.32	0.11	-0.36	-0.01	-4.81	-0.21
34	2.45E-03	-0.27	0.46	-0.31	0.62	-4.83	-0.29
35	3.60E-03	-0.24	0.24	-0.28	0.24	-4.71	-0.27
36	2.81E-03	-0.25	0.35	-0.29	0.60	-4.74	-0.28
37	4.07E-03	-0.28	0.24	-0.32	0.27	-4.83	-0.34
38	3.96E-03	-0.25	0.09	-0.29	0.05	-4.59	-0.34
39	3.05E-03	-0.21	0.22	-0.25	0.13	-4.56	-0.33
40	2.62E-03	-0.36	0.42	-0.40	0.65	-4.87	-0.31
41	3.00E-03	-0.19	0.22	-0.23	0.21	-4.53	-0.31
42	2.48E-03	-0.21	0.33	-0.24	0.37	-4.60	-0.32
43	3.73E-03	-0.27	0.25	-0.30	0.29	-4.69	-0.30
44	4.85E-03	-0.21	0.02	-0.25	-0.23	-4.48	-0.29
45	2.91E-03	-0.21	0.21	-0.25	0.16	-4.59	-0.30
46	1.60E-03	-0.19	0.39	-0.23	0.47	-4.53	-0.33
47	4.23E-03	-0.25	0.14	-0.29	0.05	-4.61	-0.32
Min.	**0.00132**	**-0.41**	**-0.19**	**-0.44**	**-0.70**	**-5.27**	**-0.37**
Max.	**0.00823**	**-0.02**	**0.80**	**-0.06**	**1.40**	**-4.38**	**-0.12**
Ave.	**0.00378**	**-0.24**	**0.27**	**-0.28**	**0.26**	**-4.71**	**-0.24**

Table 1. Results of thermodynamic speciation calculation of the study area.

http://dx.doi.org/10.5772/intechopen.71577

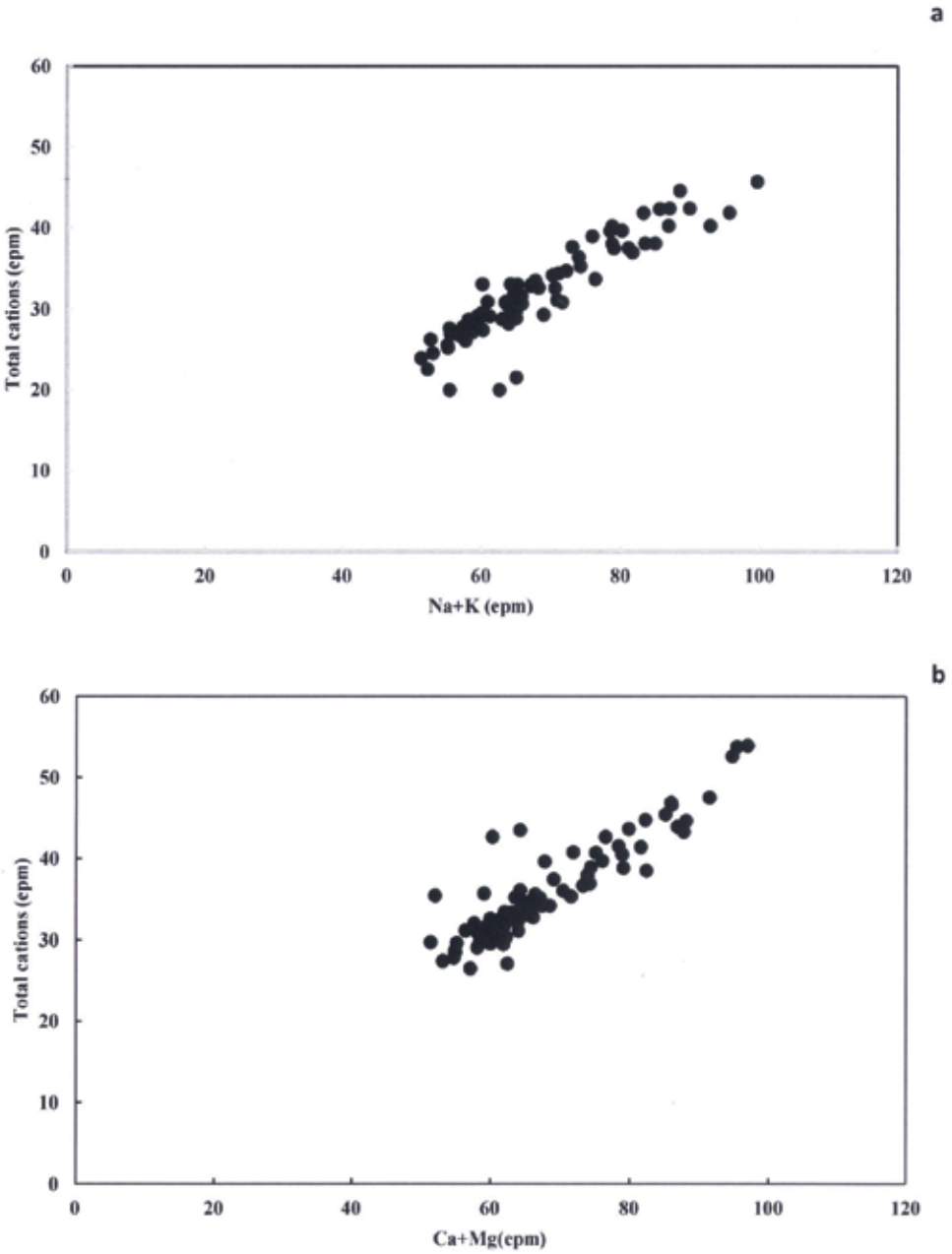

Figure 6. (a) Relation between total cations and (Na+K) in the study area. (b) Relation between total cations and (Ca+Mg) in the study area.

and $10^{-6.4}$ atm., it represents a closed system. Since the Kuwait Group aquifer is acting as a confined to semi-confined aquifer, it is more likely that the groundwater represents a deep, closed environment system. The mass-balance modeling as mentioned in Ref. [11] has been applied to specify the amounts of reacting minerals and to determine the possible source of the

major ions in a specific groundwater system. This is in order to deduce groundwater source rock and to determine the nature and the extent of the geochemical reactions that occur in this system, that is, water-rock interaction. By the application of Hounslow concept, all groundwater samples of the study area showed that $Cl^- > Na^+$ indicating that the reverse ion exchange is likely to occur in aquifer. The ratio $Ca^{2+} / Ca^{2+} + SO_4^{2-}$ of most groundwater samples ranged between 0.41 and <0.5 indicating calcium removed by ion exchange or calcite precipitation, and few groundwater samples show a range value of 0.5–0.6, which is due to gypsum dissolution. According to reference [11], waters with $HCO_3^-/SiO_2 < 5$ indicated mainly silicate weathering. However, the ratio HCO_3^-/SiO_2 of the groundwater samples found to be ranged between 1.45 and 4.77 which indicate that silicate weathering is a dominant chemical process in the aquifer. Dissolved silica data show the influences of silicate weathering on water chemistry in the study area. Participation of silicate minerals in the chemical reactions plays a vital role in groundwater chemistry. Silicate weathering can be evaluated by estimating the ratio between $Na^+ + K^+$ and the total cation (e.p.m) as shown in **Figure 6a**. This reveals that the silicate weathering contributes mainly Na^+ and K^+ ions to groundwater [23]. Further, the plot of $Ca^{2+} + Mg^{2+}$ versus total cations of the groundwater samples as in **Figure 6b** has a linear spread, indicating that some of these ions ($Ca^{2+} + Mg^{2+}$) are resulted from the weathering of silicate minerals. In addition, all the groundwater samples exhibited an oversaturation with respect to calcite, which suggest the prevailing of calcite precipitation process in the aquifer.

7. Geochemical evolution of groundwater

The initial composition of groundwater originates from rainfall with low concentrations of dissolved ions. During its return path to the ocean, the water composition is altered by rock weathering and evaporation causing more Ca^{2+}, Mg^{2+}, Na^+, SO_4^{2-}, HCO_3^-, Cl^-, and SiO_2 to be added. The concentration of these ions depends on the rock mineralogy that the water encounters and its rapidity along the flow path. The abundance of the major cations in Al-Atraf field is in the order of $Na^+ > Ca^{2+} > Mg^{2+} > K^+$. The sequence of the anions is in the order of $Cl^- > SO_4^{2-} > HCO_3^-$. The majority of the groundwater samples of the study area (75.36%) exhibited NaCl water chemical type, followed by (23.19%) of Na_2SO_4 and (1.45%) of $CaSO_4$ water chemical types. The average TDS of 4441 mg/l represents brackish groundwater as presented in **Table 2**. Calcium and magnesium present in the groundwater are mainly due to the dissolution of gypsum and anhydrite, the most rock-forming minerals of the Kuwait Group aquifer of the study area. Calcium ions are derived also from cation exchange process. The concentration of calcium ions in the study area ranges from 332 to 743 mg/l with an average value of 484.23 mg/l and magnesium ranges from 85 to 203 mg/l, with an average value of 140.87 mg/l. This indicates that the Ca^{2+} ion concentration in the study area is relatively higher than magnesium ion. Alkalinity is the quantitative capacity of an aqueous solution to neutralize an acid. The ideal range of the total alkalinity is from 80 to 140 mg/l. In natural environment, carbonate alkalinity tends to make up most of the total alkalinity due to the common occurrence and dissolution of carbonate rocks and the presence of carbon dioxide in the atmosphere. The total alkalinity of the study area ranges between 51.2 and 127 mg/l as $CaCO_3$ with an average value of 91.39 mg/l. **Figure 7a** represents $Ca^{2+} + Mg^{2+}$ versus alkalinity + SO_4^{2-} in e.p.m., suggesting that these ions have resulted from weathering of carbonate and sulfate

http://dx.doi.org/10.5772/intechopen.71577

S.No.	TDS	pH	Na	K	Ca	Mg	Cl	SO_4	HCO_3	SiO_2	T. Hardnes	T. Alkalinity	Water Chemical Types
1	5974	7.5	950	20	743	203	2346	1334	90.4	36.4	2690	74.10	NaCl
2	5412	7.45	913	19.5	638	180	2068	1247	106	39.2	2333	86.80	NaCl
3	5562	7.5	863	20	630	188	2065	1247	106	42.4	2346	87.00	NaCl
4	5138	7.4	838	19.5	600	180	1850	1363	103	36	2238	85.00	NaCl
5	6366	7.3	913	20.5	720	203	2346	1291	104	39.2	2832	85.20	NaCl
6	4872	7.4	763	18.5	570	173	1525	1508	130	26.4	2134	106.00	NaCl
7	5050	7.4	850	19	578	180	1840	1247	121	41	2183	98.80	NaCl
8	5338	7.4	863	20	600	188	1925	1392	113	40	2271	92.10	NaCl
9	5006	7.3	863	19	549	162	1683	1247	104	32.4	2037	85.30	NaCl
10	4416	7.3	695	17	458	150	1316	1334	136	43.2	1760	112.00	Na_2SO_4
11	5434	7.5	705	17.5	539	156	1640	1334	124	39.9	1987	102.00	NaCl
12	4146	7	750	15.5	458	113	1417	1073	100	42	1609	82.00	NaCl
13	4294	7.5	710	15.1	471	120	1380	1073	106	33.2	1670	86.90	NaCl
14	3753	7.5	600	15.2	408	128	1026	1394	144	26.8	1545	118.00	NaCl
15	3687	7.5	595	14	391	85	1099	1160	121	26.8	1326	99.30	NaCl
16	3860	7.5	660	14.7	408	128	1208	1073	109	33.4	1545	89.50	NaCl
17	4043	7.4	650	17.5	450	143	1495	1125	111	30.4	1711	90.70	NaCl
18	3983	7.3	650	16	383	126	1240	1189	131	41	1482	107.00	NaCl
19	4312	7.3	670	17.5	459	143	1343	1218	125	37.6	1734	102.00	NaCl
20	4181	7.9	675	15.5	459	150	1157	1378	137	39.4	1763	112.00	Na_2SO_4
21	4213	7.15	625	15	440	119	1114	1349	148	40	1588	121.00	Na_2SO_4
22	3784	7.35	610	13.8	408	113	1118	1044	117	33.2	1483	96.10	NaCl
23	4043	7.35	620	15.6	411	150	1230	1204	124	29.4	1643	102.00	NaCl
24	5624	7.2	963	15.5	645	135	2005	1450	62.5	26.8	2166	51.20	NaCl
25	4222	7.45	695	14.5	434	143	1255	1189	116	35.6	1671	95.00	NaCl
26	3883	7.4	590	16.5	451	111	1185	1225	122	37	1583	102.00	Na_2SO_4
27	3763	7.3	640	14	464	153	1193	1125	125	34.8	1787	103.00	NaCl
28	3960	7.3	700	16.5	443	128	1423	1044	94.8	27.6	1632	77.70	NaCl
29	6060	7.2	963	18.5	705	150	2300	1218	75.3	27.2	2378	61.70	NaCl
30	4550	7.2	775	17	512	128	1572	1175	101	27.2	1805	82.40	NaCl
31	4180	7.4	715	15.5	465	120	1424	1131	103	29.2	1655	84.50	NaCl
32	4257	7.35	690	14.3	458	129	1411	1131	100	31.6	1674	82.20	NaCl
33	4442	7.45	700	14.25	456	120	1361	957	103	34	1632	84.10	NaCl
34	3719	7.3	570	16	419	111	1208	1175	120	36.6	1503	98.40	NaCl
35	3575	7.4	540	16	367	111	923	1200	133	34.6	1373	109.00	NaCl
36	3686	7.5	630	14.5	424	122	1025	1218	132	34	1560	108.00	NaCl
37	4976	7.5	700	15.5	570	150	1691	1088	95.9	29	4040	78.60	NaCl
38	4711	7.5	750	17	332	128	1350	1102	87.1	32	1355	71.40	NaCl
39	4505	7.35	740	16.4	503	128	1482	1112	93	29	1782	76.20	Na_2SO_4
40	4261	7.5	655	14	482	147	1118	1450	156	27.6	1808	127.00	NaCl
41	4107	7.5	580	12.5	410	111	1171	1131	112	29.2	1480	91.70	NaCl
42	4357	7.4	450	16	525	113	900	1204	99.4	28.6	1776	81.50	$CaSO_4$
43	4582	7.4	780	30	515	143	1585	1102	88.7	28.8	1874	72.70	NaCl
44	3882	7.3	630	15.4	395	120	1226	1131	115	35	1480	94.20	NaCl
45	3590	7.3	555	15	374	120	997	1189	132	33.6	1427	108.00	Na_2SO_4
46	4070	7.6	670	14.5	425	114	1113	1204	122	29.2	1530	99.80	Na_2SO_4
47	3504	7.6	510	14	375	134	846	1218	137	29.6	1487	112.00	Na_2SO_4
48	4226	7.4	750	16.5	458	138	1316	1305	113	30.4	1711	92.20	Na_2SO_4
49	3618	7.5	615	15	435	120	999	1392	126	30	1580	103.00	Na_2SO_4
50	4092	7.5	665	14.5	473	195	1397	1276	113	29.4	1982	92.60	NaCl
51	3792	7.7	660	16	420	135	1138	1131	125	26.6	1604	103.00	NaCl
52	3784	7.4	650	16	399	128	1152	1276	126	26	1522	103.00	Na_2SO_4
53	3642	7.45	610	15.5	368	125	908	1305	130	25.6	1433	106.00	Na_2SO_4
54	4526	7.3	855	18	473	143	1539	1276	99	26	1769	81.20	NaCl
55	4030	7.4	750	17	413	128	1284	1247	113	26.4	1557	92.40	NaCl
56	4588	7.4	885	18	518	135	1614	1305	97	26.4	1849	79.40	NaCl
57	4180	7.4	745	17	450	143	1241	1363	114	30	1711	94.00	Na_2SO_4
58	3552	7.6	625	16	360	120	1053	1102	129	28	1329	106.00	Na_2SO_4
59	5163	7.4	950	19	570	158	1923	1247	86	30.4	2073	70.00	NaCl
60	4909	7.4	900	19	540	165	1714	1392	96.1	27.2	2500	79.00	NaCl
61	5188	7.4	900	18	518	158	1670	1450	109	28	1943	89.30	NaCl
62	4584	7.5	825	18	518	143	1579	1334	100	27.2	1881	82.00	NaCl
63	5394	7.1	1013	20	608	165	1943	1479	78.2	26	2197	64.10	NaCl
64	4303	7.4	715	18	450	143	1442	1247	117	28	1711	96.10	NaCl
65	3988	7.4	700	17	390	128	1215	1160	108	30	1500	88.70	NaCl
66	5260	7.2	913	19	525	150	1881	1334	97	29	1928	79.40	NaCl
67	4785	7.4	800	18	533	150	1643	1276	93	28.4	1948	76.20	NaCl
68	4964	7.6	850	20	585	150	1790	1276	83	26.4	2078	68.00	NaCl
69	4546	7.3	780	18	488	150	1617	1247	106	27.2	1835	87.00	NaCl
Min.	3504.00	7.00	450.00	12.50	332.00	85.00	846.00	957.00	62.50	25.60	1326.00	51.20	
Max.	6366.00	7.90	1013.00	30.00	743.00	203.00	2346.00	1508.00	156.00	43.20	4040.00	127.00	
Ave.	4440.97	7.40	730.12	16.85	484.23	140.87	1438.45	1237.87	111.51	31.73	1826.22	91.39	

Table 2. Report of physico-chemical parameters of the studied groundwater samples of the study area.

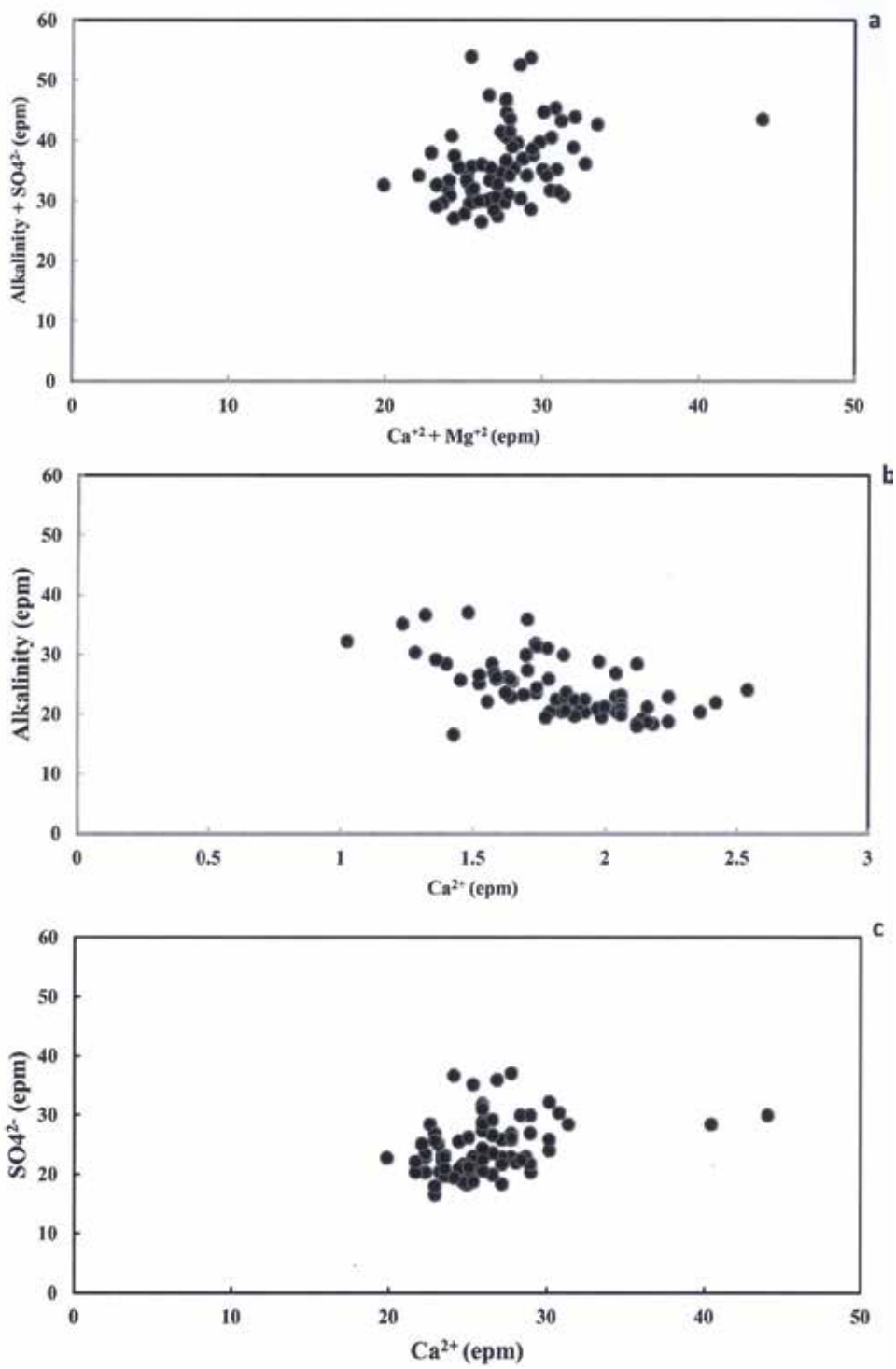

Figure 7. (a) Relation between Ca+Mg and alkalinity + SO_4. (b) Relation between Ca^{2+} and alkalinity. (c) Relation between Ca^{2+} and SO^{2-}_4.

http://dx.doi.org/10.5772/intechopen.71577

S.No.	EC	SAR	% Na	RSC	Kelly's ratio	MgR	CAI	P.I %	P.S.
1	7720	7.97	43.22	-52.29	0.77	31.05	0.37	44.73	80.07
2	8230	8.69	45.32	-52.63	0.84	32.02	0.36	46.72	83.56
3	7380	8.22	45.73	-44.91	0.85	31.74	0.31	47.52	71.32
4	7280	7.75	44.19	-45.16	0.80	32.97	0.35	46.02	71.23
5	6750	7.71	44.62	-43.06	0.81	33.09	0.29	46.49	66.38
6	7140	8.86	48.14	-42.89	0.94	30.39	0.30	49.94	73.35
7	7670	7.74	42.77	-50.92	0.75	31.73	0.39	44.42	79.62
8	6330	7.19	43.48	-40.54	0.78	33.35	0.22	45.67	58.72
9	6560	7.91	45.59	-41.67	0.85	33.92	0.28	47.61	64.89
10	7050	7.88	44.98	-43.55	0.83	34.06	0.30	46.90	68.79
11	6250	8.32	47.67	-39.02	0.92	32.73	0.20	49.64	60.46
12	5600	7.21	45.90	-32.96	0.86	35.06	0.17	48.49	51.01
13	6670	6.88	43.29	-37.70	0.77	32.30	0.33	45.59	60.15
14	5650	8.14	50.06	-30.51	1.01	28.91	0.17	52.34	51.14
15	5590	7.56	47.78	-31.64	0.93	29.58	0.20	50.11	50.10
16	5100	6.64	45.49	-28.53	0.84	34.09	0.08	48.49	43.46
17	5070	7.11	49.07	-24.52	0.98	26.38	0.15	52.10	43.08
18	5510	7.31	47.87	-29.10	0.93	34.09	0.15	50.42	45.25
19	5500	6.84	44.92	-32.40	0.83	34.38	0.32	47.40	53.89
20	5110	7.37	48.62	-27.33	0.96	35.16	0.18	51.50	47.36
21	5620	7.00	45.35	-32.62	0.84	33.93	0.22	47.92	50.57
22	5310	6.99	45.17	-33.00	0.83	35.01	0.09	47.77	46.98
23	5110	6.82	45.84	-29.32	0.86	30.84	0.12	48.78	45.47
24	4500	6.89	46.93	-27.74	0.89	31.35	0.15	49.69	42.41
25	5570	6.65	44.79	-30.82	0.82	37.56	0.21	47.47	47.23
26	7550	9.00	48.95	-42.27	0.97	25.65	0.25	50.37	71.66
27	5260	7.40	47.22	-31.52	0.90	35.20	0.14	49.66	47.78
28	5240	6.45	44.46	-29.64	0.81	28.86	0.22	47.26	46.18
29	4970	6.59	43.54	-33.69	0.78	35.22	0.16	46.04	45.37
30	5280	7.54	47.95	-31.08	0.93	32.26	0.23	50.24	51.01
31	7350	8.59	46.61	-46.28	0.88	25.97	0.35	48.10	77.56
32	5510	7.94	48.01	-34.42	0.93	29.18	0.23	50.15	56.58
33	5040	7.65	48.17	-31.39	0.94	29.85	0.22	50.49	51.94
34	6100	7.34	47.01	-31.83	0.90	31.71	0.24	49.30	51.58
35	5210	7.54	48.00	-30.94	0.93	30.26	0.20	50.34	48.36
36	4820	6.40	44.88	-28.07	0.83	30.40	0.26	47.78	46.31
37	4560	6.34	45.75	-25.26	0.86	33.27	0.08	49.02	38.53
38	4370	6.94	46.47	-29.03	0.88	32.17	0.04	49.28	41.59
39	6410	6.74	42.51	-39.21	0.75	30.26	0.35	44.51	59.03
40	6120	8.86	54.23	-25.67	1.20	38.86	0.13	56.63	49.56
41	5830	7.63	47.17	-34.10	0.90	29.55	0.22	49.29	53.38
42	5560	6.70	43.84	-33.59	0.79	33.46	0.09	46.55	46.63
43	5020	6.56	45.76	-27.75	0.85	30.86	0.23	48.49	44.81
44	5800	4.65	35.28	-33.86	0.55	26.19	0.21	37.86	37.92
45	6150	7.84	47.02	-36.01	0.91	31.40	0.22	49.22	56.18
46	4950	7.13	47.76	-27.70	0.93	33.37	0.20	50.50	46.36
47	4630	6.39	45.50	-26.37	0.85	34.59	0.13	48.62	40.50
48	5020	7.45	48.49	-28.59	0.95	30.66	0.06	51.16	43.93
49	4520	5.75	42.44	-27.49	0.75	37.07	0.06	45.62	36.55
50	5700	7.89	48.51	-32.35	0.95	33.19	0.11	50.85	50.71
51	4850	6.73	45.56	-29.51	0.85	31.26	0.04	48.33	42.67
52	5730	6.50	41.96	-37.79	0.73	40.46	0.26	44.17	52.69
53	4540	7.17	46.93	-30.01	0.90	34.64	0.09	49.60	43.88
54	4980	7.25	47.82	-28.37	0.93	34.59	0.12	50.60	45.78
55	4500	7.01	47.74	-26.52	0.93	35.90	-0.05	50.73	39.20
56	5810	8.84	50.94	-33.74	1.05	33.26	0.13	53.01	56.70
57	5390	8.27	50.82	-29.29	1.05	33.81	0.09	53.30	49.20
58	6030	8.96	50.71	-35.36	1.04	30.05	0.14	52.69	59.12
59	5680	7.83	48.33	-32.35	0.95	34.38	0.06	50.69	49.20
60	4620	7.29	49.05	-25.72	0.98	35.46	0.07	52.05	41.18
61	6910	9.08	49.64	-40.03	1.00	31.36	0.23	51.36	67.23
62	6760	8.70	48.84	-38.94	0.97	33.50	0.18	50.72	62.84
63	6690	8.88	49.90	-37.06	1.01	33.46	0.16	51.91	62.21
64	6020	8.28	48.52	-35.97	0.95	31.28	0.18	50.57	58.43
65	7400	9.40	49.80	-42.63	1.00	30.91	0.19	51.37	70.21
66	5670	7.52	47.28	-32.30	0.91	34.38	0.22	49.74	53.66
67	5320	7.86	50.02	-28.22	1.02	35.11	0.10	52.58	46.35
68	7080	9.05	50.44	-36.95	1.03	32.02	0.24	52.36	66.95
69	6250	7.89	46.90	-37.41	0.89	31.69	0.24	48.87	59.63
70	6910	8.11	46.79	-40.17	0.89	29.71	0.26	48.58	63.78
71	6030	7.92	47.73	-34.95	0.92	33.63	0.25	49.91	58.60
Min.	**4370**	**4.65**	**35.28**	**-52.63**	**0.55**	**25.65**	**-0.05**	**37.86**	**36.55**
Max.	**8230**	**9.40**	**54.23**	**-24.52**	**1.20**	**40.46**	**0.39**	**56.63**	**83.56**
Ave.	**5837**	**7.54**	**46.73**	**-34.31**	**0.89**	**32.48**	**0.19**	**49.07**	**54.17**

Table 3. Irrigation water quality parameters for groundwater samples of the study area.

minerals (gypsum and anhydrite). However, most of the points are placed in Ca^{2+} + Mg^{2+} side, which indicates excess calcium and magnesium derived from other processes such as reverse ion exchange reactions. In Ca^{2+} versus alkalinity diagram, **Figure 7b** indicates the contribution of both calcite and dolomite weathering on groundwater chemistry of the study area. Moreover, in Ca^{2+} versus SO_4^{2-} diagram (**Figure 7c**), most of the sample show excess calcium over sulfate, which reveal that the groundwater samples seem to be derived from gypsum or anhydrite dissolution. Moreover, excess sulfate over calcium in few samples expresses the removal of calcium from the system likely by calcite precipitation. Therefore, silicate weathering and carbonate dissolution are the prevailing geochemical processes in the aquifer of the study area.

7.1. Ion exchange

Ion exchange is one of the important processes responsible for the concentration of ions in groundwater.

$$\mathrm{CAI}-1=\frac{\mathrm{Cl}^{-}-(\mathrm{Na}^{+}+\mathrm{K}^{+})}{\mathrm{Cl}^{-}} \tag{2}$$

Where all values are expressed in meq/l. When there is an exchange between Ca^{2+} or Mg^{2+} in groundwater with Na^+ and K^+ in the aquifer material, the CAI-1 is negative, and if there is a reverse ion exchange, CAI-1 will be positive [24]. The values of CAI-1 of the study area are positive in most wells, and very few wells show negative, and the CAI-1 ranges from −0.05 to 0.39 with an average value of 0.19 as presented in **Table 3**. Thus, it reveals that reverse ion exchange is the dominant process in the groundwater, whereas normal ion exchange is also noticed in a very few wells.

8. Drinking and irrigation water quality

The assessment of suitability of the groundwater for drinking and irrigation purposes can be determined through the parameters such as EC, TDS, pH, SAR, %Na, RSC, Kelley's ratio, MgR, CAI-1, P.I, and P.S as displayed in **Table 3**.

8.1. Drinking water quality

The suitability of the groundwater in the study area is evaluated for drinking by comparing with the standard guideline values [25]. According to WHO specifications, TDS up to 500 mg/l is the highest desirable and up to 1500 mg/l is the maximum permissible level. Based on this classification, the TDS of the groundwater of the study area ranges between 3504 and 6366 mg/l with an average value of 4441 mg/l, which exceeds the recommended limit. However, the major cations and anions composition of the study area are all above the standard guideline of the WHO for drinking purposes. Water hardness causes more consumption of detergents at the time of cleaning, and some evidences indicate its role in heart disease [26]. The total hardness was determining by the following equation according to [27]:

$$TH = 2.5\,Ca^{2+} + 4.1\,Mg^{2+}. \quad (3)$$

where Ca^{2+} and Mg^{2+} concentrations are expressed in mg/l as $CaCO_3$. Hardness of water is due to the precipitation of Ca^{2+} and Mg^{2+} salts like carbonate, sulfates, and chlorides. Hardness of water causes scaling of pots, boilers, and irrigation pipes. However, the total hardness of the study area is varying from 1326 to 4040 mg/l as $CaCO_3$, with an average value of 1826.22 mg/l as shown in **Table 2**. The analytical result of TH indicates that the groundwater of the study area is exceeding very hard water type according to [28] as shown in **Table 4**. Therefore, according to TDS and TH standards the groundwater is not suitable for drinking purposes.

8.2. Irrigational suitability

The suitability of groundwater for irrigation depends on the effect of mineral composition of water on the soil and plants. The effect of the salt on soils causes change in soil structure, permeability, and hence it effects on plant growth.

8.2.1. Residual sodium carbonate

Residual sodium carbonate has been calculated to determine the hazard effects of carbonate and bicarbonate on the quality of water for irrigation and is expressed by the equation:

$$RSC = \left(HCO_3^- + {CO_3}^{2-}\right) - \left(Ca^{2+} + Mg^{2+}\right) \quad (4)$$

Where all ionic concentrations are expressed in meq/l. The classification of irrigation water according to the RSC presents in **Table 5** after [29], where water containing more than 2.5 meq/l of RSC are not suitable for irrigation, while those having <1.25 meq/l are good for irrigation. Eaton (1950) indicated that if waters which are used for irrigation contain excess of $HCO_3^- + {CO_3}^{2-}$ than its equivalent $Ca^{2+} + Mg^{2+}$, there will be a residue of $Na^+ + HCO_3^-$ when evaporation takes place and the pH of the soil increases up to 3 [30]. When total carbonate levels exceed the total amount of calcium and magnesium, the water quality diminished [31]. The calculated RSC values of the groundwater samples of the study area are ranged from −52.63 to

Total Hardness as $CaCO_3$ (mg/l)	Water Class
< 75	Soft
75-150	Moderately hard
150-300	Hard
>300	Very hard

Table 4. Water classes (After [28]).

RSC value	Water quality
<1.25	suitable
1.25-2.5	marginal
>2.5	Not suitable

Table 5. Water classes based on RSC (after [29]).

−24.52 meq/l with an average value of −34.31 meq/l. Negative RSC indicates that sodium buildup is unlikely, since sufficient calcium and magnesium are in excess of what can be precipitated as carbonates [32]. Hence, the groundwater of the study area is safe for irrigation.

8.2.2. Permeability index

The permeability of soil is affected by long-term use of irrigation water and is influenced by sodium, calcium, magnesium, and bicarbonate contents in soil. Doneen (1964) set a criteria for assessing the suitability of water for irrigation based on permeability index; accordingly, waters can be classified as Class I, Class II, and Class III. The Class I and Class II waters are suitable for irrigation with 50–75% or more of maximum permeability, whereas Class III water is unsuitable with 25% of maximum permeability. Therefore, soil permeability is affected by consistent use of irrigation water which increases the presence of sodium, calcium, magnesium, and bicarbonate in the soil [33].

The permeability index is used to measure the suitability of water for irrigation purpose when compared with the total ions in meq/l, and it is expressed as follows:

$$\mathrm{PI} = \frac{\mathrm{Na}^{+} + \sqrt{\mathrm{HCO}_3^{-}}}{\mathrm{Ca}^{2+} + \mathrm{Mg}^{2+} + \mathrm{Na}^{+}} * 100 \tag{5}$$

In the present study, the P.I of the groundwater samples ranged from 37.86 to 56.63% with a mean value of 49.1%, and it is observed that all the groundwater samples fall in Class II category of Doneen Chart (**Figure 8**). Therefore, the groundwater of the study area is good for use in irrigation.

8.2.3. Potential salinity

Doneen as in Ref. [17] introduced an important parameter "Potential Salinity" for assessing the suitability of water for irrigation uses, which defined as chloride concentration plus half of the sulfate concentration expressed in meq/l.

Potential salinity = Cl^{-} + ½ SO_4^{2-}. On the basis of the potential salinity, Doneen [17] subdivided the irrigation water into three classes as presented in **Table 6**. The potential salinity of the majority of the analyzed groundwater samples of the study area ranges between 36.55 and 83.56 meq/l with an average value of 54.17 meq/l, indicating high values of potential

http://dx.doi.org/10.5772/intechopen.71577

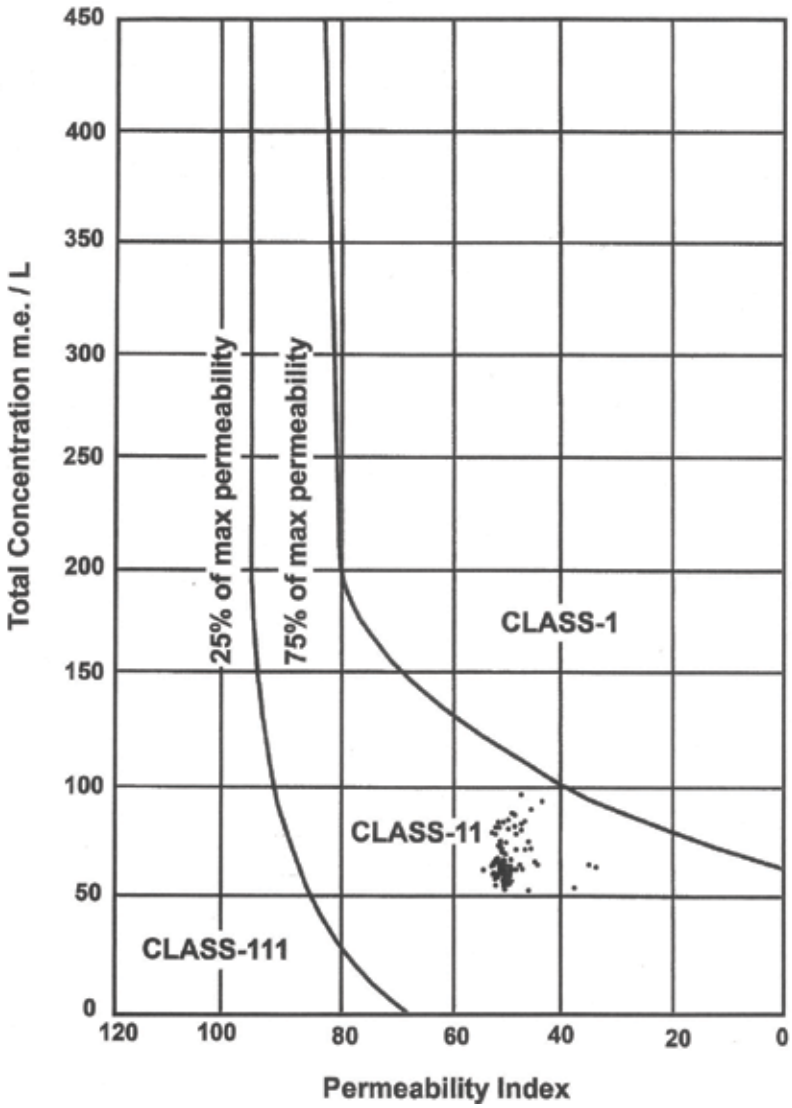

Figure 8. Permeability index diagram of the study area.

Soil Characteristics	Class of Water		
	Class 1	Class 11	Class 111
Soil of low Permeability	<3	3-5	>5
Soil of medium Permeability	<5	5-10	>10
Soil of high Permeability	<7	7-15	>15

Table 6. Classification of irrigation water based on potential salinity.

salinity. However, it is found that the classification of the groundwater of the study area for irrigation purposes fall in Class III; therefore, the groundwater should be used in case of a soil of high permeability.

8.2.4. Sodium adsorption ratio

Sodium concentration is considered an important factor to express reaction with the soil and reduction in its permeability. Therefore, sodium adsorption ratio is considered as a better measure of sodium (alkali) hazard in irrigation water as it is directly related to the adsorption of Na^+ on soil and is the important criteria for estimating the suitability of the water for irrigation. SAR can be computed as follows:

$$\text{SAR} = \frac{Na^+}{\sqrt{\frac{Ca^{2+}+Mg^{2+}}{2}}} \tag{6}$$

Where all ionic concentrations are expressed in meq/l. The SAR of the study area ranges between 4.65 and 9.4, with an average value of 7.54. The SAR values of all the study area are found to be <10 and are classified as categories S_1 and S_2, as low and medium sodium water, respectively. Therefore, based on the sodium hazard class the groundwater of the study area is suitable for irrigation.

8.2.5. Salinity hazard

The most important criteria regarding salinity and water availability to the plant is the total salt concentration. Since there exists a straight line correlation between electrical conductivity (EC) and total salt concentration of waters, the most expedient procedure to evaluate salinity hazard is to measure its electrical conductivity measured in (μmohs/cm) [34]. On the basis of salt concentration, the US Salinity Laboratory Staff divided the irrigation waters into four classes. Later on, another class was added to it [35] as given in **Table 7**. Waters having EC values above 1500 μmohs/cm can cause serious damage.

For rating irrigation waters, the US salinity diagram was used, in which the SAR is plotted against EC as shown in **Figure 9**, where the EC values of samples of the study area range from 4370 to 8230 with an average value of 5837 μmohs/cm and water exhibited very high to extensively high water salinity and medium sodium, high sodium type (C_4-S_2, C_4-S_3). Few samples are located on C_4-S_4 type. Therefore, the groundwater can be used with tolerant crops of clayey, sandy loam, and loamy sand soil texture, and special management for salinity control.

8.2.6. Magnesium ratio

In most waters, calcium and magnesium maintain a state of equilibrium. A ratio namely index of magnesium hazard was developed by [36]. According to this, a high magnesium hazard value of >50% has an adverse effect on the crop yield as the soil becomes more alkaline, and effect on the agricultural yield, and a harmful effect on soil will appear.

http://dx.doi.org/10.5772/intechopen.71577

$$\text{Mg ratio} = \frac{Mg^{2+}}{\left(Ca^{2+} + Mg^{2+}\right)} \times 100 \tag{7}$$

Where all ionic concentrations are expressed in meq/l.

In the study area, the magnesium hazard values fall in the range value of 25.65–40.46% with an average value of 32.48%, that is, magnesium hazard ratio is <50%, which is recognized as suitable for irrigation.

8.2.7. Sodium percentage (%Na)

Sodium is an important ion used for the classification of irrigation water due to its reaction with soil, reduces its permeability. The %Na is computed as:

$$\%\text{Na}^{+} = \left(\frac{(Na + K)^{+}}{Ca^{2+} + Mg^{2+} + K^{+} + Na^{+}}\right) \times 100 \tag{8}$$

Where all ionic concentrations are expressed in meq/l. According to [15], in all natural waters, $\%Na^{+}$ is a common parameter to assess its suitability for irrigation purpose as shown in **Table 8**. If the concentration of Na^{+} is high in irrigation water, Na^{+} gets absorbed by clay particles, displacing Mg^{2+} and Ca^{2+} ions. This exchange process of Na^{+} in water for Ca^{2+} and Mg^{2+} in soil reduces the permeability of soil and eventually results in poor internal drainage of

EC (µmohs/cm)	Water Salinity
00 - 250	Low (Excellent quality)
251 -750	Medium (Good quality)
751 - 2250	High (Permissible quality)
2251 - 6000	Very high
6001 - 10000	Extensively high
10001 - 20000	Brines weakly conc.
20001 - 50000	Brines moderately conc.
50001 - 100000	Brines highly conc.
> 100000	Brines extremely conc.

Table 7. Classification of waters based on EC [35].

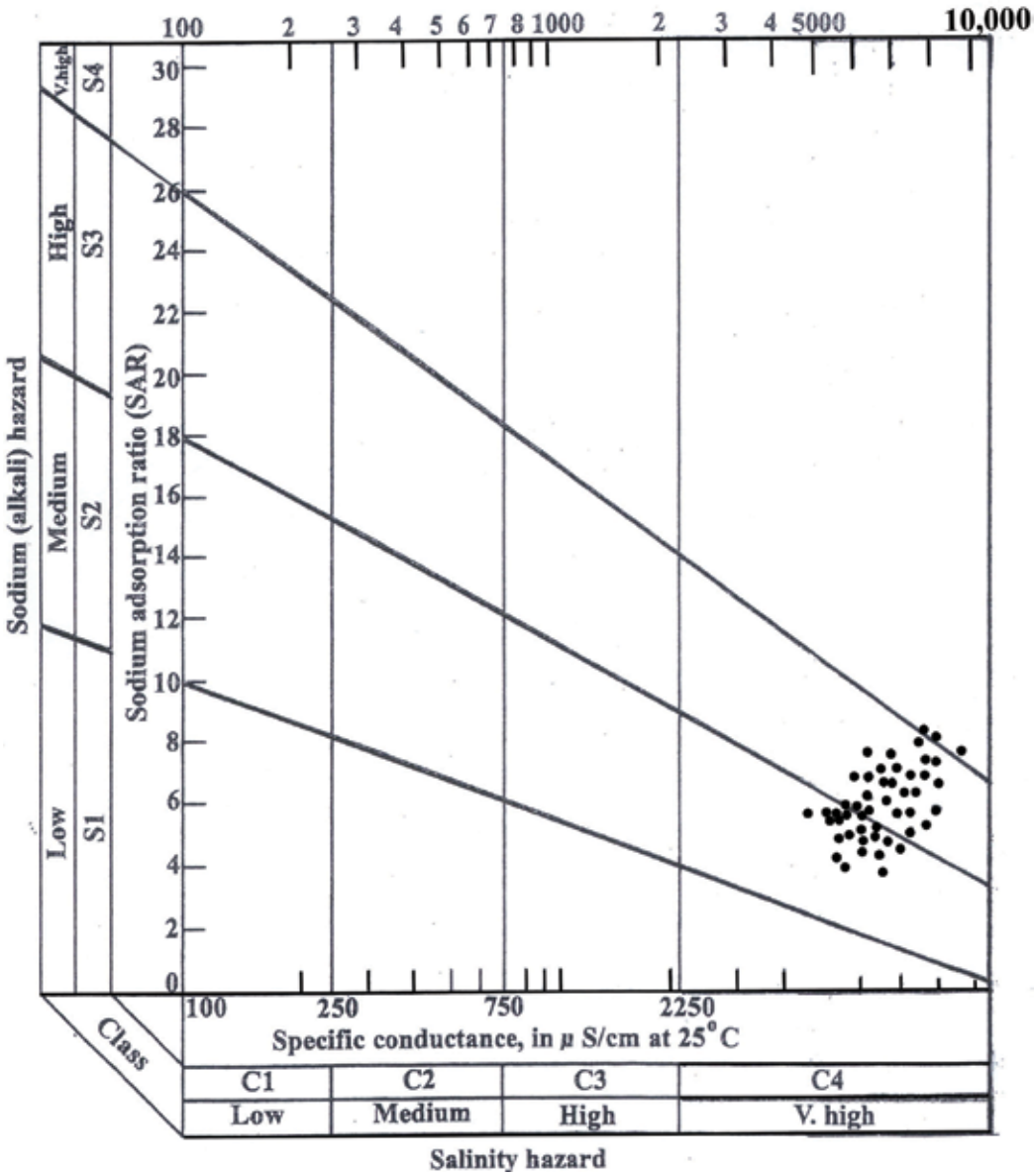

Figure 9. Wilcox diagram illustrating the groundwater quality of the study area.

the soil, and such soils are usually hard when dry [37]. The values of $\%Na^+$ of the study area varies from 35.28 to 54.23% with an average value of 46.73% which fall in good to permissible category, showing that the groundwater of the study area is suitable for irrigation; meanwhile, the EC ranges between 4370 and 8230 μmohs/cm, in which the groundwater salinity is classified as very extensively high as presented in **Figure 10**; therefore, the groundwater can be used for irrigation under specific conditions.

Water Quality	Sodium %
Excellent	< 20
Good	20 – 40
Permissible	40 – 60
Doubtful	60 – 80
Unsuitable	> 80

Table 8. Classification of groundwater based on %Na [15].

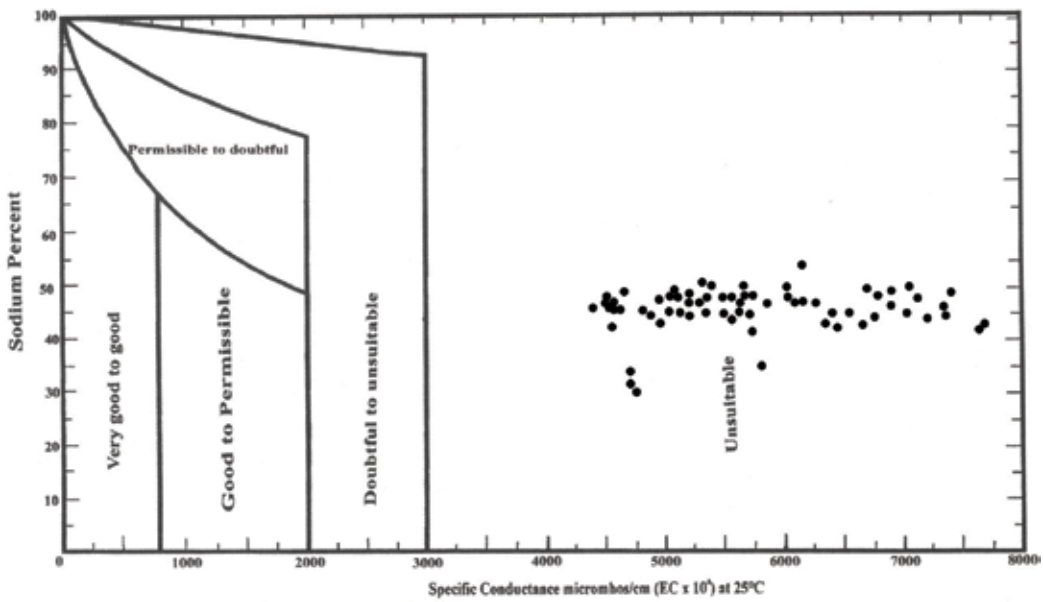

Figure 10. A plot of percentage of sodium vs. electrical conductivity of groundwater of the study area.

8.2.8. Kelly's ratio

Kelly's ratio is used for the classification of water for irrigation purposes. A Kelly's index (>1) indicates an excess level of sodium in waters [38]. Therefore, water with a KR (<1) is suitable for irrigation. KR is calculated by using the formulae, where all the ions are expressed in meq/l.

$$\text{Kelly}^{'}\text{s ratio} = \frac{Na^{+}}{\left(Ca^{2+} + Mg^{2+}\right)} \tag{9}$$

The values of the KR in the present study varied between 0.55 and 1.2 with an average value of 0.89 which is <1. It is found that 87.32% of the groundwater samples have KR <1, and 12.68% KR > 1. Accordingly, the groundwater of the study area is suitable for irrigation.

9. Conclusion

The study area is located in the southwest of Kuwait. It includes 83 wells that produce brackish groundwater from Kuwait Group aquifer. Pumping test analyses revealed that the aquifer is acting as a confined to semi-confined aquifer, and transmissivity ranges between 62.03 and 320.51 m^2/day and increases toward N-NE. The estimated storage coefficient is 7.5×10^{-4}.

In the present study, the pH values range from 7 to 7.9, indicating an alkaline type of groundwater. The total alkalinity ranges from 51.2 to 127 mg/l with an average value of 91.39 mg/l. The electrical conductivity values range from 4370 to 8230 μmohs/cm with an average value of 5837 μmohs/cm. Total dissolved solids vary from 3504 to 6366 mg/l, with an average value of 4441 mg/l representing brackish groundwater. The majority of the groundwater samples of the study area exhibited NaCl water chemical type, followed by Na_2SO_4, and $CaSO_4$ water chemical types, respectively.

The groundwater is very hard, where the average TH is 1826 mg/l as $CaCO_3$. The sequence of the abundance of the major cations and anions is $Na^+ > Ca^{2+} > Mg^{2+} > K^+$ and $Cl^- > SO_4{}^{2-} > HCO_3{}^-$. The dominant hydrochemical facies of the groundwater in the study area is Ca-Na-Cl. According to Gibb's plot, most of the samples of the study area are under the category of rock interaction and few samples are found to have the category of evaporation. Few samples fall in the precipitation-dominance area suggesting the influence of precipitation on the groundwater. Silicate weathering is the dominant weathering process in the study area; however, the carbonate weathering processes are also responsible for the supply of some ionic species to the groundwater. The calculation of the saturation indices revealed that the groundwater is oversaturated with respect to calcite and dolomite and undersaturated with respect to gypsum, anhydrite, halite, and SiO_2.

The positive index of base exchange for most of the samples (>98%) indicates that there exists a chloro-alkaline equilibrium, and there is an ion exchange of Na^+ and K^+ from water with magnesium and calcium in the rock, except one well, where the value is negative, revealed cation-anion exchange (chloro-alkaline disequilibrium).

Most of the TDS and TH values obtained are beyond the permissible limits making the groundwater of the study area unsuitable for drinking and for various domestic activities.

The suitability of groundwater for irrigation was evaluated based on the irrigation quality parameters like RSC, permeability index, potential salinity, SAR, salinity hazard, magnesium ratio, %Na, and Kelley's ratio. The majority of the groundwater samples exhibited very high salinity to extensively high water salinity class, medium and high sodium water type, respectively, According to the values of these parameters, the groundwater of the study area was found to be used for irrigation under high soil permeability, good drainage, and plants with good salt tolerance should be selected.

http://dx.doi.org/10.5772/intechopen.71577

Acknowledgements

The author would like to thank the Ministry of Electricity and Water for providing the chemical and pumping test data of Al-Atraf field.

Author details

Fawzia Mohammad Al-Ruwaih

Address all correspondence to: farhdana@yahoo.com

Department of Earth and Environmental Sciences, Kuwait University, Safat, Kuwait

References

[1] Milton DI. Geology of the Arabian Peninsula, Kuwait. Geological Survey Professional Paper 560-F. U.S Government Printing Office, Washington, U.S.A; 1967. pp. 1-7 F

[2] Fuchs W, Gattinger TE, Holzer HF. Explanatory Text to the Synoptic Geologic Map of Kuwait. A Surface Geology of Kuwait and the Neutral Zone. Vienn: Geological Survey of Austria; 1968. 87 pp

[3] Al-Sharhan AS, Nairn AE. Sedimentary Basins and Petroleum Geology of the Middle East. Amsterdam, Netherlands: Elsevier Science B.V; 1997. p. 843

[4] Besharah J, Al-Saad A. Oil Lakes Formation and Means of Remediation, Petroleum, Petrochemicals and Materials Division. Unpublished report. Kuwait Institute for Scientific Research, Kuwait; 1992

[5] Omar SA, Al-Yaqubi AS, Senay Y. Geology and groundwater hydrology of the State of Kuwait. Journal of the Gulf and Arabian Peninsula Studies. 1981;**1**:5-51

[6] Al-Ruwaih FM, Al-Awadi E. Groundwater utilization and Management in the State of Kuwait. Water International. 2000;**25**(3):378-389

[7] Fetter WC. Applied hydrogeology. 4th ed. Prentice-Hall, Inc; 2001. 598pp

[8] Saether OM, De-Caritat P. Geochemical processes, weathering and groundwater recharge in catchments. Balkema, Rotterdam. The Netherlands; 1997. 400pp

[9] Hem JD. Study and Interpretation of Chemical Characteristics of Natural Water. 3rd ed. Jodhpur, India: Book 2254: Scientific publ; 1991

[10] Ball JW, Nordstrom DK. Geochemical Model to Calculate Speciation of Major, Trace and Redox Elements in Natural Waters. Report, U.S. U.S.A: Geological Survey, International Groundwater Modeling Center; 1992

[11] Hounslow AW. Water Quality Data. Analysis and Interpretation. New York: Lewis Publishers; 1995

[12] Gibbs RT. Mechanisms controlling world's water chemistry. Science. 1970;**170**:1088-1090

[13] Piper AM. A graphical procedure in geochemical interpretation of water analyses. Transactions of the American Geophysical Union. 1953;**25**:914-923

[14] Al-Ruwaih FM, Shaflullah GS. Geochemical processes and assessment of irrigation water quality using GIS for Al-Shagaya Field-C, Kuwait. International Journal of Environment, Agriculture and Biotechnology (IJEAB). 2017;**2**(1):165-180

[15] Wilcox LV. Classification and Use of Irrigation Waters. Washington. D.C: US Department of Agriculture; 1955. 19pp

[16] Doneen LD. In: Davis CA, editor. Notes on Water Quality in Agriculture. Water Science and Engineering, University of California; 1964

[17] Doneen LD. The influence of crop and soil on percolating water. Proceedings of Groundwater Recharge Conference. California, U.S.A. 1961

[18] Theis CV. The relation between the lowering of the Piezometric surface and the rate and duration of discharge of a well using groundwater storage. Transactions of the American Geophysical Union. 1935;**25**:519-524

[19] Cooper HH, Jacob CE. A generalized graphical method for evaluating formation constants and summarizing well-field history. Transactions of the American Geophysical Union. 1946;**27**:526-534

[20] Walton WC. Groundwater Resources Evaluation. Tokyo, Japan: McGraw Hill Book Company; 1970. 664 P

[21] Deutsch WJ. Groundwater Geochemistry: Fundamentals and Applications to Contamination. U.S.A: Lewis Publishers, New York; 1997. 221pp

[22] Appelo CAJ, Postma D. Geochemistry, Groundwater and Pollution. Rotterdam, The Netherlands: Balkema; 2005. 649pp

[23] Stallard RF, Edmond JM. Geochemistry of the Amazon, the influence of geology and weathering environment on the dissolved load. Journal of Geophysical Research. 1983; **88**:9671-9688

[24] Schoeller H. Geochemistry of groundwater. In: groundwater Studies- An international guide for research and practice (ch. 15, p.p. 1-18). Paris: UNESCO; 1977

[25] WHO, editor. Guidelines for Drinking-Water Quality [Electronic Source]: Incorporations. 3rd ed. Geneva: WHO; 2008. 515pp

[26] Schroeder HA. Relations between hardness of water and death rate from certain chronic and degenerative diseases in the United States. Journal of Chronic Diseases. 1960;**12**:586-591

[27] Todd DK, Mays LW. Groundwater Hydrology. 3rd ed. John Wiley & sons, Inc; 2005. 636 pp

[28] Sawyer GN, McCarthy DL. Chemistry of Sanitary Engineers. 2nd ed. New York: Mc Grow Hill; 1967. 518pp

[29] Richards LA. Diagnosis and improvement of saline and alkaline soils. In: US Department of Agriculture Hand Book. 1954. 60pp

[30] Eaton EM. Significance of carbonate in irrigation water. Soil Science. 1950;**69**:12-133

[31] Sundaray SK, Nayak BB, Bhatta D. Environmental studies on river waters quality with reference to suitability for agricultural purposes: Mahanadi river esturarine system. India- a case study, Environmental Monitoring and Assessment. 2009;**155**:227243

[32] Satyanarayanan M, Balaram V, Al Hussin MS, Al Jemaili MA, Rao TG, Mathur R, Dasaram B, Ramesh SL. Assessment of groundwater quality in structurally deformed granitic terrain in Hyderabad, India. Environmental Monitoring and Assessment. 2007;**113**:117-127

[33] Chandu SN, Subbarao NV, Prakash SR. Suitability of groundwater for domestic and irrigation purposes in some part of Jhansi District, U. P. Bhujal Newa. 1995;**10**(1):12-17

[34] Chhabra R. Soil Salinity and Water Quality. U.S.A.: A.A. Balkema Publishers; 1996. 284pp

[35] Handa BK. Groundwater pollution in India. In: Proceedings of National Symposium on Hydrology. IAHS, publ. Univ. Roorkee, India. 1969. pp. 34-49

[36] Paliwal KV. Irrigation with Saline Water. Monogram No.2 (new series). New Delhi: I A R I; 1972. 198pp

[37] Saleh A, Al-Ruwaih FM, Shehata M. Hydrogeochemical processes operating within the main aquifers of Kuwait. Journal of Arid Environments. 1999;**42**:195-209

[38] Kelly WP. Alkali Soils- their Formation Properties and Reclamation. 3rd ed. New York, U.S.A: Reinhold publication; 1951. 92pp

Edited by Muhammad Salik Javaid and Shaukat Ali Khan

The rock matrix and the fluids contained therein define the aquifer as a whole, the custodian of continuity of life on this planet Earth. Its sustainable development, equitable utilization, quality maintenance, and balanced discharge and recharge are the essential elements to ensure that the next generation receives the resource baton passed on by the current generation. Spanning across the political and regional frontiers, transboundary aquifers have the potential to provide a uniting platform to the participatory nations. The common good of water can be enhanced by synergized research, data and knowledge sharing, joint development ventures, and hazard mitigation.

Covering the multifarious facets of aquifers, this book will form an essential and interesting reading for all stakeholders—researchers, engineers, academia, intelligentsia, and the common consumer.

Published in London, UK

IntechOpen

ISBN 978-1-83881-370-3